UNIVERSITÀ DEGLI STUDI DI MESSINA

TESI DI DOTTORATO DI RICERCA IN BIOLOGIA APPLICATA E MEDICINA SPERIMENTALE

CURRICULUM IN SCIENZE BIOLOGICHE ED AMBIENTALI

XXXIV CICLO

SSD BIO/07

Ecological and Hygienic-Sanitary Implications Related to the Diseases of the Mugilidae from ONR Capo Peloro

Canditato:

Dott.ssa Sabrina Natale

Tutor

Chiar.ma Prof.ssa Nunziacarla Spanò

Co-Tutor

Chiar.mo Prof. Fabio Marino

Coordinatore: Chiar.ma Prof.ssa Nunziacarla Spanò

Anno Accademico 2020/2021

ABSTRACT

The aim of this thesis is to identify the different mullet species present in the Ganzirri Lagoon located in Messina, in order to study the main parasitic diseases and to deepen the knowledge of a wide range of morphometric and morphological characteristics of otoliths. One of the most common problems in fish is parasitic diseases. The presence of organisms that parasitize in the living tissues of other organisms involves a chronic inflammatory reaction, which causes an immune reaction with the formation of granulomas, typical lesions of chronic inflammation with different histological characteristics. Mullets (Osteichthyes: Mugilidae) represent a widespread species, they are euryhaline fish species capable of living and adapting to any habitat and represent a suitable study model for the development of lesions in the host-parasite interface. In this study 150 mullets, of three different species *C. labrosus* (99/150), *C. auratus /L. aurata* (37/150) and *O. labeo* (14/150), were studied. Initially, dichotomous keys were used to identify the three species. Subsequently, a fresh parasitological examination of the gastrointestinal tract (GIT) was carried out in which, acanthocephalan parasites were found in two specimens of *C. labrosus*, together with some cysts probably attributable to digenean trematodes metacercariae. in two specimens of *C. labrosus.* About 44.66% of the tested specimens were positive for digenean trematodes *(C. labrosus*, 49.5 %; *C. aurata,* 27% and *O. labeo,* 50%). In addition, the present work focuses on identifying the stages of granuloma development from the initial to the final phase of infection, characterizing the immune cells and the non-inflammatory components of the granuloma in the different phases. All mullet specimens were sampled, and the different organs were examined by histological analysis. Granulomas associated with trematode metacercariae parasites were classified into five developmental stages: (1) Free parasite, (2) Encysted parasite,

(3) Early-stage granuloma, (4) Intermediate stage granuloma and, (5) Late-stage granuloma. This staging represents an effort in the knowledge of parasite-related granulomatous inflammation in fish organs as well as an attempt to relate granuloma stages to specific periods of the life cycle of the parasites. Moreover, in this study, a wide range of intra- and interspecific morphometric and morphological features in the otoliths of the three mugilid species has been investigated. In this regard, differences in otoliths among individual species were analyzed and compared. Scanning electron microscopy and stereomicroscopy were used to evaluate morphometric characteristics, variability between pairs of otoliths, and the external crystal structure of the acoustic sulcus. The positive correlation between the ratio of *sulcus acusticus* surface to the entire sagitta and the increase in specimens' size was related to an accentuated sulcal growth, which could depend on species ecology and its adaptation to studied area. Furthermore, in the case of *C. labrosus,* a different morphology has been highlighted from those reported in the literature in fish from the western Mediterranean and Atlantic Ocean, showing a remarkably higher rectangularity, while the circularity was by far lower. *C. labrosus* was the only one species to show a slight difference between the left and the right sagitta, particularly with reference to the acoustic sulcus. These small changes between left and right sagitta are most probably due to ecology and feeding strategies. Morphological differences between specimens from different geographical areas could lead to changes in sagitta among stocks and could depend on the environmental characteristics of Ganzirri lagoon. This study may expand the knowledge of sagitta morphological functionality, fish adaptation to different environmental factors, and give a better understanding of tissue reaction associated with trematodes metacercariae.

DECLARATION

I hereby declare that the results presented are to the best of my knowledge correct, and that this thesis represents my own original work, carried out during the designated research project period, and has not been taken from the work of others save and to the extent that such work has been cited and acknowledged within the text of my work. I therefore had a major role in the study design and execution of the experiments, in sampling, in the acquisition of most data, their analysis and interpretation. The thesis project (2018-2021) was a joint effort of several research teams from different institutes, mainly: The Department of Chemical, Biological, Pharmaceutical, and Environmental Sciences, the Department of Veterinary Science and the Department of Mathematical and Computational Sciences, Physical Science and Earth Science, University of Messina. Moreover, permission has been obtained from the journals to use the data to support the thesis. I am responsible for any eventual plagiarism. This thesis was verified with the software Plagiarism Checker X 2021, showing a percentage lower than 19% following five words check method.

ACKNOWLEDGEMENT

To begin with, I would like to express my sincere gratitude to my supervisor Professor Nunziacarla Spanò and co-supervisor Professor Fabio Marino (University of Messina) for their teachings, support, guidance and valuable advice on all aspects of the thesis. A special thanks to Professor Giovanni Lanteri, Professor Alessia Giannetto and all my colleagues of University of Messina, in particular Dr. Carmelo Iaria for helping out whenever needed, Dr. Serena Savoca, Dr. Gioele Capillo Dr. Claudio Gervasi, Dr. Sergio Famulari, Dr. Giuseppe Panarello and Dr. Fabiano Capparucci for help and advice on the field; Dr. Giovanni De Benedetto, Dr. Claudio Diglio, Dr. Marco Albano in all kinds of laboratory activities and sampling procedures that were essential to the success of this thesis, Dr Jessica Abbate, Dr. Dario Di Fresco and Dr Davide di Paola for their support.

I would like to thank the ARPA Sicilia (general management department state of the environment and ecosystems complex operating unit - sea area) for sharing the parameters of the environmental monitoring date of Ganzirri Lagoon and Torre Faro for the year 2020-2021

Thank you to my family for the support they provided, it was invaluable. I certainly would not be where I am today without their help.

TABLE OF CONTENTS

LEGEND TO FIGURES

Figure 1: Location of the Strait of Messina, in the central part of the Mediterranean Sea, between the Italian peninsula and Sicily. The Strait of Messina can be compared to a funnel that bends the narrowest part to the north, located between Cape Peloro (Sicily) and Torre Cavallo (Calabria), while to the south it gradually opens, the point of conjunction between the Ionian Sea and the Tyrrhenian Sea. FL (Faro Lagoon), GL (Ganzirri Lagoon), SA (Sampling Area)

Figure 2: *Liza aurata* synonymous with *Chelon auratus* (Risso, 1810), a species belonging to the Mugilidae family.

Figure 3: *Chelon labrosus* (Risso, 1827), commonly known as bosega mullet, a species belonging to the Mugilidae family.

Figure 4: *Oedalechilus labeo* (Cuvier, 1829), the gray mullet or skimmer mullet, a species belonging to the Mugilidae family.

Figure 5: Location of the studied area (a,b); particular of Ganzirri Lagoon (c) with sampling point in blue.

Figure 6: Parasitological examination: (a) Stomach and intestines sampling, (b, c) scarping and sedimentation process (d). Glass Petri plate observation by Stereo microscope Discovery.V12 ZEISS with a built-in LEICA IC80 digital camera.

Figure 7: Location of otoliths in the inner ear of fish a) Dorsal view of the vestibular apparatus; b) Otoliths within the apparatus

Figure 8: Representative stereomicroscope pictures of left sagittal otoliths of *C. labrosus* examined in the study. Scale bar: 3mm.

Figure 9: Representative stereomicroscope pictures of left sagittal otoliths of *O. labeo* examined in the study. Scale bar: 3mm.

Figure 10: Representative stereomicroscope pictures of left sagittal otoliths of *C. auratus* examined in the study. Scale bar: 3mm.

Figure 11: Mean and standard deviation (SD) of Wavelet coefficients for all combined otoliths and the proportion of variance among species (black line). The horizontal axis shows angle in degrees (°) based on the polar coordinates of Figure 8b. The centroid of the otolith is the centre point of polar coordinates.

Figure 12: Plotting the quality of Wavelet and Fourier outline reconstruction. The red lines indicate the level of Wavelet and number of Fourier harmonics needed for a 98.5% accuracy of the remodelling.

Figure 13: Specimens positive to Acanthocephala. CL: *Chelon labrosus*, CA: *Chelon aurata*, *OL: Oedalechilus labeo. X-axis: species of mugilidae, Y-axis: number of acatontocephiles*

Figure 14: *Neoechinorhynchus agilis* cranial and posterior end: **A.** proboscis (P), proboscis receptacle (R), lemnisci (L1, L2). **B.** proboscis (P), proboscis receptacle (R), hooks system (H). **C.** *N. agilis* male posterior end: seminal vesicle (SV), saefftigen's pouch (SP), bursa (BU), calotte (CA), genital pore (GP).

Figure 15. Specimens positive to Cysts. CL: *Chelon labrosus,* CA: *Chelon aurata,* OL: *Oedalechilus labeo*

Figure 16: Trematodes found in all the three mullet species, CL: *Chelon labrosus*, CA: *Chelon aurata,* OL: *Oedalechilus labeo* Data are shown as mean± SD. Letters are only present in the case of significant statistical differences. Different letters refer to significant differences between different species. Differences were considered significant when $p<0.05$.

Figure 17: Positivity of the three species to trematodes in the stomach and in the intestine. CL: *Chelon labrosus,* CA: *Chelon aurata,* OL: *Oedalechilus labeo.* Data are shown as mean± SD. Letters are only present in the case of significant statistical differences. Different letters refer to significant differences between different species. Differences were considered significant when $p<0.05$.

Figure 18: Total number of granulomas in *C. aurata, C labrosus and O. labeo.* Data are shown as mean± SD.

Figure 19: Abundance of granulomas in the organs in *C. aurata, C labrosus and O. labeo*. Data are shown as mean± SD. Different numbers represent significant differences between the species. Letters are only present in the case of significant statistical differences. Different letters refer to significant differences between specimens within the same species. Differences were considered significant when $p<0.05$.

Figure 20: Aetiology of granulomas in *C. aurata, C labrosus and O. labeo*. Data are shown as mean± SD. Different numbers represent significant differences between the species. Letters are only present in the case of significant statistical differences. Different letters refer to significant

differences between specimens within the same species. Differences were considered significant when $p<0.05$.

Figure 21: Stage I: Free Larvae H&E stained section of (a) a bile duct (b) intestine. Scale bar = 200 μm

Figure 22: H&E stained section of a a) Stage II, Encysted larva: liver Scale bar = 100 μm. b) and d) Stage III, Early Granuloma, b) liver, Scale bar = 100 μm d) liver, Scale bar = 100 μm. c) Mix of encysted metacercaria and Early Granuloma in the liver. Scale bar = 200 μm

Figure 23: Stage IV, Intermediate Stage: H&E stained section of (a) liver (b) muscle. Scale bar = 100 μm.

Figure 24: Stage V, Late-Stage Granuloma: H&E stained section a) and (b) spleen. c) gills. Scale bar = 100 μm.

Figure 25: Difference stage of granulomas in *C. aurata, C. labrosus and O. labeo*. Data are shown as mean± SD. Different numbers represent significant differences between the species. Letters are only present in the case of significant statistical differences. Different letters refer to significant differences between specimens within the same species. Differences were considered significant when $p<0.05$.

Figure 26: Left sagittae of *C. auratus* with scale bar. (a) Medial view; (b) Lateral view; (c) Mean shape.

Figure 27. Left sagittae of *C. labrosus* with scale bar. (a) Medial viex; (b) Lateral view; (c) Mean shape.

Figure 28. Left sagittae of *O. labeo* with scale bar. (a) Medial view; (b) Lateral view; (c) Mean shape.

Figure 29. Linear Discriminant Analysis (LDA) of the sulcus acusticus computed between the species *C. auratus*, *C. labrosus* and *O. labeo*. The LDA was based on selected *sulcus acusticus* parameters: Sulcus acusticus area, sulcus aucusticus perimeter, sulcus acusticus length, ostium area, ostium perimeter, ostium length, ostium width, cauda area, cauda perimiter, cauda length, cauda width, percentage of the otolith surface occupied by the sulcus (SS/OS, %), percentage of the sulcus length occupied by the cauda length (CL/SL, %), percentage of the sulcus length occupied by the ostium length (OSL/SL, %). 95% probability ellipses are shown.

Figure 30: (a) Mean shapes of left otolith contours. CA is *Chelon auratus*, CL is *Chelon labrosus*, and OE is *Oedalechilus labeo.* (b) Linear Discriminant Analysis plot between the species *Chelon auratus*, *Chelon labrosus* and *Oedalechilus labeo*, calculated on elliptic Fourier descriptors. Ellipses include 95% confidence interval.

Figure 31. SEM imaging of left sagittae proximal surface; (a-d) *C. auratus*; (b-e) *C. labrosus*; (c-f) *O. labeo*. (r) Indicates the rostrum and (*) indicates the dorsal rim.

Figure 32. SEM imaging of left *sagitta* proximal surface in *C. auratus* (a), with details of external textural organization of *ostium* (b), area between *cauda* and dorsal rim (c) and *cauda* (d-e)*;* (r) Indicates the rostrum and (*) indicates the dorsal rim.

Figure 33. SEM imaging of left *sagitta* proximal surface in *C. labrosus* (a) with details of external textural organization of *cauda* (b), dorsal area (c) and *ostium* (d)*;* (r) Indicates the rostrum and (*) indicates the dorsal rim.

Figure 34. SEM imaging of left *sagitta* proximal surface in *O. labeo* (a) with details of external textural organization of *ostium* (b) and *cauda* (c-d-e)*;* (r) Indicates the rostrum and (*) indicates the dorsal rim.

Figure 35. SEM imaging of left *sagitta* proximal surface in *C. labrosus* (a) with details of several calcium carbonates habits in posterior area (b), ventral area (c-g-h), *cauda* (d-e) and *ostium* (f); (r) Indicates the rostrum and (*) indicates the dorsal rim.

Figure 36. SEM imaging of left *sagitta* proximal surface in *O. labeo* (a) with details of several calcium carbonates habits in *ostium* (b), dorsal area (c-e) and *cauda* (d); (r) Indicates the rostrum and (*) indicates the dorsal rim.

Figure 37. SEM imaging of left *sagitta* proximal surface in *C. labrosus* (a) with details of granular crystalline habit in ventral area (b-c); (r) Indicates the rostrum and (*) indicates the dorsal rim.

Figure 38. SEM imaging of large prismatic crystals in *C. labrosus* (a-b-c-d).

Figure 39. Parameters of pH, air temperature (°C), water temperature (°C), salinity (psu), oxygen (mg/l), and oxygen O_2 (%sat) from June 2020 to December 2020.

Figure 40. Parameters of pH, air temperature(°C), water temperature(°C), salinity (psu), oxygen (mg/l), and oxygen O_2 (%sat) from January 2021 to June 2021.

LEGEND TO TABLES

Table 1: Morphological characters of studied species used for taxonomical identification.

Table2: Morphometric mean values with standard deviation (SD) and range of *C. auratus* and *O. labeo* individuals: OL (otolith length), OW (otolith width), OP (otolith perimeter), OS (otolith surface), SP (sulcus perimeter), SS (sulcus surface), SL (sulcus length), CL (cauda length), CW (cauda width), CP (cauda perimeter), CS (cauda surface), OSL (ostium length), OSW (ostial width), OSP (ostium perimeter), OSS (ostium surface), CI (circularity), RE (rectangularity), aspect ratio (OW/OL %), the ratio of otolith length to total fish length (OL/TL), percentage of the otolith surface occupied by the sulcus (SS/OS%), percentage of the sulcus length occupied by the cauda length (CL/SL%), percentage of the sulcus length occupied by the ostium length (OSL/SL%).

Table3: Morphometric mean values with standard deviation (SD) and range of right (R) and left (L) *sagittae* in *C. labrosus* individuals: OL (otolith length), OW (otolith width), OP (otolith perimeter), OS (otolith surface), SP (sulcus perimeter), SS (sulcus surface), SL (sulcus length), SW (sulcus width), CL (cauda length), CW (cauda width), CP (cauda perimeter), CS (cauda surface), OSL (ostium length), OSW (ostium width), OSP (ostium perimeter), OSS (ostium surface), CI (circularity), RE (rectangularity), aspect ratio (OW/OL%), the ratio of otolith length to total fish length (OL/TL), percentage of otolith surface occupied by the sulcus (SS/OS%), percentage of the sulcus length occupied by the cauda length (CL/SL%), percentage of the sulcus length occupied by the ostium length (OSL/SL%). (R = right, L = left).

Table 4: Medium lengths and medium weight of the three species CL: *Chelon labrosus*, CA: *Chelon aurata, OL: Oedalechilus labeo*.

Table 5: Descriptive statistic on morphological data and trematodes occurrence found in the *Chelon aurata specimens*. TL (Total Length), BW (Body Weight), PS (Positive Samples Stomach) PI (Positive Samples Intestine) TT (Total Trematode) TS (Trematode Stomach) TI (Trematode Intestine).

Table 6: Descriptive statistic on morphological data and trematodes occurrence found in the *Chelon labrosus* specimens. TL (Total Length), BW (Body Weight), PS (Positive Samples Stomach) PI (Positive Samples Intestine) TT (Total Trematode) TS (Trematode Stomach) TI (Trematode Intestine).

Table 7: Descriptive statistic on morphological data and trematodes occurrence found in the *Oedalechilus labeo* specimens. TL (Total Length), BW (Body Weight), PS (Positive Samples Stomach) PI (Positive Samples Intestine) TT (Total Trematode) TS (Trematode Stomach) TI (Trematode Intestine).

Table 8: Pearson Correlation results between total length, weight and selected morphometric parameters of *C. auratus, C. labrosus* and *O. labeo*. P= 0.05 value was used to set the significant result., OP^2/OS (circularity), OS/(OLxOW) (rectangularity), aspect ratio (OW/OL; %), the ratio of the otolith length to the total fish length (OL/TL), percentage of the otolith surface occupied by the sulcus (SS/OS, %), percentage of the sulcus length occupied by the cauda length (CL/SL, %), percentage of the sulcus length occupied by the ostium length (OSL/SL, %). ns= not significant.

Table 9: Results of t-test and ANOVA carried out on selected morphometric parameters between left and wright *sagitta* and among left *sagittae* of *C. auratus, C. labrosus* and *O. labeo*. Significant result was set at P= 0.05. OP^2/OS (circularity), OS/(OLxOW) (rectangularity), aspect ratio (OW/OL; %), the ratio of the otolith length to the total fish length (OL/TL), percentage of the otolith surface occupied by the sulcus (SS/OS, %), percentage of the sulcus length occupied by the cauda length (CL/SL, %), percentage of the sulcus length occupied by the ostium length (OSL/SL, %). ns=not significant.

Table 10: Parameters of ph, air temperature(°C), water temperature(°C), salinity (psu), oxygen (mg/l), and oxygen O_2 (%sat) from June 2020 to December 2020.

Table 11: Parameters of ph, air temperature(°C), water temperature(°C), salinity (psu), oxygen (mg/l), and oxygen O_2 (%sat) from January 2021 to June 2021.

1. INTRODUCTION

1.1 Mugilidae

The Mugilidae, commonly known as grey mullets, are a family of teleost fish belonging to the Actinopterygii, a class that groups the highest number of species with the greatest expansion and with remarkable evolutionary lines (González-Castro et al. 2011). They are secondary producers and are positioned at the basis of the food chain as they consume organic particles, debris, and benthic microalgae. They are able to 'telescope' the food chain and produce high quality fish protein available for the top predators (Whitfield et al. 2012). This class of fish which groups the largest number of species, is the most recent in terms of expansion, and it manifests the more notable evolutionary lines toward the slender, that are one of the most ubiquitous teleost families in the coastal waters worldwide (Whitfield et al. 2012). They are found in most temperate, sub-tropical and tropical waters, of both hemispheres. Since this species fits very easily any environment, it often dominates the fish fauna. As a result of this peculiarity, it is possible to find them both in clear and uncontaminated water of the coral reef and in highly turbid estuaries. Not only they can survive in some of the most polluted waters in the world, but they can spend part or even their whole life cycle in coastal lagoons, lakes and/or rivers it depends on the species.

The Mugilids present a characteristic uniform morphology and anatomy; they can reach an average size of 30 cm in standard length (SL) with a maximum size of 120 cm SL. They have two widely separated dorsal fins, the first one consists of four spines and the second one usually shows an unbranched ray (often called "spine") and 6 to10 branched rays. The pelvic fins are sub-abdominal, with a spine and five branched rays. The anal fin has two–three spines and 8 to 12 branched rays. The lateral line is absent, and an adult mullet usually has ctenoid scales. The mouth is of a moderate size, with small (labial) or missing teeth. They have 24–26 vertebrae (Harrison, I. J., Howes 1991); a subcylindrical body; the head is often broad and flattened dorsally (rounded in *Agonostomus* sp. and *Joturus pichardi*) (Serventi et al. 1996). Mullets also possess a characteristic oral and branchial filter-feeding-mechanism involving gill rakers and a specialized pharyngobranchial organ comprising a large, denticulate pharyngeal pad and a pharyngeal sulcus on each side of the pharyngobranchial chamber

(Harrison 2002). The family is widespread in tropical and temperate waters around the globe. Mugilids contain 17 genera divided into approximately 72 species; specifically in the Mediterranean Sea mullets and exotic mullets can be distinguished. They include four genera (Chelon, Liza, Mugil and Oedalechilus) and six species: thick lip mullet *C. labrosus*, golden mullet L. aurata, thin lip mullet *L. ramada*, sharpnose mullet *L. saliens*, flathead mullet M. cephalus, boxlip mullet *O. labeo*, (Cambrony 1980, Hastings 2011, Turan 2014). Taxonomical discrimination among species may be difficult, due to their complicated internal anatomy and external morphology. They are of great importance for professional and artisanal fishing, being of high commercial value, they are fished for food purposes (Marin E. et al. 2003, González Castro et al. 2009, González-Castro et al. 2011, Gallardo-Cabello et al. 2012). They are farmed both in extensive systems, such as more or less limited coastal lagoon areas in Mediterranean regions, and in semi-intensive and intensive systems, often in polyculture together with other species, although still based on the collection of wild fry, as induced spawning it is not practiced commercially. The identification of the species and the taxonomy of mullets have been processed on the external morphology, meristics, morphometrics and the structure of some internal organs. Mullets have a remarkably uniform external morphology and internal anatomy. These features can be observed by using different scales, such as the adipose membrane, that may look like a third eyelid but it is simply a fat deposition on the head around the eyes, which is absent during the lifetime and opaque after the death. This tissue does not develop in newly hatched fish but only when the fish reaches the size of 4-5 cm, after which the covered eye area can continuously increase during their lifetime (*Mugil cephalus*) or remain relatively insignificant as in some species of the genus Liza. The number of pyloric caeca (Perlmutter et al. 1957, Hotta & Tung 1966, Luther 1975), varies among mullet species, and it can be of some taxonomic importance, especially among different genera. The number of pyloric caeca varies within a certain range in specimens of the same species, but it is common to find well-differentiated species of the same genus sharing the same number of pyloric caeca. The shape of the teeth and the pattern of the dentition have been widely employed in taxonomic and systematic studies of mullets (Schultz 1946). In many species, only a single row of teeth develops and this is referred to as primary teeth (Ebeling 1957), but in others there may be several internal rows called secondary teeth. In some species the shape of the primary and secondary teeth is different because the teeth of the distal type are loosely attached to the underlying bone, they are presumably regularly lost and

replaced (Ebeling 1957). The Shape of the Stomach (Thomson 1997) is muscular with a thick wall and carries out mechanical action used to reduce the walls of the alkali insoles cells. The head is often broad and flattened dorsally, a wide variation in shape and size can be observed among Mugilidae species. The mouth is usually small/moderate in size. Lips can be tight or thick, smooth, lamellar or papillate. The upper lip can be terminal or surmounted by a protrusion of the muzzle. The jaw structure belongs to the percoid type, distinguished by the premaxillary having short pedicels and the shaft is broadest at the blade-like distal end (Thomson 1997), (Ghasemzadeh 1998). The number of scales in the lateral and transverse series, the number of scales in the lateral series (Ll) can be counted over the left side of specimens, from the scale located just behind the head, immediately above the insertion of the pectoral fin to the caudal flexure (hypural plate limit). Its number varies approximately from 24 to almost 63. The most relevant characteristics is the first dorsal fin, which is constituted by 4 fins, the first 3 of which are close while the fourth is separated from the others. Each spine is supported by a single basal pterygiophore. The second spine usually ranges from 7 to 10 rays but varies by species, the most anterior ray is a short, thin ray which is often unbranched and segmented only near its tip in adults (Ghasemzadeh 1998) it is very often confused with the spine. The rays of the anal fin also vary according to the species and can range from 8 to 13. Pectoral fins have one spine and 14–20 rays in different genera of mullets. Pelvic fins typically have one spine and five rays. Other very important characteristics for the identification of the species and the taxonomy of mullets are the Preorbital, that changes according to the species and can take a straight or bended curved shape. The nostrils can be variously placed in different species of mullet. The intestinal convolution (Hotta & Tung 1966) and osteology (Hotta & Tung 1966, Sunny 1971, Kobelkowsky & Reséndez 1972, Luther 1975, Senou 1988, Ghasemzadeh 1998), and otoliths (González-Castro & Ghasemzadeh 2016), are the most studied parts among teleost fish's anatomic structures, because they represent a permanent record of their life history. For their species-specific morphology, they are very important for the taxonomic use, representing a useful tool in species discrimination of a large number of bony fishes (D'Iglio et al. 2021). The inner ears are fundamental for vestibular and acoustic functions (the balance and hearing). In the teleost fishes, they consist of calcium carbonate crystals and organic materials of protein origin. The otoliths of teleost fish are basically made up of aragonite crystals. There are three pairs of otolithic organs (three for side), in the inner ear of the fish: the utriculus, the lagena and the

saccule. Each Otolith is characterized by the presence of an epithelium that surrounds it; within it there is an area made up of sensorial cells called the Macula. There is a depression in the otolith called the Sulcus Acusticus**,** which is the related to the sensory macula. Otoliths are found in the back of the fish head. Each otolithic organ is associated with a certain type of otolith. The lapillus is found in the utricle, the asterisk in the lagena and the *sagitta* is found in the saccule. *Sagitta* is the otolith with the greatest morphological variability and therefore it is the most studied. In fishes, the inner ear has two basic functions: the perception of sounds (acoustic function) and the perception of the angular acceleration and gravity (balance function). These two functions correspond to two morphologically different parts. The upper part of the inner ear (utriculus and semicircular canals) mainly controls the balance function. The lower part (sacculus and lagena) is specialized in the reception of sounds. When a sound wave arrives, the otolith acts as a transducer of the wave for the nervous system of the fish. Each teleost species has been reported to be characterized by otoliths with peculiar characteristics (shape and size). The morphology of the otoliths was studied to identify species and fauna fossils, to analyze the diets of fish species from the stomach contents as well as for archaeological research purposes. Furthermore, in the last decades, the otoliths shape analysis has become fundamental in the fisheries management in order to discriminate between the fish stock and the populations, as well as their migration and eco-geochemistry (D'Iglio et al. 2021). Otolith *sagittae* are also used to identify intraspecific and interspecific relationships (establishing affinities and differences between species). The morphological features, shape and crystalline structure of sulcus are increasingly used as a tool to discriminate from different fish stock, species and size-related within population, in relation with the environmental, biological and ecological behavior of the species. First of all, the otoliths morphology has long been mainly used both to discriminate among species and in stomach contents analysis for the preys identification, since they are often the only identifiable components (D'Iglio et al. 2021). Moreover, otolith growth is related to fish growth and any environmental changes in the fish habitat. The variation in the proportions of the components that constitute the otolith causes the formation of growth rings, following a daily and seasonal periodicity (Freeburg 2014). Growth rings are used to determine the age of the fish and they are very useful in the studies on growth, recruitment and mortality, which are necessary for the knowledge on population dynamics. Other current studies focus on the chemical composition and microstructures of otoliths and their relationship with the environment. Also very important

is the morphology of the cephalic lateral line canals (Song 1981), pharyngeal branchial organs (Harrison, I. J., Howes 1991) and the dentition, pigmentation and melanophore patterns in identification of fry and juveniles (van der Elst & Wallace 1976, Cambrony 1980, Reay & Cornell 1988, Serventi et al. 1996, Minos et al. 2002). Depending on the availability of different taxa within each region, harvested mugilids will vary in species composition, but *M. cephalus* is often an important species in capture (Chaoui et al. 2006, Katselis et al. 2006). Adults are mainly targeted by small-scale fishing, while fry and juvenile fish are caught for aquaculture in some areas (Whitfield et al. 2012). Very often they are introduced into inland waters, where they cannot reproduce, since in subjects placed in freshwater basins not communicating with the sea, the gonads degenerate. Egypt is by far the largest producer of farmed mullets, with 84% of world mullet aquaculture production (Gautier & Hussenot 2005)

1.2 Biogeography and Distribution of Mugilidae in the World

1.2.1 Biogeography and Distribution of Mugilidae in the Americas

Most Mugilidae species are found in the Indo-Western Pacific region (Harrison 2002); The family includes about 78 species in 20 genera but 2 in particular (*Liza and Mugil)* represent the 40% of the species within the family (Eschmeyer et al. 2015). The American continent, on the Atlantic and Pacific coasts, hosts 14 recognized species, distributed in five genera: *Agonostomus, Chaenomugil, Joturus, Mugil and Xenomugil* (Eschmeyer et al. 2015). *M. cephalus* and *M. curema* species have a widespread distribution and an unusual amount of variations geographically distant from each other, which certainly complicates the taxonomy of these species (Harrison, I. J., Howes 1991). The south part of the eastern Pacific region is affected by the cold Humboldt Current, also called the Peru Current, which runs along the entire coast of Peru and prevents tropical waters from flowing beyond ~ 30°C (Briggs 1995). The north part of the eastern Pacific region is influenced by the California Current, which moves west of the southern part of Baja California (Briggs 1995). For the West Atlantic region, the eastward projection of Brazil divides the warm southern equatorial current into two branches, the former running south Brazilian Current and remains within the south Atlantic system, the latter flowing northwest, parallel to the shore and accelerating when it meets the flow of Northern Equatorial Current (Briggs 1995).

1.2.2 Biogeography and Distribution of Mugilidae in India, South-East and East Asia

India, Southeast and East Asia host high marine biodiversity, with a hotspot located between the Indo-Malay and Philippine archipelagos (IMPA). The hypotheses of this biodiversity are different such as the high rates of local speciation, a greater accumulation of species formed elsewhere, the presence of refugia and the overlap of a distinct biogeographical ichthyofauna (Bellwood & Wainwright 2002, Carpenter & Springer 2005, Gallardo-Cabello et al. 2012, Hubert et al. 2012, Kulbicki et al. 2015). Recent phylogeographic molecular taxonomic investigations have shown that biodiversity is often underestimated and consequently also the geographic distribution of poorly valued species (Carpenter & Springer 2005, Hubert et al. 2012). Given the scarcity of taxonomic characters, making taxonomy, biogeography and biological research for mugilidae is challenging (Durand et al. 2012). India, South-East and East Asia lie on the intersection of four tectonic plates (the Indo-Australian, Sunda, Eurasian, and the Philippines Sea plates) that have experienced important volcanic activities since Cenozoic (Rangin et al. 1990). For this reason, many of the islands in East and South-East Asia were raised as a consequence of tectonic activities and volcanism providing habitat diversity for marine life and pivotal factors in determining the current distribution of species, particularly in South-East Asia. In this context, molecular studies offer a valid alternative to morpho-anatomic characters, which can highlight both phylogenetic relationships among taxa and species diversity.

1.2.3 Biogeography and Distribution of Mugilidae in Australia and Oceania.

In this area several studies have been conducted on Australian mullets and the descriptions of new genera and species of Mugilidae have been reported. In 1981, the distribution of mullets had remarkably increased between latitudes 65° N and 50° S in Europe, Africa, Asia, Australia and New Zealand, and between 40° N and 37° S along the east coast and between 30° N and 5° S on the west coast of the American continent; whereas *Mugil cephalus* is the only cosmopolitan species, present in between the latitudes 42° N and 42° S in all coastal waters of the world (Thomson 1963). Due to its ubiquity, size and palatability as a food fish, *M. cephalus* is one of the most important fish species, inhabiting thousands of islands in Oceania. Over the years there have been numerous reviews about this topic reporting 27 species

(Ghasemzadeh 1998). Phylogenetic analysis of Indo-Pacific mullets, based on traits derived from external morphology, morphometric and meristic, osteology and splanchnology, suggests that *Cestraeus and Aldrichetta* are the most plesiomorphic taxa in this area.

1.2.4 Biogeography and Distribution of Mugilidae in the Western, Central and Southern Regions of Africa

The African continent has a coastline of 26,000 km which extends from latitude 37°21' N to 34°51' S. This wide latitudinal interval, in addition to the presence of important oceanographic and topographical features, is the main factor responsible for the delimitation of four marine regions: the temperate region of the north-eastern Atlantic, the tropical region of eastern Atlantic, the temperate region of the Southern Africa and the western Indo-Pacific region (Spalding & Phillips 2007). During the Pleistocene, glaciations had a major impact on coastal marine life and distribution due to both sea level lowering and surface temperature changes of the sea. Beyond the physical factors and the physiological tolerance of species, a range of species is also shaped by its evolutionary history. It is therefore evident that the geographical distribution and the genetic structure of a species is given by the evolutionary factors and processes that significantly affect the opportunities for dispersal and determine the demographic characteristics. However, the diversity of Mugilids in the western, central and southern regions of Africa consists of 31 mitochondrial lineages corresponding to 26 morphological species and five putative species, all belonging to 10 genera according to the taxonomic review based on mitochondrial phylogeny (Durand et al. 2012).

1.2.5 Biogeography and Distribution of Mugilidae in the Mediterranean Sea, Black Sea, and North-East Atlantic

The biodiversity of the Mediterranean Sea has a great biological, economic and cultural importance. Approximately 8500 marine species live in the Mediterranean Sea, which corrisponds 4% and 18% of the world marine species, but protection measures, both for species and ecosystems, are still scarce (Bianchi & Morri 2000, Turan et al. 2005, Turan 2014). In the Black Sea a noticeable decrease in native fishes has been reported and related to

eutrophication, overfishing, poaching, and physical destruction of the breeding grounds caused by alien species. The Black Sea is connected to the Mediterranean Sea through the Turkish Strait, which includes the Strait of Istanbul, the Marmara Sea and the Çanakkale Strait. Therefore, the arrival of new species in the Black Sea is precisely due to the connection with the Mediterranean Sea. The effects of Mediterranean water and ballast waters have removed geographical barriers and modified geographic distribution of species, in addition to changes in biological and genetic diversity in the Black Sea (Oğuz & Öztürk 2015). Mugilidae are distributed all over the world, and generally considered important from an ecological point of view and are a major food resource for humans in some parts of the world (Whitfield et al. 2012).They are the target of commercial catch fishing, and they are mainly caught with gillnets, seines, and hooks. They are also grown in some regions of the Mediterranean Sea and Black Sea, mainly in large ponds or limited coastal lagoons. In the Mediterranean Sea mullets and exotic mullets can be distinguished. They include four genera (*Chelon, Liza, Mugil* and *Oedalechilus*) and six species: thick lip mullet *C. labrosus,* golden mullet *L. aurata,* thin lip mullet *L. ramada,* sharpnose mullet *L. saliens,* flathead mullet *M. cephalus,* boxlip mullet *O. labeo* , (Cambrony 1980, Hastings 2011, Turan 2014), distributed in the Mediterranean Sea, whereas the lessepsian keeled mullet *Liza carinata* and the introduced redlip mullet *Liza haematocheila* (Daan 1987, Turan et al. 2005, Kottelat & Freyhof 2007) are found in the Black Sea.

1.3 Biogeography and Distribution of Mugilidae in the Island of Sicily

The Strait of Messina (Central Mediterranean Sea) can be compared to a funnel that splits the Ionian Sea waters in the north from the Tyrrhenian Sea waters in the south, located between Capo Peloro (Sicily) and Torre Cavallo (Calabria) (Fig.1). Although Ionian and Tyrrhenian basins are contiguous, they are physiographically distinct, having waters with different physico-chemical and oscillatory characteristics that determine the onset of peculiar hydrodynamic phenomena. This hydrodynamic conditions are reflected on the conformation of the seabed and on the sedimentation rhythms (Tramontana et al. 1995) favouring the establishment of particular biocenosis (Giaccone et al. 1972, Fredj & Giaccone 1995, Zampino & Di Martino 2000). At the level of the submarine saddle, the stationary currents flow southwards from the surface at 30m and in the opposite direction from this depth towards

the bottom, with speeds that can reach up to 50cm/sec under certain weather-marine situations. The co-oscillation of the water masses of the Strait with the tides of the adjacent seas originates the tidal currents which, with an almost opposite phase and with the same amplitude. The relative velocities reached along the stretch corresponding to the Sella Ganzirri - Punta Pezzo, score maximum values of over 200cm/sec both in the northbound ("rising" current) and in the southbound ("descending" current) current. The hydrodynamic characteristics and the peculiar ecological conditions determine an extraordinary ecosystem for what concerns the variety of species and the biocenoses (Poluzzi et al. 1997). From a wildlife point of view, the Strait of Messina has always been considered as the "paradise of zoologists", due to the enormous biodiversity that characterizes it, (De Domenico 1987). The species of benthic invertebrates are those that arouse the greatest interest. The seabed is enriched by a great variety of shapes and colours given by the abundance of coelenterates (actinia, madrepores and corals). A clear example of this is the forests of yellow and red gorgonians (*Paramuricea clavata*) in the depths of Scilla (Northern part of the Strait). The Strait of Messina represents a crucial point for the migration of numerous species, being along one of the main routes of the Mediterranean (Poluzzi et al. 1997). The migration route of large pelagics fish is of great economic and environmental interest. Other migration routes of ecological interest are those carried out by cetaceans. In fact, the Strait of Messina is what Cetologists call a "Whale Gate", which is an obligatory passage for migrations and displacements.

Torre Faro Lagoon and Ganzirri Lagoon (Northern Sicily) are connected by several canals to the norther part of the Strait of Messina and form two small ecosystems characterized by brackish water, high levels of biodiversity and primary productivity, making them suitable for the exploitation of biological resources and for shellfish farming, an activity that has been practiced for several centuries in both lagoons. The area between Ganzirri and Torre Faro remains one of the most interesting lagoon systems in Italy from a scientific point of view and it is protected by naturalistic and landscape constraints (Poluzzi et al. 1997). Technically, they are brackish coastal ponds which, due to their communication with the sea, represent an environment of transition in dynamic equilibrium with the marine environment. They house specialized flora of brackish humid environments, and they characterize a staging area for migratory birds. Due to its conformation, Torre Faro Lagoon, also represents a rare example of a meromictic basin (Montenat et al. 1987). It is the object of study and research by

international specialists of floristically rich biotopes, with species of *Psammophilus* vegetation with high risk of disappearing, as well as some plant species typical of halophilic environments and coastal sandy coasts, found in few environments of the Mediterranean basin. The Torre Faro Lagoon is included in the area named “Capo Peloro” which is an Oriented Natural Reserve (ONR), established by the Sicilian Region (Southern Italy) with D.A. 21/6/01, as well as a Site of Community Importance (SCI) according to Directive 92/43/EEC and a Special Protection Area (SPA) according to Directive 79/409/EEC. Moreover, these two basins have unique hydrological and environmental characteristics, mainly due to the constant temperature peaks, during specific times of the year (11°C in January and 31°C in August), and due to the presence of a rich flora and fauna. The two lagoons differ mainly in their depth and size. In 1932 several studies were also conducted by the Civil Office of Messina, which it was asserted that the water was unpoluted due to/because of the groundwater crops, emerging in the depressions of the soil located between hills and sea. Flowing from these hills the water gradually became salty due also to the influx of the sea water. Ganzirri Lagoon extends over an area of about 400,000 square meters. It extends 2km long from north to south and over 200m wide, with a depth of 8 m. The Torre Faro Lagoon has a diameter of 665 m and covers an area of 263,600 square meters. The greater volume of water is due to the depth of the lagoon itself, which is approximately 28m in the deepest part. Particularly, Lagoon Ganzirri and Lagoon Torre Faro are connected each other by the Margi canal and with the sea, thanks to the presence of four canals: Canale degli Inglesi, Faro, Due Torri and Catuso. (Bottari et al. 2005), allowing water exchange with the Tyrrhenian and Ionian seas. Differently from Ganzirri Lagoon, the introduction of water here is modest. The water supply is due to the presence of small canals, aquifers and streams that connect it to the sea. Some of these channels, are artificial origin, and date back to the mid-19th century. The entrance of sea water and the following increase or decrease in the levels of salinity of its water depends on the tide and this affecting the oxygen gradient of the lake, In the canals between the two lagoon there is no large water exchange. As a result, we have the creation of two distinct and separate environments, both physically and chemically. Several algal species are found in the predominantly sandy depths of both lakes that decompose in spring because of lack of oxygenation, deriving from the little water supply through the channels, which causes visible agglomerations on the surface. Unfortunately, due to pollution and human neglect, the lakes have undergone serious alterations over the years,

finding themselves in disastrous conditions (Montenat et al. 1987). Over time, and with conscience, an attempt was made to redevelop both areas, through nature trails (bird watching and excursions around the lakes). Regrettably, the little attention paid to these areas in terms of care, maintenance, and investments, has left these wonderful scenarios on standby. It is worth noting that Torre Faro Lagoon has got an unusual and long-studied peculiarity: the presence of hydrogen sulphide gas that, rising to the surface, causes the death of marine organisms. The particular distribution of the gas is linked to the phenomenon of red water, repeatedly found in the lake itself. The flora and fauna of the two lakes are very varied. In addition to mussels (mussels, cockles, oysters, and clams), which for centuries have represented one of the main cultivation activities in the lakes, there are numerous fish families, one of the most common are the Mugilidae which, entering the lakes through the connecting canals. They are an important food resource for man, they are the target of commercial fishing, and are mainly caught with gill nets, seines or beach nets, with nets up to 50 meters long. They reproduce at sea and colonize the waters. Each species migrates towards the channels of the lagoons, according to a precise calendar typical of each species, in the period following reproduction, to colonize the most trophically rich waters. Clarify, the most common sexual species are: *Chelon labrosus, Liza aurata, L. ramada, L. saliens, Mugil cephalus and Oedalechilus labeo* (Genovese 1961).

Figure 1: Location of the Strait of Messina, in the central part of the Mediterranean Sea, between the Italian peninsula and Sicily. The Strait of Messina can be compared to a funnel that bends the narrowest part to the north, located between Cape Peloro (Sicily) and Torre Cavallo (Calabria), while to the south it gradually opens, the point of conjunction between the Ionian Sea and the Tyrrhenian Sea. FL (Faro Lagoon), GL (Ganzirri Lagoon), SA (Sampling Area)

1.3.1 *Chelon aurata* / *Liza aurata*

The golden mullet or lotregano (*Liza aurata* synonymous with *Chelon auratus* (Risso, 1810) (Fig. 2), is a fish of the Mugilidae family. Very similar to *Mugil Cephalus* (common mullet), it has a smaller and narrower head, thin upper lip and a large, very noticeable golden spot on the operculum. It is rather difficult to recognize the three European species belonging to the genus Liza. This is perhaps the easiest to identify due to the golden spot on the operculum, always clearly visible (and often accompanied by another smaller spot closer to the eye). Furthermore, unlike other species of the genus, the black spot on the axilla of the pectoral fins is absent. It has a slender body, with subcircular section in the front, progressively laterally

compressed moving towards the tail. Stocky head, relatively broad, and with a flat upper profile. Scales of the predorsal area extended anteriorly up to the height of the nostrils. Mouth in terminal position. Minute teeth arranged in several series on both jaws, vomer, palatine, and tongue. Smooth and thin upper lip. Maxilla not visible with closed mouth. The upper jaw reaches posteriorly the level of the posterior nostril, the only species of the genus with this characteristic. (Arechavala-Lopez et al. 2012). Rudimentary fatty eyelid. Preorbital with almost straight lower margin and clearly oblique and pointed posterior margin. Fine and numerous gills, the number increases as the size increases. Jugular space of oval shape. Predorsal scales with only one central furrow or without veins. Posterior angle of the pointed preorbital bone. Stomach provided of 6-11 pyloric ceca, of approximately equal or gradually longer length proceeding from the ventral to the dorsal region. Elongated intestine, after the muscular stomach there are several anterior and posterior convolutions. Pectoral fins without axillary process, when folded forward they go beyond the posterior edge of the orbit. Back of ash grey or blue grey colour, paler sides with silvery sheen scales, white belly. On the flanks some dark longitudinal bands are observed. Pectoral spot absent. Very evident golden spot on the operculum and flanked by another smaller one, located behind the eye. Translucent fins translucent, greyish or of the same colour as the back. Peritoneum ranging in colour from dark brown to black (Whitfield et al. 2012). Larvae and fry are recognizable by the presence of rows of dark chromatophores arranged in a herringbone pattern on the sides, and by two dark vertical stripes at the base of the rays of the caudal fin. Euryhaline species, catadromous migratory, is encountered in the sea, in the brackish waters of coastal mouths and lagoons, and in freshwater habitats. In the sea it stays close to the coast, and it is rarely encountered over 10 meters deep. Frequent in lagoons with muddy bottoms rich in coastal vegetation. It goes up the lower reaches of rivers, sometimes inside connected freshwater lakes. The eggs develop in the open sea, the larvae migrate towards the coast, and the fry carry out the trophic phase in shallow coastal waters or in the brackish waters of lagoons and mouths. The optimum water temperature for the species is 23-25 ºC, whereas at 6-8 ºC fish stop feeding and death occurs below 1.5 ºC. Fry can also be found in shallow, warm (up to at 37.5 ºC) water. This species easily adapts to fresh water and withstands saline concentrations up to 57‰, at higher concentrations it suffers from mass mortality phenomena in waters with a salinity of 65‰ or higher. It is a gregarious species; it also forms numerous shoals. After birth, the fry moves to shallow coastal waters or brackish waters for the trophic phase. In the Italian coastal lagoons,

the whipping of the fry takes place from March to June with the maximum number of arrivals between April and May. In the Caspian Sea, where the species was introduced to increase commercial fishing, seasonal migrations occur (Baldwin 2003). When the first colds arrive in autumn, the shoals from the northern and central areas of the basin migrate to the south to winter along the Iranian coasts. Trophic migration to return to the shallows of the central Caspian Sea begins in March, in response to the spring temperature rise. The diet includes a wide range of small benthic invertebrates, plankton, algae, and organic detritus, in fresh and brackish waters also insects, especially chironomid larvae. Adults scrape the periphyton from rocks and anthropic structures, or graze over beds of mud or sand. The ingested material is filtered by the pharyngo-branchial apparatus to extract the food, and, because of these feeding habits, a certain amount of sand is found in the gastric contents of many specimens. In the gastric contents of specimens captured in the southern Caspian Sea, the main elements of food consisted of small bivalve molluscs, foraminifera, and calanoid copepod crustaceans, and to a lesser extent ostracod crustacean, fish eggs, nematodes, worms of the genus Nereis, and crustaceans' cycloid copepods (Ghadirnejad & Ryland 1996). Larvae and fry feed on zooplankton and benthic macroinvertebrates. Adults prefer to live in the neritic zone, which is a shallow marine environment. They enter in the lagoons and avoid fresh water. Juveniles move to coastal lagoons and estuaries in winter and especially in spring. They feed on small benthic organisms, debris and occasionally on insects and plankton. The juveniles feed only on zooplankton. The reproductive season generally runs from September to December, in the Caspian Sea basin (where the species is allochthonous) begins in the central part of the basin in July and ends in the southern areas between mid-October and early November. The scrub takes place in the sea with collective modalities, generally at a depth of above 5 and 10 meters, at water temperatures between 16 and 26 ° C with greater intensity when the surface water reaches a temperature of 20-22°C. The eggs are pelagic and after fertilization, they are carried by the current. Each egg has a diameter between 1.08 and 1.14 mm. The absolute individual fecundity is very high, depending on the size of the female. It ranges from about 113,000 to 1,470,000 eggs, with an average of about 452,000 eggs. At hatching, the larvae measure about 4 mm. They are recognizable by the yellow pigmentation concentrated along the trunk and the dorsal and ventral profiles outlined by black pigments. The sexual maturity is reached at the length of about 20 - 30 cm, the males mature earlier than the females. In natural populations, males are numerically dominant in the lower age groups, while females in the

higher ones. Maximum length reported: 590 mm TL. Generally, most common size: 300mm SL. Maximum age: about 12 years. It is a species subject to viral and bacterial diseases. In February 2004 a strong death was recorded among the specimens of this species present in the waters of the Gilan region (Iran), due to a viral epidemic from betanovirus (Hassantabar et al. 2021). Fish affected by these diseases swim irregularly or belly up and, on post-mortem examination of the internal organs revealed gas accumulation and distension of the swim bladder, yellowish liver with liquefaction of the gallbladder, and hyperaemia of the intestine with excess sand in the cecum. *L. aurata* is a potential host to various species of parasites, such as *Saccocoelium obesum*, parasite of the intestine, and *Microcotyle mugilis* which infests the gills. The presence of monogeneous flukes of the genus Ligophorus was found in the gills of specimens captured in the delta of the river Safid (Iran) (Naem et al., 2002). Specimens of this species prey on many species of carnivorous fish, marine mammals, and ichthyophagous birds. In the Caspian Sea, *L. aurata* is included in the diet of seals *(Pusa caspica*). *L. aurata* is common and locally abundant throughout its distribution area (Dmitrieva et al. 2013). No particular threats to its survival are known. Breeding in captivity guarantees the possibility of replenishing wild stocks. Locally, some populations may decline or disappear due to pollution, as in the case of oil spills from extraction plants or the sinking of oil tankers. In some countries, there are protective measures as a minimum size fishable and fishing-ban periods. Positive effects on the growth of wild populations have been obtained thanks to the bans on trawling along the coasts. In the IUCN Red List (International Union for Conservation of Nature and Natural Resources), *L. aurata* is included among the low-risk species (LC, Least Concern). *L. aurata* also has good commercial importance but breeding is not very widespread in Western Europe. Generally, wild specimens are caught together with other fish and arrive on the market. On the contrary, in the Caspian Sea basin the species is among those most intensely exploited by industrial fishing. In Italy this species is captured together with other mullets. *L. aurata* is also popular among sport fishermen, who target it with various techniques, and among spearfishers. It can be found in the Atlantic coasts from the Azores and Madeira northwards to the British Isles and the southern coasts of Norway and Sweden (but not in the Baltic Sea) and in the whole Mediterranean and the Black Sea (Assis et al. 2018). Moreover, it is present in the south of the Cape Verde Islands, in Senegal, and in the northern part of the Red Sea. It has also been introduced into the Caspian Sea.

Figure 2: *Liza aurata* synonymous with *Chelon auratus (Risso, 1810)*, a species belonging to the Mugilidae family.

1.3.2 *Chelon labrosus*

The mullet or Bosega (*Chelon labrosus Risso, 1827*), (Fig.3) commonly known as mullet bosega, is species belonging to the Mugilidae family characterized by a slender body, with a subcircular section in the anterior part, progressively compressed laterally moving towards the tail. Stocky head, dorsally flattened, relatively broad. Cephalic scales extended from the back to the end of the muzzle. Mouth in terminal position. Small teeth are placed on the upper jaw and vomer. Large upper lip, approximately equal to the diameter of the pupil, and with 2-3 series of horny papillae arranged centrally over 1/4-1/3 of its total extension. Lower lip incised centrally, with both halves joined at an open angle, and a straight or slightly concave margin (Khemis et al. 2013). Maxilla visible with closed mouth. Very reduced fatty eyelid. Preorbital inclined posteriorly and with a straight lower margin. Reduced jugular space. Dorsal scales only one short central dimple. Stomach with 5-8 pyloric appendages of equal length. Two clearly separated dorsal fins. Pectoral fins without axillary process, folded forward, extend to the anterior edge of the eye. Silver grey livery, with a darker back with metallic reflections, lighter sides, and a whitish belly with golden reflections. On the flanks there are 6 to 7 dark longitudinal bands, well-marked. A dark spot is visible at the base of the pectoral fins. Translucent fins, pectoral fins and unequal dark greyish fins with blue or yellowish-brown reflections, ventral fins and anal fin lighter, whitish in colour with more or

764 less marked yellowish-brown reflections. Females reach larger sizes than males. The species
765 reproduces only in the sea (Whitfield et al. 2012). Like all species that possess pelagic eggs,
766 the grey mullet is very prolific, each female can lay about 100,000 to 7 million eggs. Each
767 egg has a diameter ranging from 1.1 to 1.5 mm and has some oily drops inside to favour its
768 buoyancy. At hatching, the larvae measure from 4 to 4.2 mm. Minimum population doubling
769 time, mean: 1.4-4.4 years (K = 0.12-0.17; tm = 3; tmax = 25). Males reach sexual maturity in
770 their second year of life, while females tend to reach sexual maturity one year later. In the
771 northern areas of the range, maturity is reached later, between the third and fifth year of life.
772 The growth rate is relatively high, immature ones can reach the size of 150 mm TL already at
773 class 1+. Maximum length reported: 750 mm SL. Maximum published weight: 4,500 g. Most
774 common size: 320mm SL. Maximum age reported: 25 years. Average age: about 10 years. It
775 is an euryhaline species, catadromous migratory (Boglione et al. 1992). Widespread in the sea
776 along the coasts, in brackish lagoons and in the terminal stretch of rivers, frequent in ports.
777 Of gregarious nature, they often swim in a large shoal. The number of specimens for each
778 shoal is inversely proportional to age and size; in fact, the most numerous groups are formed
779 by immature individuals. The peak movement of the shoal occurs in the central daylight hours,
780 when the sun is at its zenith, but the food activity reaches its peak before twilight and shortly
781 after dawn. Generally, the shoals of adults enter the brackish waters in the spring to feed and
782 return to the sea in the autumn. Some specimens remain at sea all year long, others overwinter
783 in relatively shallow lagoons thanks to their considerable thermal tolerance (from 4 to 37 °C).
784 The fry makes their first entry into the brackish waters from April to June, with maximum
785 arrivals in May. They usually stay until the first colds arrive in autumn. In some cases, when
786 the percentage of dissolved oxygen drops to unsustainable levels in the summer, they move
787 into the sea until the right environmental conditions are restored. The diet includes organic
788 detritus, epilithic algae, diatoms, plankton, and a wide range of invertebrates, in exceptional
789 cases the larger specimens can prey on small fish (Arechavala-Lopez et al. 2012). The
790 opportunistic feeding behaviour of the species can be easily observed inside the harbours,
791 shoals of these fish stationed near the fishing boats to feed on the waste overboard. Mullets
792 are subjected to viral and bacterial diseases; they host several species of parasites. Among the
793 most common parasites reported there are the protozoan *Myxosporidium mugilis*, the
794 trematodes *Microtyle mugilis*, *Tetraonchus vanbenedenii* and *Bedenia monticellii*, and the
795 crustaceans copepod *Ergasilus nanus*, *Caligus bonito* and *Lernanthropus mugilis*,

Lernaenicus neglectus. The main mullet's predators are represented by various species of carnivorous fish, marine mammals and i*chthyophagou*s birds, including the cormorant (*Phalacrocorax carbo*) which annually causes huge losses to aquaculture companies specialized in the breeding of this species. *C. labrosus* is also common and locally abundant throughout its distribution area. No particular threats to its survival are known. Locally, some populations may decline or disappear due to pollution, as in the case of oil spills from extraction plants and the sinking of oil tankers (Brooks et al. 2011). In many countries there are protective measures such as a minimum size to be fished and fishing ban periods. Positive effects on the growth of wild populations have been obtained thanks to the bans on trawling along the coasts. In the IUCN Red List (International Union for Conservation of Nature and Natural Resources), *C. labrosus* is included among the low-risk species (LC, Least Concern) (Reay & Cornell 1988). The species has considerable fishery and commercial interest. It is farmed in aquaculture in many countries. Their meats have different value depending on the place of origin. Specimens caught near drains or in harbours often have an unpleasant taste. The taste of mullets caught in the brackish waters of the valleys is more delicate, even if they often have a slight muddy taste. The highest quality specimens are fished in the open sea. Salted and dried ovaries are used for the preparation of mullet bottarga. Mullets are a very important fish for sport and professional fishing. The most used technique by sport fishermen is fishing with a fixed rod or reel. Professional fishermen catch mullets with pots and other types of nets. *C. labrosus* is among the most common species object of spearfishing.

Figure 3: *Chelon labrosus* (Risso, 1827), commonly known as mullet bosega, is a fish belonging to the Mugilidae family

1.3.3 *Oedalechilus labeo*

The skimmer mullet (*Oedalechilus labeo* Cuvier, 1829) (Fig.4) is another species belonging to the Mugilidae family. It has an elongated body, with a subcircular section in the anterior part, progressively compressed in a lateral direction proceeding in a caudal direction. Head is broad and flattened dorsally. The infraorbital space is almost equivalent in length to that of the oral opening. Mouth in terminal position. Minute teeth are arranged in several series on both jaws. Palate without teeth. Posterior angle of the maxilla strongly curved downwards and visible with the mouth closed. Upper lip thick, devoid of papillae but with a margin formed by a row of densely assembled horny projections. Small horny formations are also present on the lower lip. Presence of Rudimentary fatty eyelid. Preorbital with concave anterior margin and lower margin notched and curved at the bottom. (Boglione et al. 1992). Linear and very narrow jugular space. Internal space without scales. Rudimentary pectoral axillary scale. Dimple-free predorsal scales. Stomach provided with 6 or 7 (rarely 5) pyloric blinds of equal length. Pectoral fins devoid of axillary process, folded forward they reach the level of the posterior edge of the eye or slightly exceed. It also has 45-48 squamosas in series Back livery of ash grey or blue grey colour, clear and silver sides, white belly. On the sides there are some more or less marked longitudinal golden stripes. Pectoral dark spot is absent or barely mentioned. Dorsal, pectoral, and caudal fins are greyish, with shades of the same colour as the back. Ventral fins and anal fin are clear, whitish or semi-transparent. It is a species widespread in coastal marine waters, it does not seem to enter fresh or brackish waters. Of gregarious nature, it forms large shoal generally composed of individuals of the same age and size (Turan et al. 2011). Typical of the coastal strip, it is stationed on any type of seabed. It hardly tolerates variations in temperature and salinity. Compared to other Mugilid species, it is not frequent in harbours with polluted waters. This is a diurnal species, with maximum peak of feeding activity in the twilight hours. Fry and juveniles carry out the trophic phase in shallow coastal waters. The feeding habits vary in relation to the size: the fry have a diet almost entirely composed of plankton and macroinvertebrates, while the adults tend to feed mainly on filamentous algae, together with diatoms, sand and detritus, nematodes,

polychaetas, bivalves and a certain zooplanktonic percentage represented by nauplii of copepods, barnacles and larvae of gastropods. The reproductive period goes from July to September. The scrub takes place in the sea, in surface waters near the edge of the continental shelf, in a collective way. Despite their small size and high fecundity, each female produces several hundred thousand eggs per season. Micromeritic eggs, with a diameter of about 0.75 mm, straw yellow in colour, and with a large oily drop of golden yellow colour. Eggs and larvae are pelagic. Short embryonic development takes about a couple of days. At hatching, the larvae measure about 2 mm. They lead pelagic life for a couple of months, up to 20 - 30 mm in size, then the fry gathers and migrate towards the coast (Hubbs 1976, Matić-Skoko et al. 2012). The scrub occurs only once a year. The minimum time of population doubling average 1.4-4.4 years. In both sexes, sexual maturity is reached at the age of about two. Maximum length reported: 250 mm TL. Generally, most common size: 200mm TL. It is a species subject to fungal infestations (*Ichthyophonus* sp.) and bacterial (streptococcosis, epitheliocystitis, edwardsiellosis) diseases. Host of various species of parasites, such as protozoa, flukes, and crustaceans. *O. labeo* is a prey of many species of carnivorous fish, marine mammals, and ichthyophagous birds. No particular threats to its survival are known. Locally, some populations may decline or disappear due to pollution, such as oil spills from oil rigs and the shipwreck of oil tankers. In some countries, protective measures exist as a minimum measure and periods of prohibition. The species is not included in the IUCN (International Union for Conservation of Nature and Natural Resources) Red List. It is also a kind of very modest interest, only occasionally present on the Italian markets. Its meats are of good quality, but the small size does not make it economically attractive. It is marketed fresh, frozen, smoked, salted, and dried. Professional fishing is carried out with seines, gillnets, and with jackets in the slums. Due to its small size, it has no particular interest for sport fishermen.

Figure 4: *Oedalechilus labeo* (Cuvier, 1829), the grey mullet or skimmer mullet a species belonging to the Mugilidae family.

1.4 Parasites and diseases of Mullets

The breeding of Mugilidae in fresh water, brackish water and sea water is constantly increasing, accordingly, the presence of diseases and parasites in confined fish has become evident. History has already shown that diseases and pests play a significantly damaging role in aquaculture, and disease outbreaks have been one of the main obstacles to the expansion of the sector. Comprehensive data on mullet culture and associated pests depend mainly on large-scale polyculture of mullet with carp and tilapia in fresh and brackish water ponds in Israel (Lahav & Sarig 1967, Paperna & Lahav 1971, Sunny 1971, Paperna 1975). Although spawning can be induced on an experimental basis, mullet rearing still depends on fry or fingerlings from natural waters. This, combined with the behaviour of the mullet, favours the spread of disease, whose transmission can occur in the water or through intermediate hosts. Infection can also be introduced by infected individuals. Once in the system, many pathogens can reproduce easily. Epizootic diseases with infectious bacteria can cause massive mortality in fish. Typically, such a disease persists for long periods, spreads from area to area and affects selected host species. *Achromobacter aquamarinus* and two *A. superficialis* strains were isolated from Mugil while *Escherichia intermedia*, *Achromobacter sp.* and four strains of *Aeromonas salmonicida* were isolated from fish without disease symptoms (Almeida et al.

1968). It was also observed that some severely injured mullets could have been directly or secondarily infected by bacterial organisms. Very often, *Pseudomonas* sp. has been isolated from lesions, from the liver and often from blood. Bullock et al. discussed several bacteria and variables in infectious bacterial diseases, some of which are likely to affect mullets. Bullock and Lewis have provided methods on how to cultivate and identify suspected pathogens (Bullock et al. 1974, Lewis et al. 1976). Secondary bacterial infections often follow ectoparasite infestations. Some of the bacteria recognised in fish are *Aeromonas hydrophilia, Mycobacterium marinum, M. fortuitum, Vibrio parahaemolyticus, Erysipelothrix rhusiopathiae and Leptospira icteroemorhagiae*. They can also cause disease in humans; for instance, Mugilidae could also act as vectors for cholera, salmonellosis, shigellosis, and presumably many other diseases. *Vibrio parahaemolyticus*, one of the commonly encountered and best studied marine organisms, causes bacterial food poisoning in thermal climates all over the world. Both the organisms and the enterotoxins responsible for the disease can be destroyed by heating at 60°C for five minutes. Most bacterial diseases that could be contracted can also be avoided simply not eating raw food. Another problem that affects the mugilids can be the aquatic mold *Sparolegnia sp*. (Lahav & Sarig 1967), which infects mullets stored in freshwater ponds. This fungus attacks mostly freshwater fish, especially those with an injured integument, as it happens after handling. Infection also occurs mainly in ponds rich in organic matter, such as heavily fertilized ponds. This problem can be eliminated with a low concentration of salt or with a variety of other treatments (Teichert-Coddington et al. 2017). Protozoa infects all mullet species internally or externally and occasionally causes disease that can be followed by death. Among the flagellates those that most affect the mugilids are *Sarcomastigophora, A. ocellatum, Oodinium cyprintum* (Rawson 1973). The parasitic dinoflagellate *Amyloodinium ocellatum (Brown) Examita sp.* have been found in the intestinal epithelial tissue of some young *Mugilidae.* The Trematodes are very frequent in mullets that can represent an intermediate host. They are a class of worms belonging to the phylum of the Platelminti *(Platyhelminthes),* a few centimeters long, with a flattened or cylindrical body. They characterized by suckers or hooks with which they adhere to the host. They can be divided into monogeneous and digenei, depending on how many hosts they have in the biological cicle. The best-known species is *Fasciola hepatica*. Like all Platelminti, Trematodes are acelomates and aprocti. All of them ore more or less endoparasites. They are believed to derive from ancestors similar to the current rhabdocelids (turbellars with

rectilinear cavities). They are hermaphrodites with indirect development. Compared to turbellars, they show structural modifications such as: loss of epithelial cilia, greater development of glandular cells, presence of structures that allow the parasite to adhere to the host (suckers, hooks or both) - loss of the eyes. Other parasites very frequent in the mugilidae are *Microspora and Myxospora*, small unicellular spores containing a single protoplasm that extrudes through an everted polar filament into a host cell. Many of these develop inside a pan sporoblast and the visible cyst includes an enormous number of spores. Microsporidans are unicellular organisms but can be formed by one or more sporoplasms, from one to three valves and from one to six polar capsules containing extrusable filaments. The spores are about the size of a human red blood cell and can sometimes be seen with the naked eye when they are more than one. In most species that infect mullet, the spores have two polar filaments and two valves, after separation of the valve sutures, sporoplasm exits and undergoes division, both in a bladder and between tissues. The most frequent species are: *Myxobolus spp.* and *Ellipsomyxa mugilis.* Many of the species that are present are hosts of parasites, including *Myxosporidium mugilis*, gill parasitic protozoan, *Microtyle mugilis* flukes, *Tetraonchus vanbenedenii* and *Bedenia monticellii*, which affect the gills, or copepod crustaceans, among the most common ones we can highlight *Ergasilus nanus*, *Caligus bonito* and *Lernanthropus mugilis* affecting the gills, *Lernaenicus neglectus* on the skin and *Branchiella oblonga* which settles on the axilla of the pectoral fins. The most common pathogens in Mugilidae, which can be zoonotic, are *Heterophyes heteropyes* and *Mycobacterium* sp. The former is a zoonosis that occurs only by ingestion while mycobacteriosis occurs also by contact. It was described by (Belousova 2019) the first case of a fluke larva of the genus *Haplosplanchnus* (Loss, in 1902), which was first recorded in the Black Sea in the gastropod mollusk *Hydrobia acuta* (Hoeksema 1998). This gastropod species was first indicated for the first time as a probable second intermediate host. *Haplosplanchidae* (Poche, 1926) is a small family of trematodes, which includes nine genera: *Haplosplanchnus* (Looss, 1902), *Schikhobalotrema* (Skrjabin et Guschanskaja, *1955), Hymenocotta (*Manter, *1961), Haplosplanchnoides (*Nahhsnuplanus, 195*5), Psuschanplanus (*Protangoplanus, 1955) *Hymenocotta (*Manter, 1961*) Provitellotrema* (Pan, 1984*), Discocephalotrema (*Machida, 1993) and *Parahaplosplanchnus Nahhas*, (Rhodes et Seeto, 1997) (Turan et al. 2005). Despite the fact that these helminths are widespread among marine and estuarine fish in the tropical and subtropical zones of the world's oceans, any information on the life cycles of the representatives of this family is

fragmentary and concerns only two species: *Schikhobalotrema acuta* (Linton, 1910) and *Haplosplanchnus pachysomus* (Eysenhardt, 1829) Looss, 1902 (Cable & Hopp 1954, Saad-Fares & Maillard 1985). The life cycle of the latter species has been studied in the Mediterranean Sea. The gastropod mollusk *Hydrobia ventrosa* (Dall et al. 2011) is indicated as an intermediate host, and is a prey of Mugilidae, which, according to the authors (Saad-Fares & Maillard 1985), become infected by eating detritus with adolescariae.

1.4.1 *Heterophyes heterophyes*

Adults of *Heterophyes heterophyes* are minute flukes, measuring 1-2 mm in length. The surface of the worm is covered with minute spines. Adults reside in the small intestine of the definitive host. At least 36 genera are known within this family, and among them, 13 genera are known to be zoonotic (Chai & Jung 2017); *Metagonimus, Heterophyes, Haplorchis, Pygidiopsis, Heterophyopsis, Stellantchasmus, Centrocestus, Stictodora Procerovum, Acanthotrema, Apophallus, Ascocotyle,* and *Cryptocotyle*. Flukes of Heterophyes are characterized by the presence of a genital sucker and armed gonoty (Chai & Jung 2017). The genus Heterophyes was raised by (Spencer Cobbold 1866) with *Heterophyes aegyptiaca* as the type; later this was synonymized with *H. heterophyes* (Witenberg 1929). This species was first discovered by Bilharz in 1851 during an Egyptian autopsy in Cairo (Chai & Draxler 2014). It is now known to cause human infections along the Nile Delta in Egypt and Sudan, the Middle East, Southeast Europe and India (Yu & Mott 1994, Chai et al. 2005, Pica 2005). Adult flukes are minute in shape, from ovoid to elliptical, elongated or piriform (Witenberg 1929). They show unique morphological peculiarities such as the presence of two testicles side by side near the posterior end of the body, a large median ventral sucker and a large submedian genital sucker armed with 70-85 chitinous rods on the gonotyl (Chai et al. 2005, Chai & Draxler 2014). Adults release embryonated eggs, each with a fully-developed miracidium, and eggs are passed in the host's faeces. After ingestion by a suitable snail (first intermediate host), the eggs hatch and release miracidia which penetrate the snail's intestine. Genera *Cerithidia* and *Pironella* are important snail hosts in Asia and the Middle East respectively. The miracidia undergo several developmental stages in the snail, sporocysts, rediae, and cercariae. Many cercariae are produced from each redia. The cercariae are released from the snail and encyst as metacercariae in the tissues of a suitable fresh/brackish water fish

(second intermediate host). The definitive host becomes infected by ingesting undercooked or salted fish containing metacercariae. After ingestion, the metacercariae excyst, attach to the mucosa of the small intestine and mature into adults (measuring 1.0 to 1.7 mm by 0.3 to 0.4 mm). In addition to humans, various fish-eating mammals (e.g., cats and dogs) and birds can be infected by *Heterophyes heterophyes (Taraschewski, 1984)*. Human and animal infections have been reported in Egypt, Sudan, Greece, Turkey, Palestine, Italy, Tunisia, India and the Middle East, including Saudi Arabia, Iran, Iraq, United Arab Emirates, Kuwait and Yemen (Yu & Mott 1994, Chai & Draxler 2014, Huval et al. 2015). An estimated 30 million people are infected with this fluke (Mehlhorn et al. 2015). In Egypt, human infections are commonly found in the north of the Nile Delta, particularly around lakes Manzala, Burullus and Edku, where fishermen and pets often consume fish (Yu & Mott 1994, Youssef & Uga 2014). In experiments with dogs and cats infected with *H. heterophyes*, involvement of Peyer's patches and mesenteric lymph nodes by adult flukes was frequently observed (Hamdy & Nicola 1980). In avian hosts, such as gulls, flukes frequently invade extraintestinal or somatic tissues and organs, particularly the liver, pancreas and bile duct (Chai & Draxler 2014). The host's immune responses against flukes or their excretory secretory products (ESP) may be too strong (hypersensitive) that the host's immunity can harm the host itself (Chai & Draxler 2014). The affected mucosa can undergo hypersensitivity and allergic reactions, including severe catarrhal inflammation and villous loss (Chai & Draxler 2014). Elevated levels of IgG, IgM and IgE were found in sera from humans infected with *H. heterophyes* (el-Ganayni et al. 1989, Fullwood et al. 1999). Elevated levels of IgG, IgM and IgA have also been reported in the intestines of infected humans (el-Ganayni et al. 1989). Pathogenicity, host-parasite relationships and clinical manifestations in each species infection are poorly understood but proper prevention and attention is needed.

1.4.2 Mycobacteriosis

Mycobacteriosis is a chronic progressive disease caused by several acid-fast bacteria of the genus Mycobacterium affecting wild and cultured fish worldwide (Yam et al. 2009). These mycobacteria are saprophytes from soil and waters, where they can live for years. In particular, *M. marinum* is a bacillus ubiquitous in nature, forming the largest portion of all mycobacteria isolated from fish (Decostere et al. 2004). The economic impact on the fish

industry due to mycobacteriosis may be underestimated because of the long incubation period of the disease and its chronic nature. Mycobacteriosis is a common disease of wild and cultured marine, brackish and freshwater fish (Decostere et al. 2004). Mycobacteria are widespread all over the world, especially in aquatic environments. Simply a small fraction causes diseases in animals and humans. In humans, it causes the formation of granulomas in the skin, especially on the extremities of the limbs (Bignal & McCracken 2000, Grodzinski et al. 2001, Carballo et al. 2003), sporadically, involves the deeper tissues, resulting in tenosynovitis, bursitis, arthritis and osteomyelitis (Piersimoni & Scarparo 2009). In immunosuppressed subjects these bacteria are able to cause disseminated infections, sometimes serious, with lymph node, bone, pulmonary and skin involvement (Ghittino & Bozzetta 1994, Requena et al. 1998, Oda et al. 2002). This risk is more concrete for aquarists and for those who work in pet shops or aquaculture farms. The most frequently isolated species in fish are *M. marinum, M. chelonae and M. fortuitum* (Gautier & Hussenot 2005) however they have been isolated in individuals with no symptoms or lesions attributable to Mycobacteriosis (Bozzetta et al. 1995) (Sala et al. 2003, Prearo et al. 2004). Many other species, such as *M. shottsii, M. pseudoshottsii and M. salmoniphilum* (Gauthier et al. 2015) *M. marinum, M. chelonae and M. fortuitum* are also frequently associated with human infections (Decostere et al. 2004). From the point of view of the zoonotic impact of this species, it is necessary to report that hand infections caused by *M. abscessus*, previously considered rare and found almost exclusively in immunocompromised individuals, have recently been reported in two cases in immunocompetent individuals. *M. abscessus* is also potentially responsible for causing severe chronic tenosynovitis even in immunocompetent subjects (Prisic et al. 2010). Among the many mycobacterial species isolated from fish tissues, the most commonly detected are *Mycobacterium marinum, M. chelona and M. fortuitum*, infecting more than 150 species of fresh and saltwater fish (Zanoni et al. 2008, Lewis & Chinabut 2011). No external signs often appear before until advanced stages of the disease are evident. These non-specific signs include emaciation, haemorrhages and dermal lesions, and abdominal swelling (Gauthier & Rhodes 2009). The chronic proliferative form of the disease is characterized by granulomas, while the subacute form is associated with necrosis and acid-fast bacilli scattered diffusely in all affected tissues, including kidneys, liver, spleen and often all visceral organs (Ferguson et al. 2006). One of the major difficulties in the identification of mycobacteria at the species level is the time required for isolating them and

biochemical characterization of the organisms. The Mugilids are coastal and brackish marine species and are distributed in all temperate and tropical seas (Griffith et al. 2006). They are a major food source in different regions of the world. Acid-fast bacterial infections in wild Mugilids are scarcely reported worldwide: (Antuofermo et al. 2017) observed several cases in *Liza aurata* from Libya; (Fernandez & Dias 2013) in a single *Mugil curema* from Brazil; (Antuofermo et al. 2017) in an adult *Mugil Cephalus* from the Gulf of Mexico; and, more recently, (Varello & Carrera 2014) in a number of Italian species. Furthermore, fish mycobacteriosis was also detected in cultured mullets (Salati & Moore 2010). Moreover, mycobacteriosis in fish has not been properly investigated by the simultaneous application of histopathological, bacteriological and molecular biology methods (Pourahmad et al. 2014, Şeleci et al. 2015). Therefore, this disease is often underdiagnosed and information on its effects on farmed fish is rather limited (Antuofermo et al. 2017). This pathology therefore requires attention not only because it suggests the need for a greater monitoring effort to determine the welfare state of farmed fish but, above all, for the potential zoonotic implications that this disease can have for fisheries and aquaculture operators.

1.4.3 Hydrobia

Hydrobia is a gastropod mollusc belonging to a family that includes species that live in fresh and brackish waters. They are very small brackish water snails with a gill and an operculum. *Hydrobia acuta* is a very small (4-6 mm) species of brackish water snail with oval-oblong shell, slightly conical, sharp in the upper part transparent, smooth, even if marked to read observed under a microscope. In nature it is greenish in colour. The shell has six or seven coils. The opening is oval and the peristome is simple with little pronounced umbilical fissure and a thin and smooth operculum. *Hydrovia ventros* is present throughout the Mediterranean Sea. It is probably the most common euryhaline between the Mediterranean gastropods. It is not uncommon to find it, with considerable population densities, even in the first concentration tanks of the salt pans where salinity level is at least double of the normal marine values, while, on the other hand, its presence characterizes very desalinated lagoon and estuary environments. It is often found on *Ulva* sp. Small, elongated shell with five convex coils and deep suture. Semi-transparent, it is whitish in colour. Maximum published size and age: Maximum length between 4 mm and 5 mm. The gastropod *Hydrobia ventrosa* (Dall et

al. 2011) is indicated as trematodes intermediate host, and fish of the family Mugilidae become infected by eating them (Galaktionov & Skirnisson 2007).

1.5 Mugilidae as a Bioindicators

One of the greatest challenges that humanity must face is the preservation of the environments. The effects of global change are having a huge impact on the ecosystems. To achieve an integrated management, scientists and ecologists must select relevant indicators that could be used as bioindicator for the health status of coastal areas. These indicators are usually selected among living species or physico-chemical parameters or a combination of both. Very few fish species have characteristics able to fulfil this function. A particular species of Mugilidae satisfies this function: The *Mugil cephalus* (Whitfield et al. 2012). This well-known species lives in all tropical, subtropical and warm temperate coastal zones and it is able to adapt to different habitats. This organism is used because it is a flat-headed fish and is distributed all over the world, from tropical to temperate seas. It is also of great commercial importance for fishing, especially in developing countries. *Mugil cephalus* is diadromous and often migrates between continental and marine environments during its life cycle. It possesses several characteristics required in a sentinel or indicator species, such as wide tolerance to salinity and temperature, which allows it to populate most of the coastal waters. Juveniles and sub-adults grow in freshwater and/or estuarine habitats, but adults undertake offshore migrations for spawning, usually grouped in large shoals (Bacheler et al. 2005). Between 2006 and 2009 the European Union funded the project *"MUGIL Project" (Main Uses of the Gray mullet as an Indicator of Littoral Environmental Changes), (INCO-CT-2006-026180)*. The aim of this project was precisely to create a collaborative network around the world using *M. cephalus* as an indicator of the state of coastal environments and to standardize methodologies for further studies. The project covered four global areas (Europe, Africa, Asia and America) and involved collaborators from southern Europe (Spain, France and Greece) and from subtropical and tropical countries (Mexico, Senegal, Benin, South Africa and Taiwan) (Panfili et al. 2016). Among the tools available to study fish migration, otolith microchemistry has proven to be one of the most effective tools for studying habitat occupation between freshwater and seawater environments by diadromous fish (Tomás-Zapico & Coto-Montes 2005, Ohji et al. 2007). In the absence of detailed studies on the use of the saline habitat by *M. cephalus* in

other parts of the world, otolith microchemistry is a very efficient approach to determine the migratory habits of this species which is seasonal, usually occurring when the water temperature is appropriate for breeding, although this too appears to be highly variable from area to area (Whitfield et al. 2012).

2 AIM OF THE PRESENT THESIS

The general aim of this study was to investigate the ecological and health condition of mugilid population in ONR Capo Peloro. The research activity was divided into three objectives:

Research objective 1: Identification of five stages of granuloma development from early to late stage: Stage I - Free parasite as without tissue reaction; Stage II - Encysted parasite as intact encysted metacercaria or spore-containing plasmodium; Stage III - Early stage as inflammatory cells and partially degenerated larvae; Stage IV - Intermediate stage granuloma as layers of flattened cells surrounding the degenerated parasite and necrosis; Stage V - Late-stage granuloma increased layers of epithelioid cells around the inner core, and the outer sheet with large fibroblasts.

Research objective 2: Study of otolith morphology, inter and intra-specific variability within Mugilidae *sagittae,* analyzing and comparing their morphology, morphometry, shape, and externa textural organization among the three species sampled: Golden grey mullet (*Chelon auratus*, Risso, 1810), Thicklip grey mullet (*Chelon labrosus,* Risso, 1827) and Boxlip mullet (*Oedalechilus labeo,* Cuvier, 1829).

Research objective 3: Parasitological study on stomach and intestine for pathogen identification

3 MATERIALS AND METHODS

3.1 Sampling

Specimens were sampled from the northern area of the Strait of Messina, Ganzirri Lagoon 38°15’41’’N, 15°37’35’’E (Fig.5). They were fished over several days using throwing nets also known as sparrow hawk or “rezzaglio” (ARPA Sicilia authorization n.1138/A of 15.03.2021) which is an ancient circular fishing net, tied to a rope in the central part. It is collected with the hands using a precise procedure that favours its subsequent opening at the time of use. Once collected, it is thrown into the water with the help of the torso twist. The weights positioned in the external perimeter make the net to fall quickly parallel to the surface, while the centre that has no additional weights can also remain on the surface of the water (depending on the mesh of the net, the tighter the mesh is the slower it sinks). Thus, a large cone is formed which has the perimeter as its base and the centre of the net as its vertex, preventing the fish from escaping. The net is recovered by means of the rope tied to the centre of it, that closes the base of the cone and forms a sort of bag in which the fish are caught. The fish were transported to the Experimental Fish Pathology Centre (Centro di Ittiopatologia Sperimentale della Sicilia – CISS), Department of Veterinary Sciences, University of Messina, Italy. CISS has been accredited since 2006 for the use and since 2010 for production of aquatic organisms for experimental research (DM n°39/ March/2006). The fish included in this work are not part of an experimental challenge, but all samples were used for diagnostic purposes commissioned by fish farmers, aimed at controlling fish diseases. For this reason, the approval of the ethical committee was not necessary, although all the treatment of animals was performed according to European and Italian guidelines on animal welfare. The analysis conducted does not fall under the provisions of Legislative Decree No. 26/2014, implementing European Directive 2010/63/EU of the European Parliament, as any waste material was used for diagnostic purposes, and therefore not regulated by the laws on animal experimentation. Therefore, the fish were placed in optimal conditions respecting the animal welfare.

Figure 5. Location of the studied area (a,b); particular of Ganzirri Lagoon (c) with sampling point in blue.

3.2 Specimens Identification

Initially the specimens were weighed, measured, and using dichotomous keys, species identification was carried out. For species identification the head was evaluated first because it is the most informative organ from a taxonomic point of view, normally employed in any identification key of the mullet. Although the head is often broad and flattened or slightly convex dorsally in mullets, a wide variation in relative shape and size can be observed among

Mugilidae species. The positional relationships between different anatomical elements such as jaws, nostrils, lips, eyes, opercular and preorbital bones, jugular space, and also their shape and size generate a variety of information useful for taxonomic identification. For a good identification of the species, we have also evaluated the number of spines and rays of paired and unpaired fins and the number of scales in the lateral series, it can be counted on the left side of the specimens, from the scale located just behind the head. Its number varies from approximately 24 to nearly 63, although sometimes different species have the same number. To have a better confirmation of the species, at the time of necropsy the pyloric caeca were taken. Normally their number varies within a certain range in specimens of the same species, it varies from 3 to 48, but more often from 5 to 10, even if it is normal to find well-differentiated species of the same genus that share the same number of pyloric blinds (Table1). Finally, the Otoliths were eventually extracted.

C. auratus	*C. labrosus*	*O. labeo*
Pure gold stain on the operculum	Jugular space very short, straight, delimiting a very narrow oval space	First anal fin with 3 spiny rays close together and 11 soft rays
Scales on head not extending beyond eyes	Upper lip very deep, larger than pupil, with 3-4 sets pf papillae	Upper lip deep more than pupil diameter with fine labial fold
Rudimentary adipose eyelid	5 pyloric caeca of equal length, rarely 6 or 7	Rudimentary adipose eyelid
Dorsal scales with a dimple	Dorsal scales with a dimple, unique and short	Dorsal scales without dimple
Space between the two nostrils devoid of scales		Space between the two nostrils devoid of scales

Table 1. Morphological characters of studied species used for taxonomical identification.

3.3 Histological Examination

The necropsy examination was conducted at the University of Messina at the Department of Chemical, Biological, Pharmaceutical and Environmental Science. At a first external examination the specimens appeared to be in good health, only some of them presented a gill pallor. The internal organs (heart, spleen, liver, gills, kidney) were removed from the fish and fixed in a 10% neutral buffered formalin for about 72h. After fixation the samples were

washed in running water and dehydrated with a battery of increasing alcohol (70, 80, 90 Absolute 1 and Absolute 2) and xylene and finally paraffin embedded. Sections of 5 µm thickness were obtained with a microtome (EG11504 Leica Biosystems). Sections were stained with haematoxylin and eosin (H&E); selected sections were also stained with Ziehl-Neelsen method (ZN). The granulomas in a visceral organ were evaluated according to the parasite class involved. They were classified in five time-dependent stages, based on the evaluation of selected histological features i.e., based on the state of parasites, necrosis, cellular components and layers formation. Stage I Free Parasite, without tissue reaction. Stage II Encysted Parasite, intact encysted metacercaria or spore-containing plasmodium. Stage III Early-Stage Inflammatory cells are observed. Stage IV Intermediate stage granuloma Stage V Late-stage granuloma, encircling layers of epithelioid cells increased around the inner core. The stomach and intestine were sampled separately as it was difficult to proceed with histological analyses as being organisms that feed on muddy plain biofilms, and associated meiofauna. The final yield did not satisfy the preparation. Therefore, they were first freshly sampled, and parasitological analyses were performed, with the use of cones and after emptying, fixed in a 10% neutral buffered formalin, for histological examination.

3.4 Parasitological Examination

External evaluation of gills and internal organ surface was performed for each specimen to investigate the presence of parasites by a Leica M205C stereomicroscope with a built-in LEICA IC80 digital camera and a organs and gills biopsy was also performed to evaluate the microparasite presence, gastrointestinal (GI) tract was inspected for helminths. The stomach and intestine were opened by scissors and the total gastric and intestinal mucosa was scraped with the aim of a microscope slide. The GI content and mucous was transferred into 1l graduated conical beakers and filled with water for the subsequent sedimentation phase, all the supernatant was replaced every hour to purify the sediment. After 2 or 3 water changes, according to the supernatant clearness, the sediment was transferred in a Petri plate to perform the Total Worm Count technic (TWC) (Arundel 1967), with the aim of the stereomicroscope. Some found parasite specimens were stored in 70% ethanol until morphological evaluation.

Other specimens were stored at -80° for subsequent molecular analyses (Fig.6). All found parasites were mounted on a microscope slide with a glycerin drop, covered by a coverslip, clarified for 24 hours, and then identified with keys suggested by (Yamaguti 1970)

Figure 6: Parasitological examination, (a) Stomach and intestines sampling, (b, c) scarping and sedimentation process (d). Glass Petri plate observation by Leica M205C stereomicroscope with a built-in LEICA IC80 digital camera.

3.5 Hydrobia identification

A Discovery V12 stereo microscope with built-in LEICA IC80 digital camera was used to observe the gastropods and the Hydrobia species was identified using dichotomic keys.

3.6 Molecular analysis

The samples were collected into Eppendorf, three series of 20 minutes washes were performed with a PBS buffer solution (Phosphate Buffer Saline). The samples were purified, and the DNA was extracted using a Wizard SV Genomic DNA Purification System (Promega).

Concentration and purity were verified using the Nanodrop spectrophotometer (Thermo Scientific). The PCR was performed using a GoTaq® Colorless Master Mix (Promega) and different primers have been used for trematodes identification: 28S, ITS-2, cox1 and 18s. The 28S DNA (y673 bp) forward primer 5' GTCCGATAGCGAACAAGTACCGT 3' and reverse primer 5' AGCATAGTTCACCATCTTTCGGGTCTCAA 3'; for the partial ITS-2 (y1.5 kb) forward 5' GTCGTAACAAGGTAGCTGTA 3' and reverse primer 5' TATGCTTAAGTTCAGCGGGT 3'; and for the mitochondrial cox1 (y800bp) was amplified by forward primer 5' TTTTTTGGGCATCCTGAGGTTTAT 3' and reverse primer 5' CAACAAATCATGATGCAAAAGG 3' (Mladineo et al. 2010). While the different 18S DNA oligonucleotide primer sets used were: Trematodes C-For ATGGCTCATTAAATCAGCTAT, Trematodes A-Rev TGCTTTGAGCACTCAAATTTG, Trematodes. C-for + A-rev (800 bp) were found to be specific for trematodes due to its higher polymorphism among trematode species. Each of the specific oligonucleotide primer sets amplified different regions of the 18S rDNA. (Routtu et al. 2014). The thermal cycling conditions were the following: for 28S rDNA consisted of initial denaturation for 30 s at 94°C, 35 cycles of denaturation for 30 seach at 94°C, annealing at 58° C for 30s, elongation for 60 s at 72° C with final extension of 10 min at 72° C. For ITS 2 and cox1: initial denaturation for 30 s at 94° C, 35 cycles of denaturation for 30 seach at 94°C, annealing at 56°C for 90s, elongation for 90 s at 72° C with final extension of 10 min at 72° C. For 18s initial denaturation at 94 °C for 2 min once, denaturation at 94 °C for 30 s, annealing at 56 °C for 30 s, elongation at 72 °C for 1 min repeated 30 cycles, followed by a final 1-min elongation at 72 °C. Positivity was assessed on 1% (w / v) agarose gel and the concentration and purity were verified using the Nanodrop spectrophotometer (Thermo Scientific). Once the presence of bands had been ascertained, a Gel extraction was carried out using the Promega kit Wizard® SV Gel and PCR Clean-Up System, and samples was sent to **Genechron Biotech** for sequencing.

3.7 Otolith Extraction

Otoliths are found in the inner ear behind the skull. The saccular otoliths were removed from otic capsule (Fig.7), cleaned from tissue with 3% H_2O_2 for 15 min and then with Milli-Q water and finally stored dry inside Eppendorf microtube, with number, date, total length and sex registered. A Leica M205C stereomicroscope with a built-in LEICA IC80 digital camera was

used to collect all the digital images of the otolith's samples. (Fig.8,9,10) Data on length and width were registered for each otolith through their observation in a stereoscopic with a graduated ocular lens. Each sagitta was photographed twice, first with the sulcus acoustics facing upwards and then with the annuli side facing up. Before being converted in binary format for contour extraction by ImageJ 1.48p software, feely available at http://rsb.info.nih.gov/ij/), the longest axis was been used to orient horizontally the images. Measurements were taken on the right and left sides of the three pairs. The constants of the relations of the *sagittae*, asterisks and lapilli for the length and width of the rostrum were calculated and the relations between the total length of the fish and all the measurements of the three otoliths were also recorded. The identification and counting of the growth rings were carried out using a stereoscopic microscope with transmitted light. Sagittas and asterisks were observed, and the average length of the fish was finally calculated.

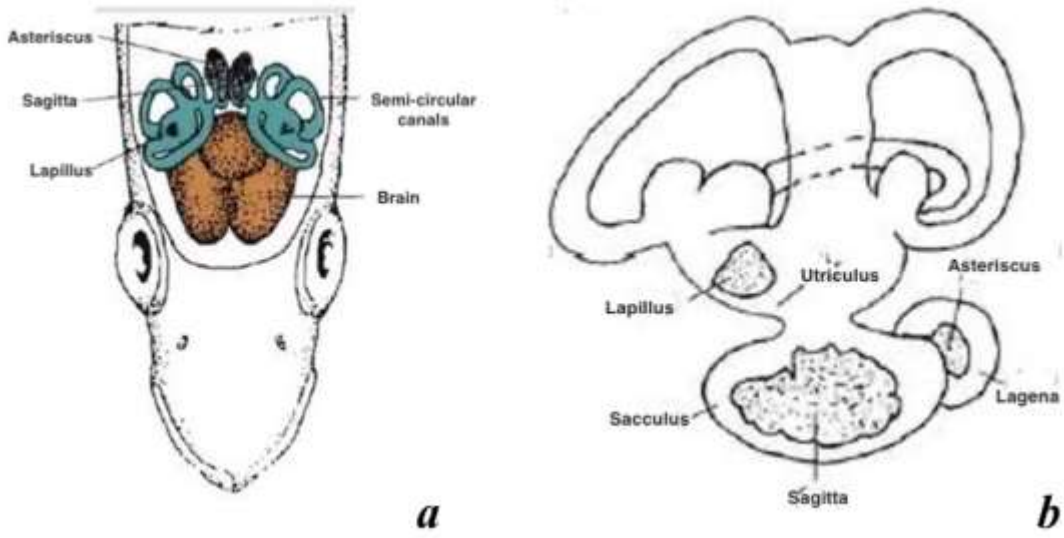

Figure 7: Location of otoliths in the inner ear of fish. a) Dorsal view of the vestibular apparatus; b) Otoliths within the apparatus

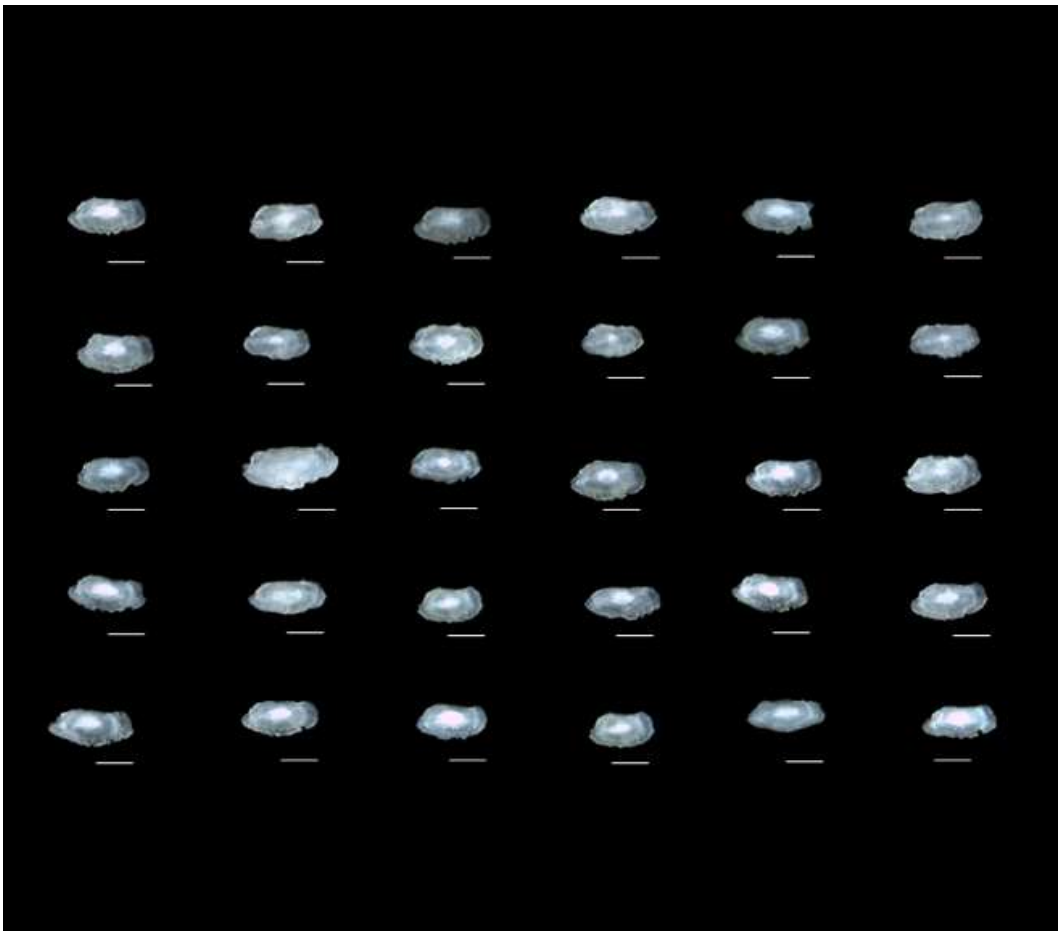

Figure 8. Representative stereomicroscope pictures of left Sagittal otoliths of *C. auratus* examined in the study. Scale bar: 3mm.

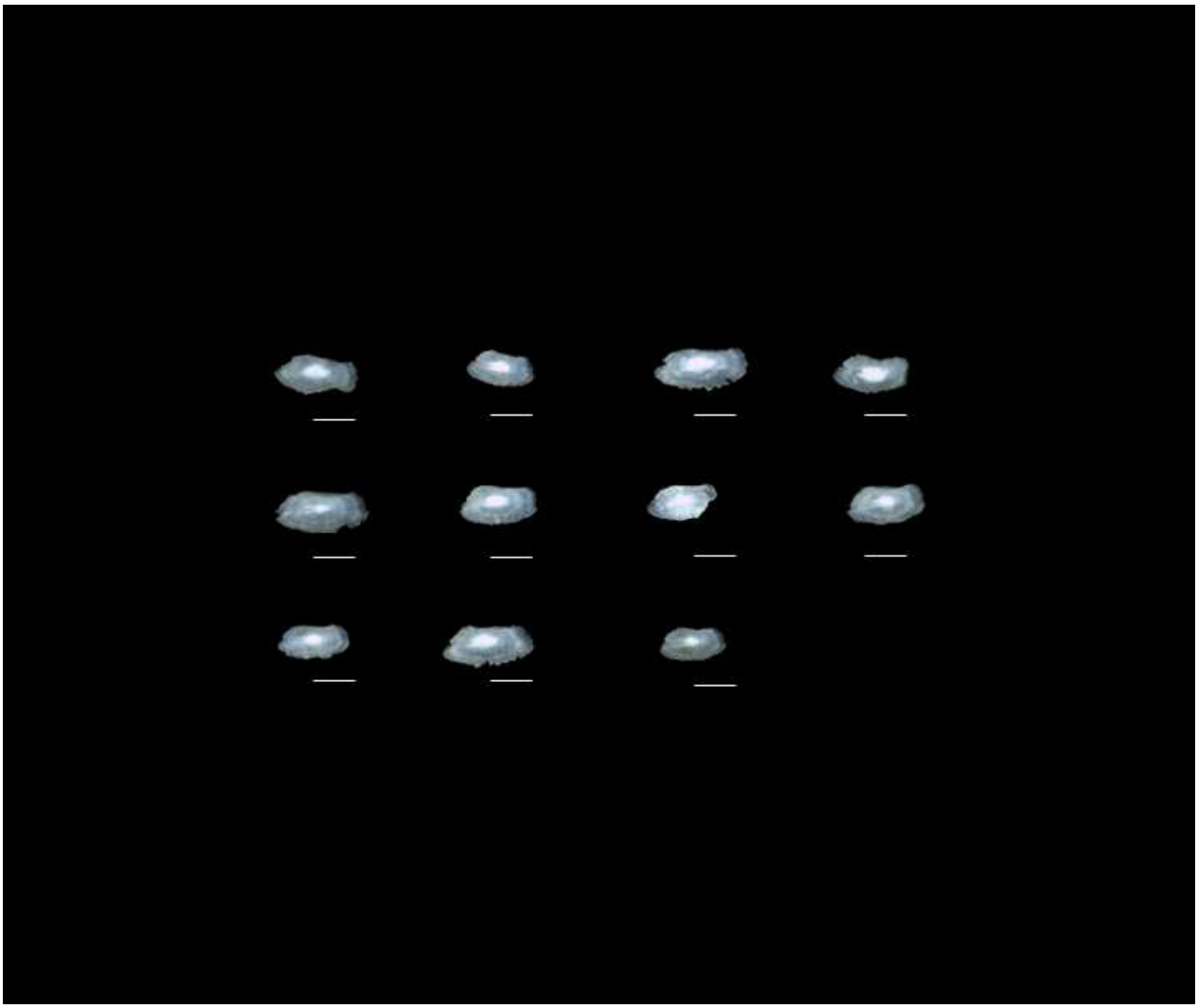

Figure 9. Representative stereomicroscope pictures of left Sagittal otoliths of *O. labeo* examined in the study. Scale bar: 3mm.

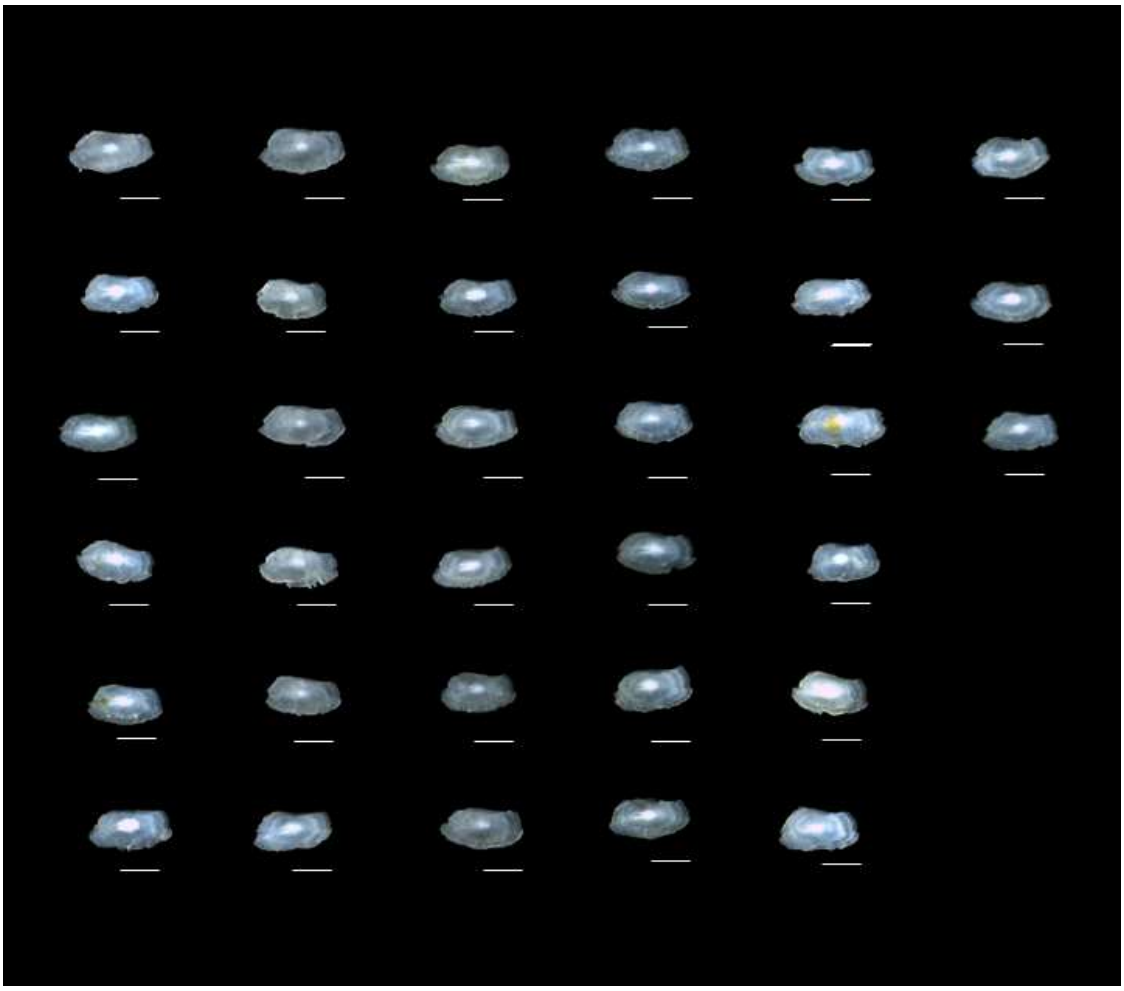

Figure 10. Representative stereomicroscope pictures of left Sagittal otoliths of *C. labrosus* examined in the study. Scale bar: 3mm.

3.7.1 Morphometry

According to literature (Tuset et al. 2008, Lombarte & Tuset 2015, Montanini et al. 2015, Jawad et al. 2018)), by ImageJ (ImageJ 1.48p software, freely available at https://imagej.nih.gov/ij/) some otolith measurements: otolith length (OL, mm), otolith width (OW, mm), otolith perimeter (OP, mm), otolith surface (OS, mm^2), sulcus perimeter (SP, mm), sulcus surface (SS, mm^2), sulcus length (SL, mm), cauda length (CL, mm), cauda width (CW, mm), cauda perimeter (CP, mm), cauda surface (CS), ostium length (OSL, mm), ostium

width (OSW, mm), ostium perimeter (OSP), ostium surface (OSS). Afterwards, other otolith shape indices were calculated: circularity (P^2/A), rectangularity (OS/(OL×OW)), aspect ratio (OW/OL; %), the ratio of the otolith length to the total fish length (OL/TL), percentage of the otolith surface occupied by the sulcus (SS/OS, %), percentage of the sulcus length occupied by the cauda length (CL/SL, %) and percentage of the sulcus length occupied by the ostium length (OSL/SL, %) (Table 2 and Table 3).

Otolith Morphological characters (mm-mm^2)	***C. auratus*** **Mean ± SD**	***C. auratus*** **Min. - Max.**	***O. labeo*** **Mean ± SD**	***O. labeo*** **Min. - Max.**
OL	6.82 ± 0.78	5.56 - 9.60	6.27 ± 0.81	5.27 - 7.43
OW	3.38 ± 0.27	2.97 - 4.24	3.27 ± 0.28	2.83 - 3.62
OP	17.32 ± 1.44	14.21 - 22.05	16.38 ± 2.39	13.46 - 20.45
OS	17.06 ± 2.38	12.71 - 26.01	15.48 ± 3.18	11.65 - 20.05
SP	14.72 ± 1.89	10.62- 19.28	14.24 ± 2.18	10.54 - 16.95
SS	0.12 ± 0.01	0.08 - 0.16	0.11 ± 0.02	0.08 - 0.13
SL	6.35 ± 0.89	4.31 - 8.41	6.05 ± 1.09	4.15 - 7.36
CL	4.12 ± 0.71	2.47- 5.92	3.72 ± 0.83	2.27 - 4.63
CW	1.08 ± 0.24	0.50 - 1.60	0.98 ± 0.23	0.57 - 1.40
CP	9.04 ± 1.54	5.69 - 12.34	8.29 ± 1.53	5.77 - 10.30
CS	0.07 ± 0.01	0.04 - 0.09	0.06 ± 0.01	0.04 - 0.08
OSL	2.23 ± 0,38	1.54 - 3.20	2.34 ± 0.47	1.69 - 3.16
OSW	1.24 ± 0.29	0.80 - 2.09	1.24 ± 0.17	1.00 - 1.45

OSP	5.69 ± 0,83	4.02 - 7.60	5.95 ± 1.01	4.75 - 7.93
OSS	0.04 ± 0.01	0.03 - 0.06	0.04 ± 0.01	0.04 - 0.06
OP^2/OS	17.65 ± 1.10	15.89 - 19.99	17.41 ± 1.73	15.55 - 20.93
OS/(OLxOW)	0.74 ± 0.04	0.52 - 0.78	0.75 ± 0.03	0.71 - 0.79
OW/OL %	49.88% ± 0.04	38.11% - 57.50%	52.44% ± 0.03	46.97% - 56.48%
OL/TL	0.04 ± 0.01	0.03 - 0.06	0.04 ± 0.01	0.02 - 0.05
SS/OS %	0.66% ± 0.001	0.42% - 1.12%	0.72% ± 0.00	0.47% - 1.02%
CL/SL %	64.76% ± 0.05	52.00% - 71.66%	0.61 ± 0.06	0.53 - 0.69
OSL/SL %	35.24% ± 0.05	28.34% - 48.00%	0.39 ± 0.06	0.31 - 0.47

Table 2: Morphometric mean values with standard deviation (SD) and range of *C. auratus* and *O. labeo* individuals: OL (otolith length), OW (otolith width), OP (otolith perimeter), OS (otolith surface), SP (sulcus perimeter), SS (sulcus surface), SL (sulcus length), CL (cauda length), CW (cauda width), CP (cauda perimeter), CS (cauda surface), OSL (ostium length), OSW (ostial width), OSP (ostium perimeter), OSS (ostium surface), CI (circularity), RE (rectangularity), aspect ratio (OW/OL %), the ratio of otolith length to total fish length (OL/TL), percentage of the otolith surface occupied by the sulcus (SS/OS%), percentage of the sulcus length occupied by the cauda length (CL/SL%), percentage of the sulcus length occupied by the ostium length (OSL/SL%).

Otolith Morphological characters (mm-mm²)	***C. labrosus*** **Mean ± SD. (L. otoliths)**	***C. labrosus*** **Min. - Max (L. otoliths)**	***C. labrosus*** **Mean ± SD (R. otoliths)**	***C. labrosus*** **Min. - Max. (R. otoliths)**
OL	6.73 ± 0.33	5.97 - 7.54	6.71 ± 0.33	6.04 - 7.45
OW	3.52 ± 0.19	3.24 - 4.00	3.48 ± 0.15	3.21 - 3.88
OP	17.36 ± 0.79	15.88 - 19.62	17.24 ± 0.72	15.93 - 18.89
OS	18,21 ± 1,44	15.98 - 21.64	17.91 ± 1.47	15.67 - 22.05
SP	15.57 ± 1.22	13.19 - 18.13	14.72 ± 1.51	12.31 - 19.30
SS	0.12 ± 0.01	0.10 - 0.13	0.11 ± 0.01	0.09 - 0.14
SL	6.29 ± 0.41	5.45 - 7.25	2.43 ± 0.77	0.93 - 5.75
CL	4.21 ± 0.39	3.39 - 4.80	1.18 ± 0.52	0.84 - 3.67
CW	1.20 ± 0.19	0.65 - 1.58	4.15 ± 0.68	1.04 - 5.13
CP	9.78 ± 1.05	7.58 - 11.68	9.51 ± 1.15	6.99 - 13.44
CS	0.07 ± 0.01	0.06 - 0.09	0.07 ± 0.01	0.05 - 0.10
OSL	2.09 ± 0.31	1.64 - 2.90	1.26 ± 0.37	0.09 - 2.07
OSW	1.43 ± 0.25	0.97 - 2.00	1.90 ± 0.34	0.94 - 2.37
OSP	5.79 ± 0.65	4.82 - 7.20	5.21 ± 0.76	3.79 - 6.98
OSS	0.04 ± 0.005	0.04 - 0.05	0.04 ± 0.01	0.03 - 0.05
OP^2/OS	16.58 ± 0.61	15.71 - 18.48	16.62 ± 0.60	15.59 - 18.69
OS/(OLxOW)	0.77 ± 0.02	0.71 - 0.81	0.77 ± 0.02	0.72 - 0.81
OW/OL %	52.43% ± 0.03	48.43 - 59.70%	51.95% ± 0.02	46.58% - 55.80%

OL/TL	0.03 ± 0.003	0.03 - 0.04	0.03 ± 0.003	0.03 - 0.04
SS/OS %	0.64% ± 0.001	0.48% - 0.78%	0.61% ± 0.00	0.46% - 0.85%
CL/SL %	66.84% ± 0.04	56.98% - 74.49%	48.51% ± 0.10	34.29% - 90.46%
OSL/SL %	33.16% ± 0.04	25.51% - 43.02%	51.49% ± 0.10	9.53% - 65.71%

Table 3: Morphometric mean values with standard deviation (SD) and range of right (R) and left (L) *sagittae* in *C. labrosus* individuals: OL (otolith length), OW (otolith width), OP (otolith perimeter), OS (otolith surface), SP (sulcus perimeter), SS (sulcus surface), SL (sulcus length), SW (sulcus width), CL (cauda length), CW (cauda width), CP (cauda perimeter), CS (cauda surface), OSL (ostium length), OSW (ostium width), OSP (ostium perimeter), OSS (ostium surface), CI (circularity), RE (rectangularity), aspect ratio (OW/OL%), the ratio of otolith length to total fish length (OL/TL), percentage of otolith surface occupied by the sulcus (SS/OS%), percentage of the sulcus length occupied by the cauda length (CL/SL%), percentage of the sulcus length occupied by the ostium length (OSL/SL%). (R = right, L = left).

3.7.2 Otolith Shape Analysis

Shape R, an open-source software package that runs on the R platform (R Gui 4.0.5), was used to carry out the analysis of otoliths shape. This is a specific package designed to study the image modification of the otolith shape of fish or species. All the otoliths' images captured were binarized using a threshold pixel value of 0.05 (intensity threshold). Each extracted outline was coupled to a master list file enclosing information on analyzed specimens (e.g., fishes' length and weight, origin). Wavelet and Fourier coefficients required for statistical analysis were both extracted and then adjusted with respect to allometric relationships with the fish lengths. Wavelet coefficient was also used to obtain the graph shown in (Fig.11), which compares the mean otolith shapes of species analysed. The quality of both Wavelet and Fourier reconstruction obtained was estimated by comparing how it deviated from the otolith

outline. The value 15 was set as maximum number of Fourier harmonics to be shown. Finally, the graph shown in figure 12 was obtained running a specific function of g-plots R package, to investigate how the variation in the Wavelet coefficients is dependent on the position along the outline.

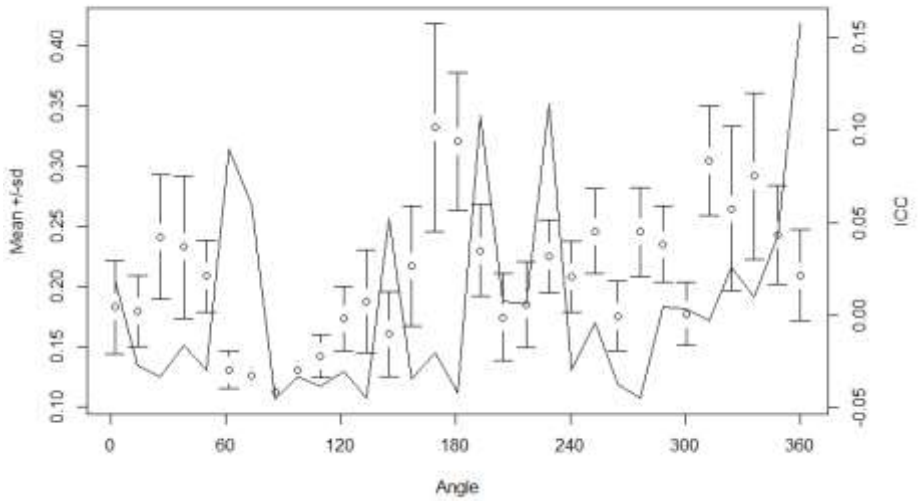

Figure 11: Mean and standard deviation (sd) of Wavelet coefficients for all combined otoliths and the proportion of variance among species (black line). The horizontal axis shows angle in degrees (°) based on the polar coordinates of Figure 8b. The centroid of the otolith is the centre point of polar coordinates.

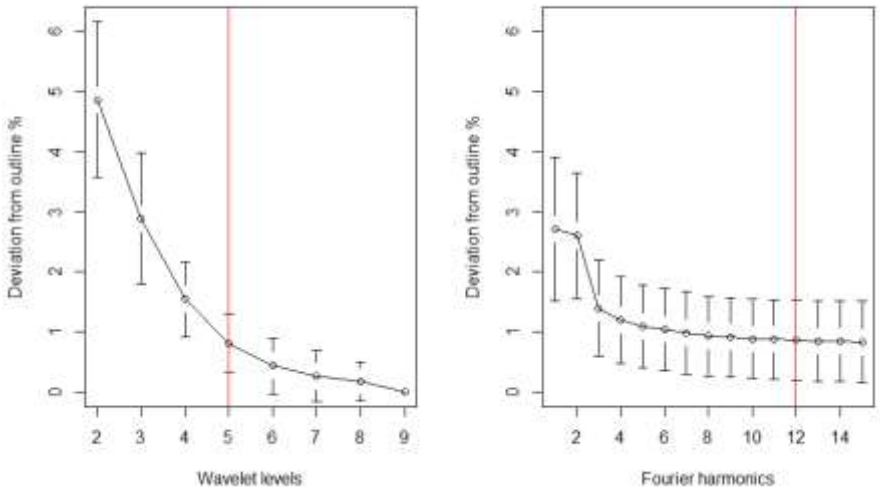

Figure 12: Plotting the quality of Wavelet and Fourier outline reconstruction. The red lines indicate the level of Wavelet and number of Fourier harmonics needed for a 98.5% accuracy of the remodelling.

3.8 SEM Analysis

A total of 9 otoliths were observed at SEM: 3 of *C. auratus/L. aurata*, 3 of *C. labrosus* and 3 of *O. labeo*. They were fixed for 48 h in 70% alcohol. Samples were dehydrated in a graded series of alcohol from 70 to 100°, for 1 h in each solution. To avoid the critical drying point, samples were placed on a stub (SEM-PT-F-12) using conductive adhesive tables (G3347) and left for 12 h at 28 °C. Finally, the samples were sputter coated with 20 nm gold palladium. The samples were examined using a Zeiss EVO MA10 operating at the acceleration voltage of 20Kv.

3.8 Microbiological Analysis of Water Samples

The data of the chemical-physical parameters of Ganzirri Lagoon in the period between June 2020 and June 2021, were measured by the technical staff of the *ARPA Sicilia* UOC sea area, shared and transferred to evaluate the Ph of the Water, Temperature of the Air (°C), Water Temperature (°C), Salinity (psu), Oxygen (mg / l) and Oxygen (% sat). Analysis of water

parameters has been performed to exclude alterations that could possible affect health status of fish sampled.

3.9 Statistical Analysis

3.9.1 Statistical Analysis of Otoliths

All statistical analyses were conducted using Sigmaplot V.14, R vegan package V.2.5, and PAST V. 2.756 software. Selected morphological parameters (OP^2/OS, OS/(OlxOW), OL/TL, OW/OL%, SS/OS%, RW/RL%, RL/OL%) were analysed using an unpaired t test to highlight any significant differences between the right and left sides of the otolith specimens within the same species. Differences in morphological parameters between specimens of different species were also analysed using one-way ANOVA or Kruskal-Wallis one-way ANOVA. Additionally, *sulcus acusticus* parameters were subjected to a Linear Discriminant Analysis (LDA) to show differences between all the analysed species. Finally, the correlation between the measured parameters and fish weight and total length was tested using the Pearson correlation coefficient. To determine differences in otolith contours, wavelet coefficients were used to analyse shape variation among species using an ANOVA-like permutation test. Moreover, shape coefficients were subjected to a LDA to obtain an overview of the differences in otolith shape between the species examined. The significance level was set at $P < 0.05$.

3.9.2 Statistical Analysis of Parasites and Granuloma

The occurrence of parasites and granulomas was analysed using univariate analysis. All the data are presented as the mean ± standard deviation (SD). One-way analysis of variance (ANOVA) followed by Tukey's test were performed to highlight any significant difference in trematode abundance between Mugilidae species investigated and between male and female specimens. Additionally, ANOVA was performed to show any significant difference in trematodes occurrence between target organs. Moreover, a correlation analysis was performed to detect any potential correlation existing between trematodes abundance and Mugilidae specimens morphological features. Regarding granulomas occurrence in analysed specimens,

the ANOVA followed by Tukey's test were performed to highlight any significant difference in granulomas abundance between Mugilidae species investigated and between male and female specimens. One-way ANOVA was also performed to show any significant difference in granulomas **occurrence** between organs and causative agents. Finally, a correlation analysis was performed to detect any potential correlation existing between granuloma abundance and Mugilidae specimens morphological measures. The significance level was set at $P<0.05$. Prior to the analysis the assumptions of normality and homoscedasticity were checked by Shapiro-Wilk test and Levene test respectively, after a data square root transformation when necessary. All statistical analysis were performed using Prism V.8.2.1 (Graphpad Software Ldt., La Jolla, CA 92037, USA).

4 RESULTS

4.1 Specimens Identification

Identification of Mugilidae species sampled revealed a heterogeneous group composed of *C. labrosus* (99/150), *C. auratus / aurata* (37/150) and *O. labeo* (14/150). In a Table 4 are reported the mean lengths and the mean weight with standard deviation (SD) of the three species are reported. Values of Std. Dev. Std. Error and C.I. Mean are showed in Appendix 5

	Length(cm) Mean ± SD	**Weight (gr) Mean ± SD**	**% Males**	**% Females**	**% Indefinite sex**
CL	20,18±3,99	91,66±139,67	44,44%	42,42%	13,14%
CA	19,75±1,9	72,08±22,19	54,05	35,13%	10,82%
OL	18,75±2,74	65,28±23,97	28,57	50%	21,43%

Table 4: Medium lengths, medium weight with standard deviation (SD) of the three species and % of sex of specimens. CL: *Chelon labrosus*, CA: *Chelon aurata*, *OL: Oedalechilus labeo*.

4.2 Parasitological Findings

Parasitological examination showed the presence of two different taxa. In two *C. labrosus* female subjects, characterized by a Body Weight (BW) of 1.453g and 61g, 16 Acanthocephala (1,3%), (Fig.13) extract from intestine and stomach respectively, were morphologically identified as *Neochinorhynchus agilis* (Neoechinorhynchidae, Rudolphi, 1819) according to the key suggested by (Sarabeev et al. 2014) (Fig.14).

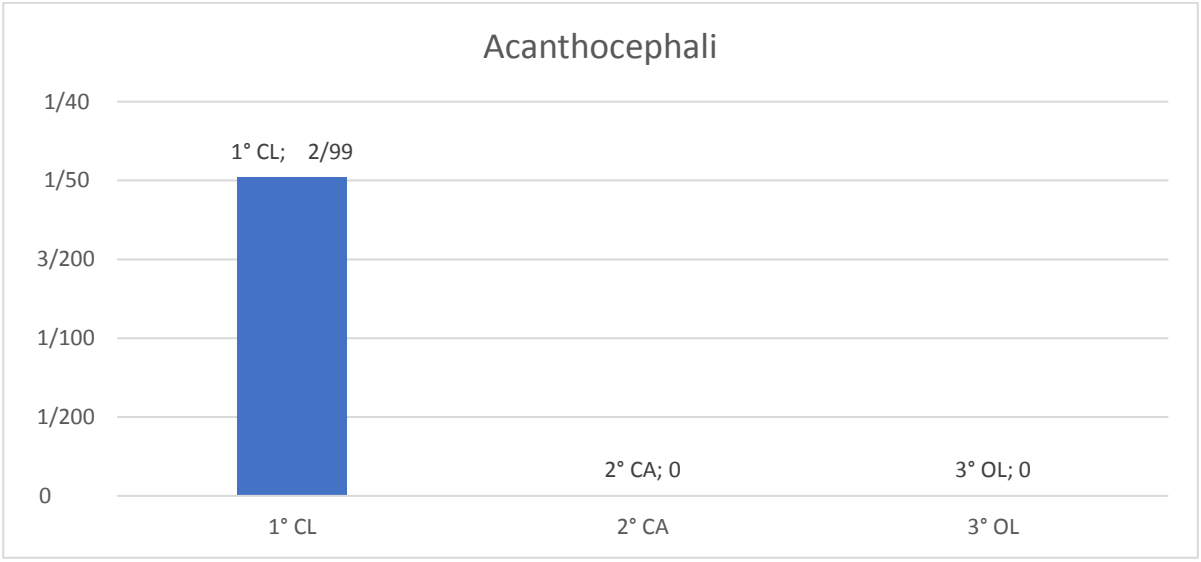

Figure 13: Specimens positive to Acantocephala. CL: *Chelon labrosus*, CA: *Chelon aurata*, *OL: Oedalechilus labeo.* X-axis: species of mugilidae, Y-axis: number of acatontocephiles

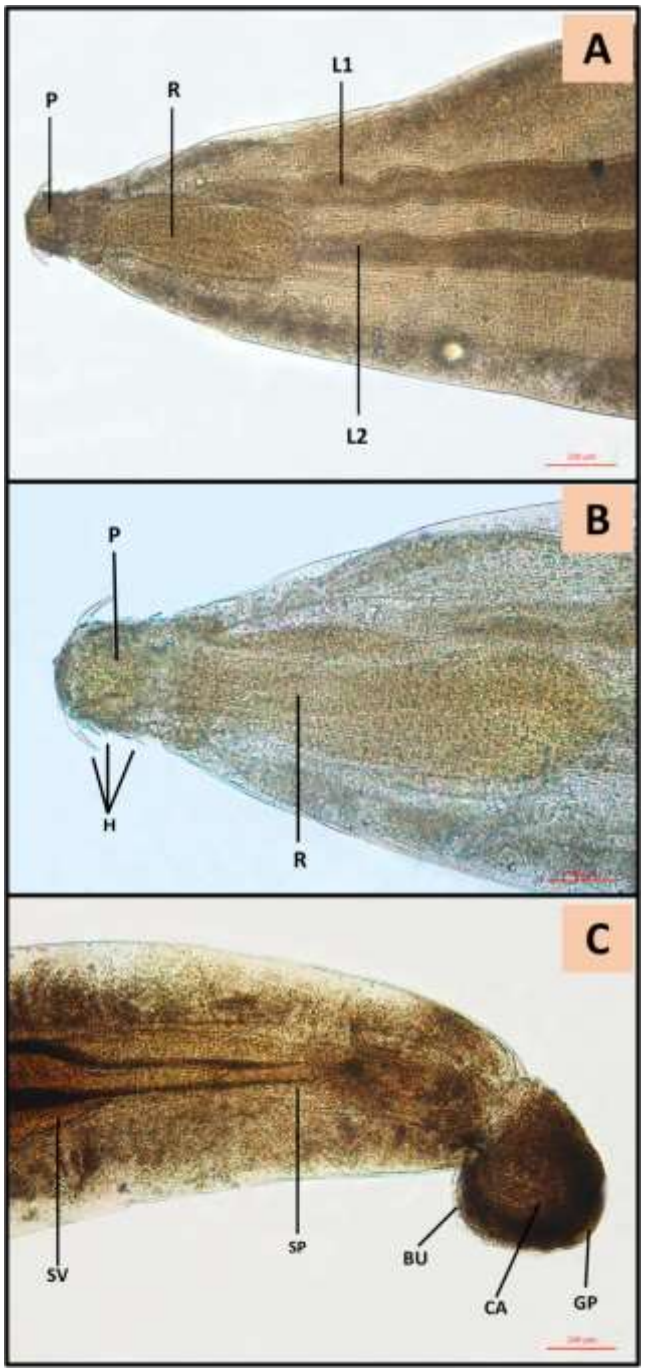

Figure 14: *Neoechinorhynchus agilis* cranial and posterior end: **A.** proboscis (P), proboscis receptacle (R), lemnisci (L1, L2). **B.** proboscis (P), proboscis receptacle (R), hooks system (H). **C.** *N. agilis* male posterior end: seminal vesicle (SV), saefftigen's pouch (SP), bursa (BU), calotte (CA), genital pore (GP).

In addition, the biggest female specimen, and a male of 69g (BW), showed also the presence of 18 and 4 cysts in the gastric wall. (Fig. 15).

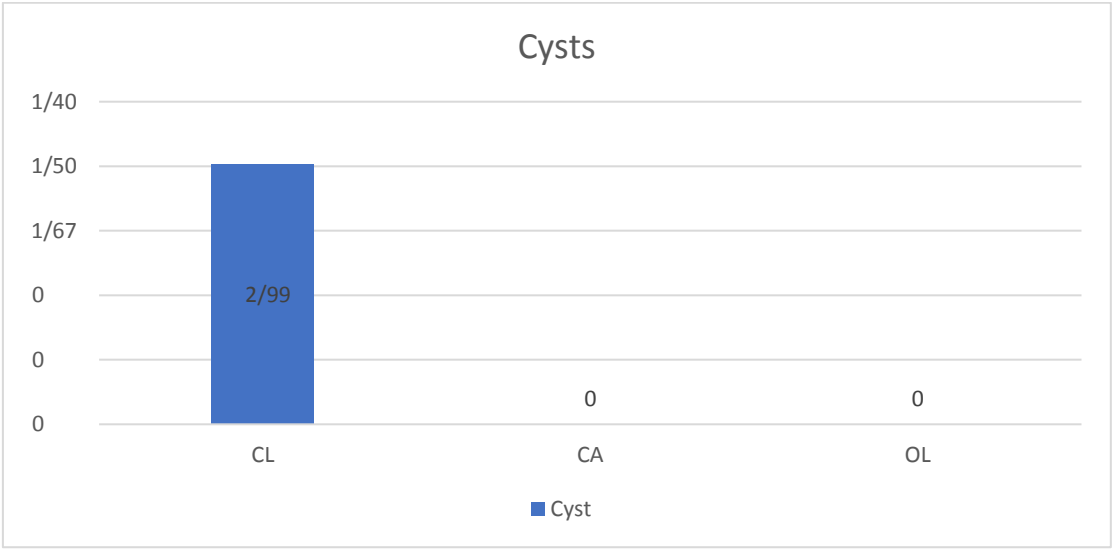

Figure 15: Specimens positive to digenean trematodes metacercariae . CL: *C. labrosus*, CA: *C. aurata*, *OL*: *O. labeo*

No nematodes were found in the gastrointestinal tract (GIT) of the 150 examined fish. Sixty-seven GIT of 150 specimens (44.7%) were positive for trematodes Fig. 16 -17.The stomach and intestine of each specimen were observed fresh and 67/150 samples proved positive for trematodes thus 44.66% of stomach and intestine showed positivity to trematodes. 48/150 samples had trematode's positivity in the stomach 32% of samples, while 51/150 samples instead had trematode's positivity in the intestine, 34% of samples. Among these it was seen that 32/150 specimens were positive to trematodes in both stomach and intestine, therefore 21.33% of the samples were positive to trematodes in both stomach and intestine. For *C. labrosus* 49/99 specimens were positive in which 11/49 of them had trematodes only in the stomach, 14/49 had trematodes only in the intestine and 24/49 had trematodes both in the stomach and in the intestine. Thus, *C. labrosus* samples proved positive for trematodes by 49,49% intraspecific and 32.66% vs. total. For *C. auratus* 10/37 specimens were positive of which in which 1/10 had trematodes only in the stomach, 9/10 had trematodes only in the intestine, and 3/10 had trematodes in both the stomach and intestine. Thus, *C. auratus* samples resulted positive for trematodes by 27,02% intraspecific and 6,66% vs. total. For *O. labeo* 7/14 specimens were positive; 3/7 of them had trematodes only in the stomach, 0/7 have trematodes only in the intestine, and 4/7 had trematodes in both the stomach and intestine. Thus, *O. labeo* samples proved positive for trematodes by 50% intraspecific and 4,66% vs. total. All these results are shown in the table below. Significant differences were observed in

trematodes abundance between the three Mugilidae species analysed (H= 6.57, df=2, p= 0.037). In addition, A significant negative correlation was found between trematodes abundance and total length (r= -0.688; p=0.005) and body weight (r=-0.645; p=0.01). Descriptive statistic of morphological data and trematodes contents found in *C. aurata*, *C. labrosus* and *O. labeo* are shown in Table 5,6 and 7. A different number of trematodes was found in the stomach and intestine of all fish samples that have been analysed. Trematodes occurred in the stomach showed a significant difference between the CA and OL specimens (p=0.01) and CA and CL (p=0.009). However, no difference was observed between the trematodes abundance in the intestine collected from fish samples (p>0.05).

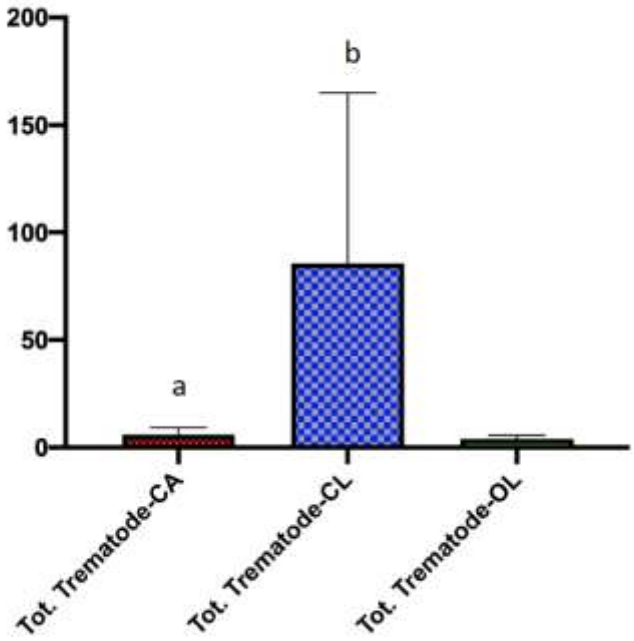

Figure 16: Trematodes found in all the three mullet species , CL: *Chelon labrosus*, CA: *Chelon aurata*, OL: *Oedalechilus labeo* Data are shown as mean± SD. Letters are only present in the case of significant statistical

differences. Different letters refer to significant differences between different species. Differences were considered significant when $p<0.05$.

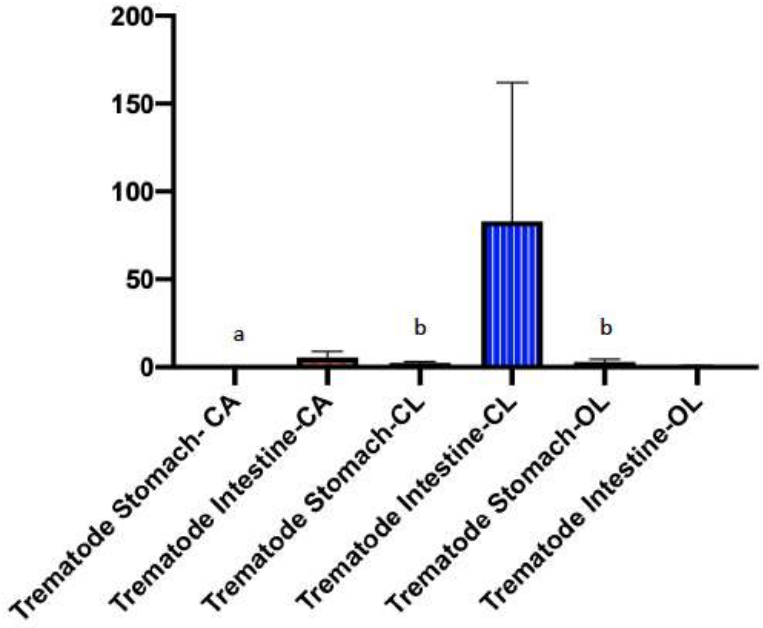

Figure 17: Positivity of the three species to trematodes in the stomach and in the intestine. CL: *Chelon labrosus*, CA: *Chelon aurata*, OL: *Oedalechilus labeo.* Data are shown as mean± SD. Letters are only present in the case of significant statistical differences. Different letters refer to significant differences between different species. Differences were considered significant when $p<0.05$.

	Mean	Std Dev	Std. Error	Range	Max	Min	Median	25%	75%
TL	19,757	1,924	0,316	11	27	16	20	19	21
BW	72,081	22,193	3,648	142	184	42	68	61	76
PS	0,108	0,315	0,0518	1	1	0	0	0	0
PI	0,243	0,435	0,0715	1	1	0	0	0	0,5
TT	0,448	0,856	0,141	3,231	3,231	0	0	0	1

TS	0,297	1,051	0,173	5	5	0	0	0	0
TI	5,622	19,897	3,271	105	105	0	0	0	0,5

Table 5: Descriptive statistic on morphological data and trematodes occurrence found in the *Chelon aurata* specimens. TL (Total Length), BW (Body Weight), PS (Positive Samples Stomach) PI (Positive Samples Intestine) TT (Total Trematode) TS (Trematode Stomach) TI (Trematode Intestine).

	Mean	**Std Dev**	**Std. Error**	**Range**	**Max**	**Min**	**Median**	**25%**	**75%**
TL	20,18	3,992	0,399	37,5	53	15,5	20	18,5	21
BW	91,66	139,679	13,968	1428	1453	25	76	61,25	90
PS	0,37	0,485	0,0485	1	1	0	0	0	1
PI	0,39	0,49	0,049	1	1	0	0	0	1
TT	0,914	1,247	0,125	9,414	9,414	0	1	0	1,565
TS	2,6	7,222	0,722	55	55	0	0	0	2
TI	82,35	779,445	77,945	7798	7798	0	0	0	2,75

Table 6: Descriptive statistic on morphological data and trematodes occurrence found in the *Chelon labrosus* specimens. TL (Total Length), BW (Body Weight), PS (Positive Samples Stomach) PI (Positive Samples Intestine) TT (Total Trematode) TS (Trematode Stomach) TI (Trematode Intestine).

	Mean	**Std Dev**	**Std. Error**	**Range**	**Max**	**Min**	**Median**	**25%**	**75%**
TL	18,75	2,744	0,733	9	23	14	19,25	16,25	21,125
BW	65,286	23,973	6,407	74	104	30	61,5	43,75	85,25
PS	0,5	0,519	0,139	1	1	0	0,5	0	1
PI	0,286	0,469	0,125	1	1	0	0	0	1
TT	0,782	0,847	0,226	2,166	2,166	0	0,595	0	1,565
TS	3	5,883	1,572	22	22	0	0,5	0	3,5
TI	0,857	1,61	0,43	5	5	0	0	0	1,5

Table 7: Descriptive statistic on morphological data and trematodes occurrence found in the *Oedalechilus labeo* specimens. TL (Total Length), BW (Body Weight), PS (Positive Samples Stomach) PI (Positive Samples Intestine) TT (Total Trematode) TS (Trematode Stomach) TI (Trematode Intestine).

4.3 Histologic Examination

From the histological analysis carried out on 150 specimens, 51 (34%) were positive to different pathogens (Fig.18, AppI). Among these 51 positive specimens, 7 (13.73%) specimens showed mature granulomas with peripheral fibroblasts and melan-macrophages incorporated, but with absence of detectable parasite, while in 44 (86.27%) specimens the parasites were present. Some of the fish showed infection limited to a single organ, while in other specimens multiple organs were affected. The liver was the most affected organ. As a matter of fact, 48/51 showed liver positivity, only 5/51in muscle, 3/51 in heart, 3/51 in intestine, 2/51 in pancreas, 1/51 in gills 2/51 in spleen and 2/51 in stomach (Fig19, App III). Microscopic examination of organs revealed a multifocal, slightly to severe granulomatous inflammation around parasites and five different stages of lesions. Most of the selected fish showed the presence of only one stage of granuloma caused by metacercaria (35/44, 79.54%) while (9/44, 18.18%) showed the presence of two or more stages of granuloma (Fig 20, App IV). Statistical difference ($p<0.05$) were observed in the occurrence of granulomas maturity stages (Fig 25), affected organs (Fig 19) and causative agents (Fig 20). Interesting, a significant correlation was found between the maturity stage of granuloma and total length and body weight of the *C. labrosus* specimens ($r=0.5$; $p=0.001$)

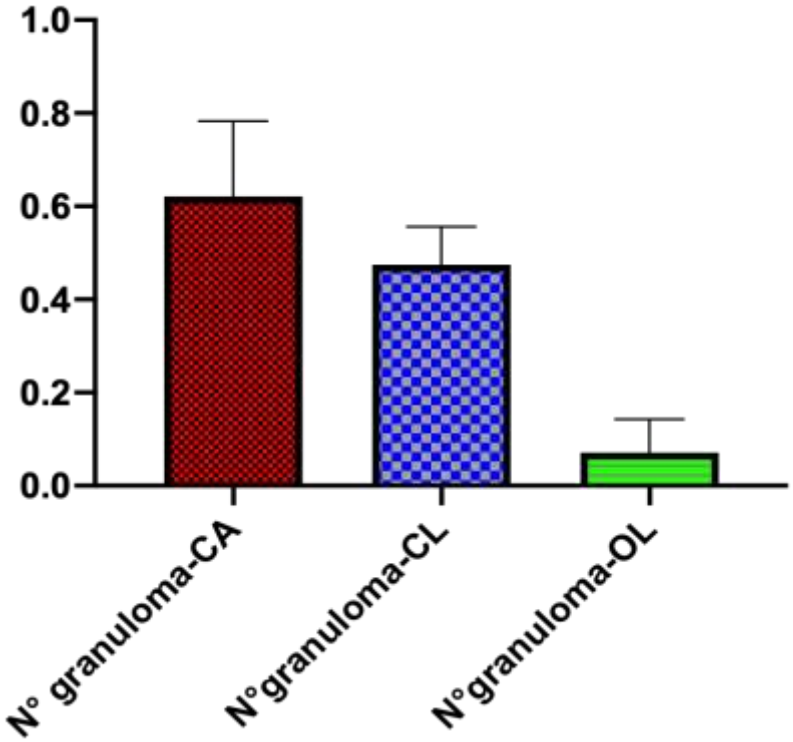

Figure 18: Total number of Granuloma in *C. aurata, C labrosus and O. labeo.* Data are shown as mean± SD.

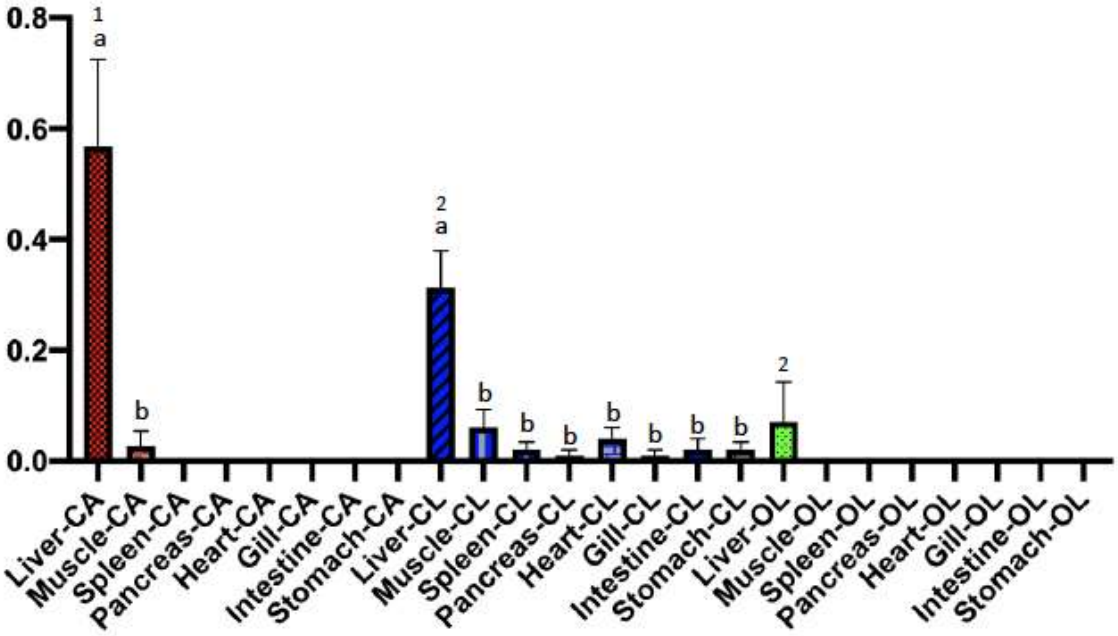

Figure 19: Abundance of Granulomas in the organs in *C. aurata, C labrosus and O. labeo*. Data are shown as mean± SD. Different numbers represent significant differences between the species. Letters are only present in the case of significant statistical differences. Different letters refer to significant differences between specimens within the same species. Differences were considered significant when $p<0.05$.

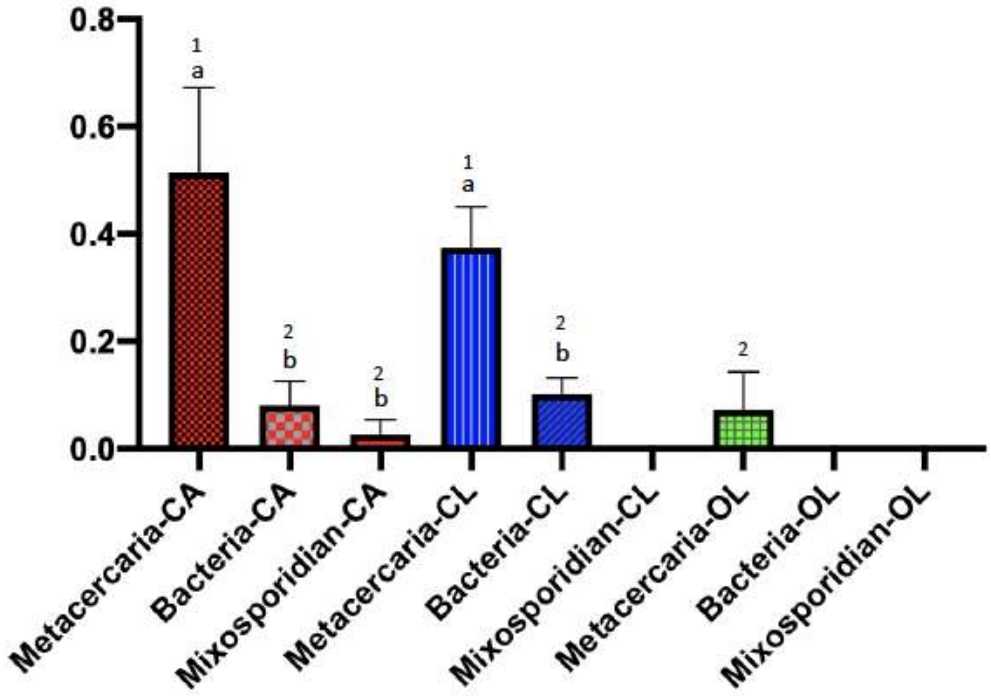

Figure 20: Aetiology of Granulomas in *C. aurata , C labrosus and O. labeo*. Data are shown as mean± SD. Different numbers represent significant differences between the species. Letters are only present in the case of significant statistical differences. Different letters refer to significant differences between specimens within the same species. Differences were considered significant when $p<0.05$.

Lesions identified as stage I (Free parasite) presented intact parasite, without any cystic wall. (Fig. 21)

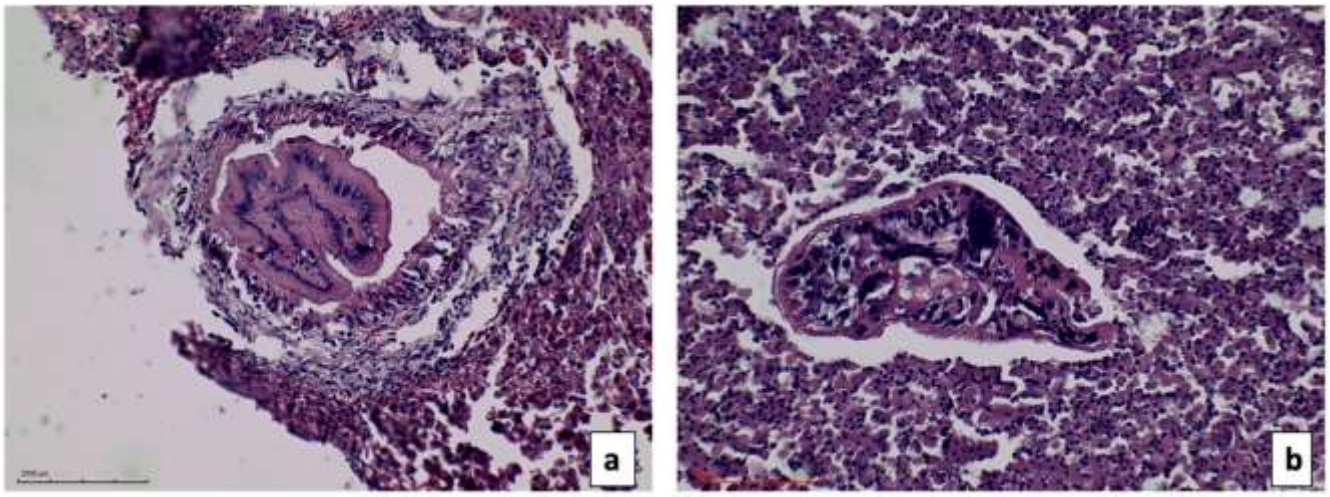

Figure 21: Stage I: Free Larvae H&E stained section of (a) a bile duct (b) intestine. Scale bar = 200 μm.

In stage II (Encysted parasite) lesions were classified as encysted parasite stage and showed an intact parasite, in or without association with sparse inflammatory cells, surrounded by a thin cystic wall. In stage III (Early stage) inflammatory cells begin to be observed arranged in one or two layers around the parasite. (Fig 22)

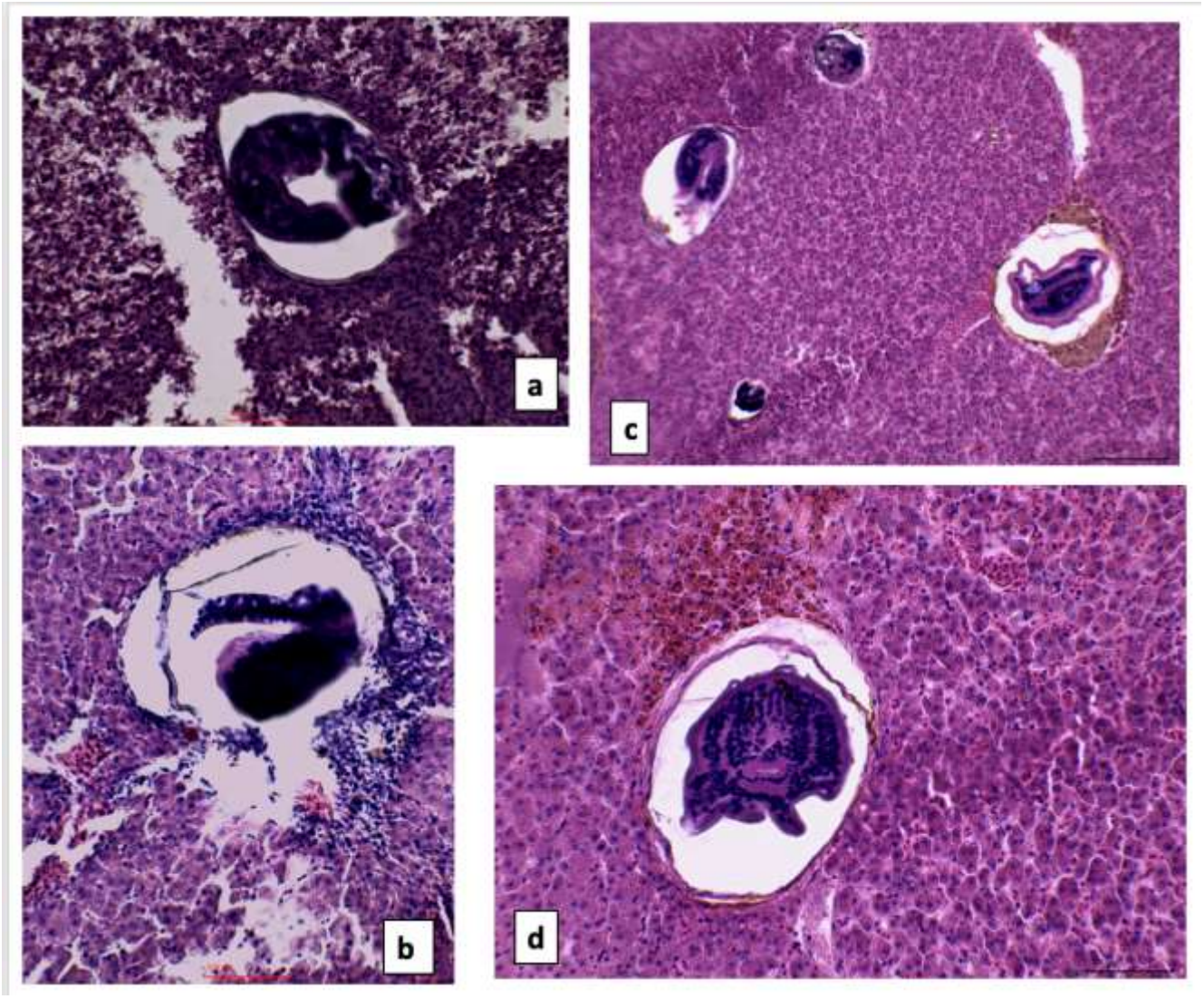

Figure 22: H&E stained section of a a) Stage II, Encysted: liver Scale bar = 100 µm. b) and d) Stage III, Early, b) liver, Scale bar = 100 µm d) liver, Scale bar = 100 µm. c) Mix of encysted larva and early granulomas in the liver. Scale bar = 200 µm

In stage IV (Intermedie stage granuloma), an outer sheet composed of different layers of flattened cells surrounding the degenerated parasite and necrosis was observed. It was characterized by a moderate to abundant eosinophilic cytoplasm, a vesicular ovoid nucleus with prominent central nucleolus, and basophilic. This stage was classified as an epithelioid cell stage. In addition, an outer covering composed of fusiform cells with sparse collagen has occasionally been found in this stage, mixed with fibroblasts. (Fig.23)

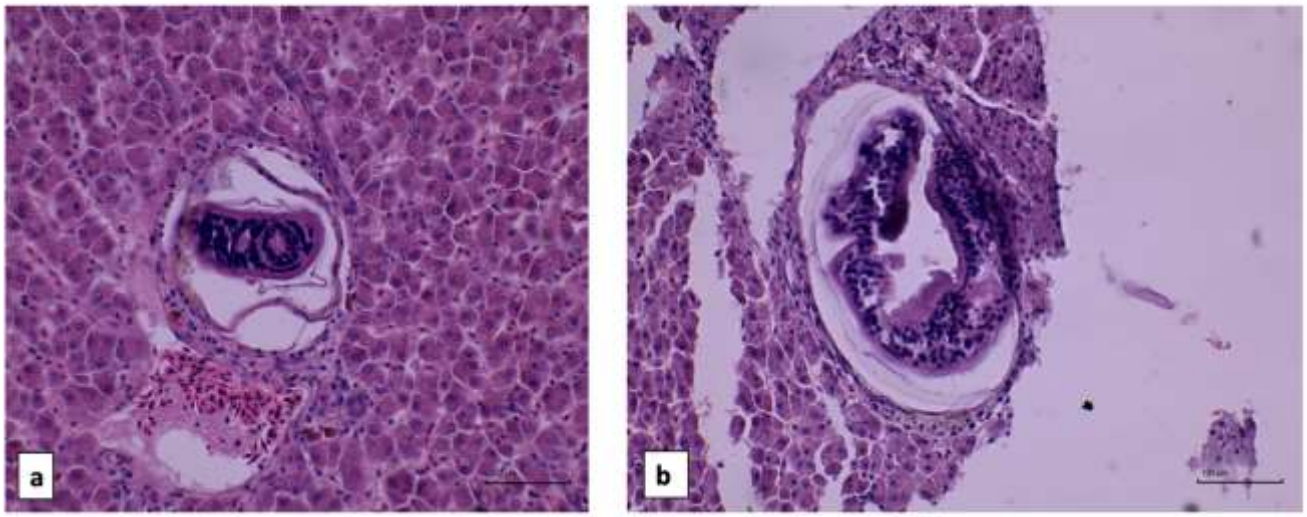

Figure 23: Stage IV, Intermediate Stage: H&E, stained section of (a) liver (b) muscle. Scale bar = 100 µm. Note macrophagic cells surrounding the cyst wall.

In stage V (Late-stage granuloma) the surrounding layers of epithelioid cells increased around the inner core, and the outer sheet consisting of fibroblasts was consistently present and larger in size, as collagen fibers were seen. This stage was classified as the fibroblast stage (Fig. 24.).

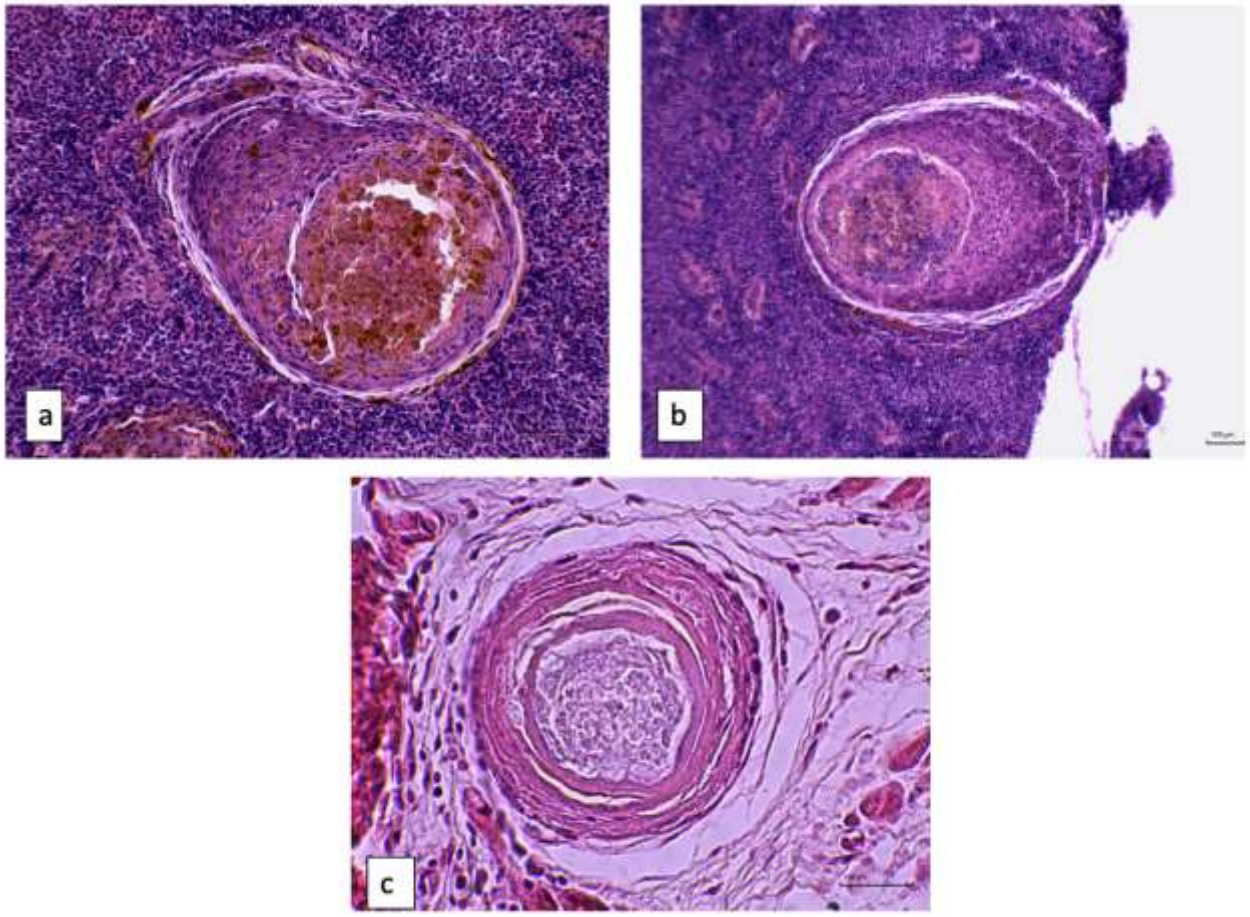

Figure 24: Stage V, Late-Stage Granuloma: H&E stained section a) and (b) spleen. c) gills. Scale bar = 100 μm.

On histological examination, the classification of the parasites was based on the characteristic features (Fig.25, AppII). In stage III near the wall of the parasitic cysts, macrophages were found scattered and/or mixed with necrotic material or scattered in the surrounding parenchyma in later stages. In addition, aggregates of macrophages, often showing pigment-laden cytoplasm, were observed in association with the outer layers of granulomas. Mast cells appeared as ovoid cells with distinct borders and abundant cytoplasm containing numerous eosinophilic granules, and a central nucleus. In phase II, mast cells were close to the parasites, whereas, in later epithelioid and fibroblast phases, mast cells migrated to the outer layers. In fact, they were most frequently observed mixed with fibroblasts and sometimes detected in close contact with the fibroblast membrane, elongated in shape with vaguely arranged granules. Rodlet cells were not found in all stages but were recognizable as ovoid cells with

distinct borders, an eccentric round nucleus, and characteristic cytoplasmic eosinophilic rodlets, mainly arranged near the parasite capsule or in the surrounding parenchyma.

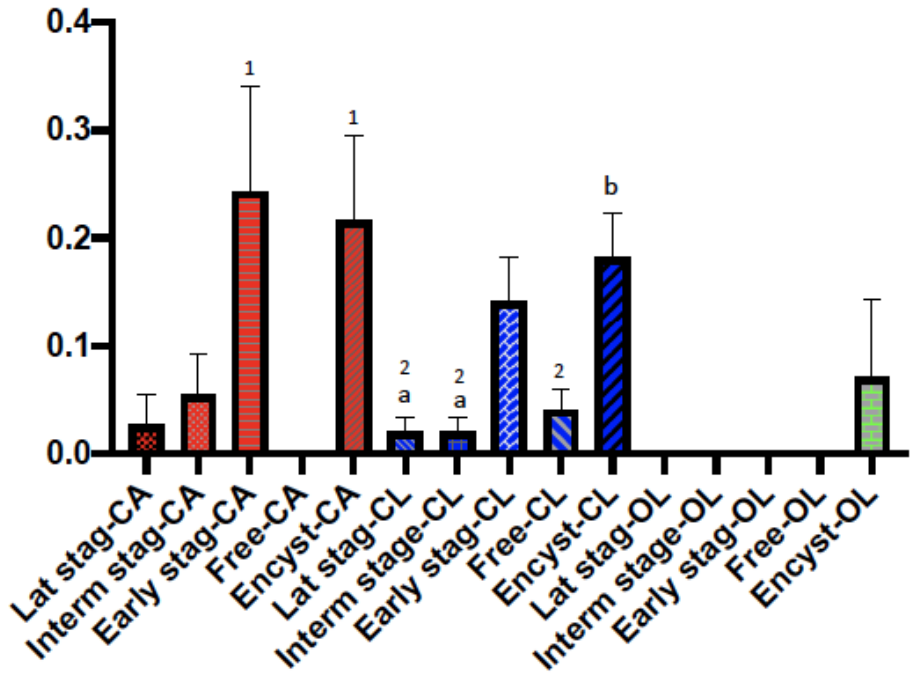

Figure 25: Difference stage of granulomas in *C. aurata* , *C labrosus and O. labeo*. Data are shown as mean± SD. Different numbers represent significant differences between the species. Letters are only present in the case of significant statistical differences. Different letters refer to significant differences between specimens within the same species. Differences were considered significant when $p<0.05$.

4.4 Molecular analysis

BLAST (NCBI) analysis of the sequence obtained from ITS gave an identification at the level of genus Haploporidae while 28s and 18s amplification showed a similarity of 99.46% for

Haploporus benedeni (Stossich,1887) (Accession number FJ211228), while from the other sequences obtained BLAST was not or little specific.

4.5 Morphometric and Shape Analysis of Otholith

For the three studied species of mugilidae, a general pattern is recognized: the Sagitta has a rectangular to oblong shape with irregular margins; the acoustic sulcus is heterosulcoid and ostial, formed by a short funnel-shaped ostium open at the anterior margin, and by a closed tubular cauda at least twice as large as the ostium. However, the morphology of the sagitta of the gray mullets studied presents some differences during their growth. Each species has distinctive morphological patterns of otoliths as described below.

Chelon auratus (Risso, 1810), golden head mullet, specimens showed a *sagitta* with rectangular to oblong shape, entire margin in dorsal rim and lobed to entire margins in ventral rim. The ostium is funnel-like, shorter than cauda. Cauda is tubular, sinuous, ends near posterior edge. Anterior region was angled-round, with a short and pointed *rostrum* and an *anti-rostrum* almost entirely absent. Posterior region was flattened to round. There is a mildly pronounced dorsal depression; ventral depression is absent (Fig.26).

Chelon labrosus (Risso, 1826), lipped mullet, Shape: Rectangular, dorsal and ventral margins are sinuate and crenate and lobed to entire margins in ventral rim. The ostium is funnel-like, shorter than cauda. Cauda is tubular, sinuous, ends close to posterior edge. Anterior region was angled-irregular, with a short and broad *rostrum.* The dorsal rim showed a marked plateau tilting toward anterior rim. The *anti-rostrum* was absent or, in some specimens, poorly marked with a wide and small *excisura.* The posterior region was slightly irregular to round. Small on the dorsal depression cauda; ventral depression is absent (Fig.27).

Oedalechilus labeo (Cuvier, 1829), gray mullet or skimmer mullet, Shape: rectangular, dorsal and ventral margins crenate. Sulcus acusticus: heterosulcoid, ostial, supramedian. Ostium: funnel-like, shorter than cauda. Cauda: tubular, sinuous, ends close to posterior edge.

The anterior region was round to irregular, with a *rostrum* short and broad, and a short and pointed *anti-rostrum.* Small on the dorsal depression cauda; ventral depression is absent (Fig.28).

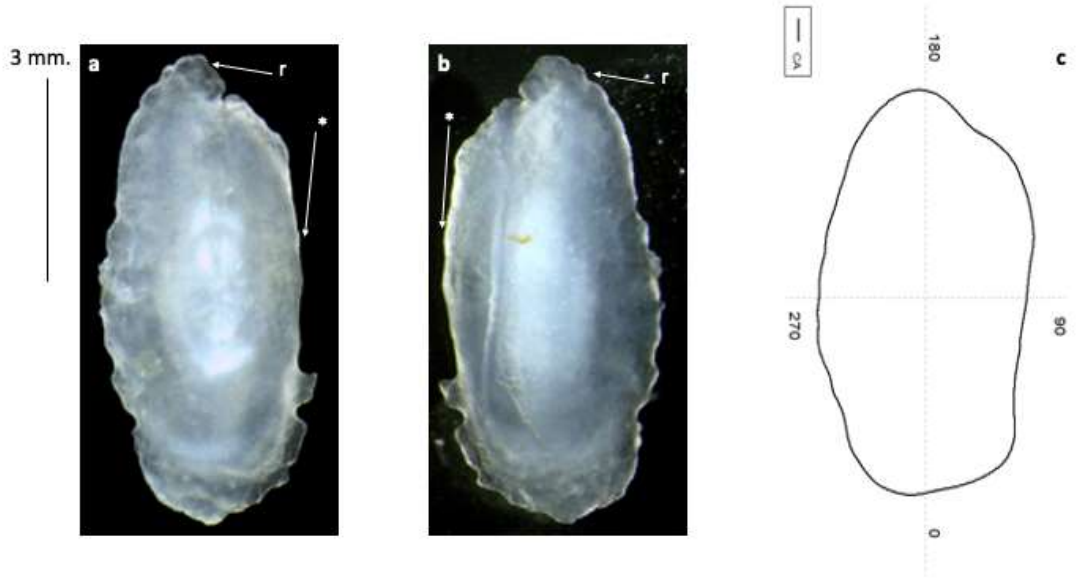

Figure 26. Left sagittae of C. auratus with scale bar. (a) Medial viex; (b) Lateral view; (c) Mean shape.

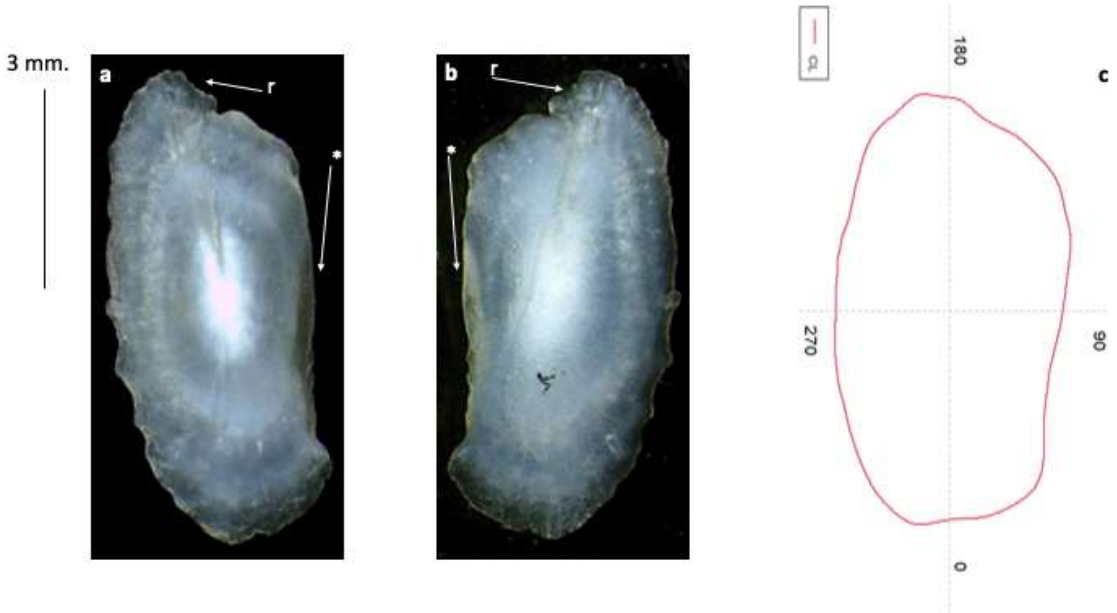

Figure 27. Left *sagittae* of *C. labrosus* with scale bar. (a) Medial viex; (b) Lateral view; (c) Mean shape.

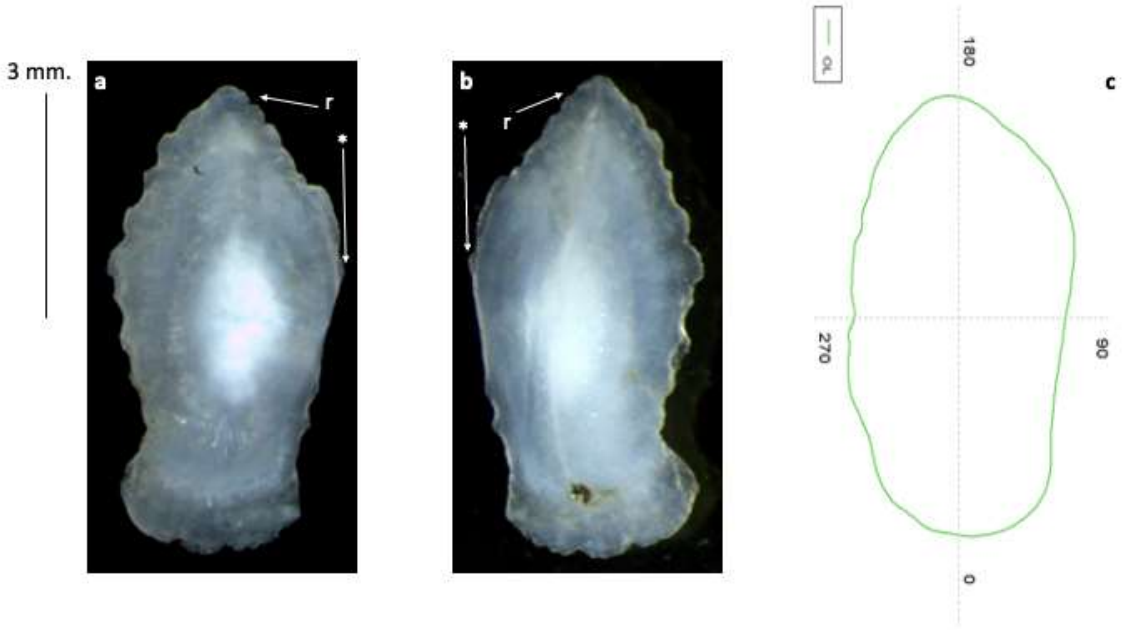

Figure 28. Left *sagittae* of *O. labeo* with scale bar. (a) Medial view; (b) Lateral view; (c) Mean shape.

The correlation analysis of intra-specific differences among morphometrical parameters of *sagittae*, revealed, in the specimens of the *C. auratus* species, a moderate significant correlation between TL and SS/OS% (ρ= 0.416; p = 0.001). *C. labrosus* was the only species to have shown differences between the right and left side of the otoliths, for the parameters CL/SL% (H = 38.48, df 1, p <0.001) and OSL/SL% (H=38.48, df 1, p<0.001). Moreover, a significantly positive correlation was noted between TL and OW/OL (ρ = 0.411; p = 0.001); while a negative correlation was noted between TL and OL/TL (ρ = - 0.366; p = 0.0029) and between BW and OL/TL (ρ = - 0.392; p = 0.001). In *O. labeo* specimens a strong negative correlation was observed between TL and OL/TL (ρ = - 0.729; p = 0.001) and between BW and OL/TL (ρ = -0.658; p = 0.001). A significant positive correlation was recorded between TL and SS/OS% (ρ = 0.561; p = 0.008) and BW and SS/OS% (ρ = 0.499; p = 0.02). For the inter-specific differences among morphometrical parameters of *sagittae,* the investigated species showed significant differences in some parameters. *C. auratus* and *C. labrosus* revealed differences in OP^2/OS (H = 20.802, DF2, P <0.001), OS/[OLXOW] (P = 0.001), OW/OL% (P <0.002) and OL/TL (H = 12.477, DF 2, P = 0.002). *C. auratus* and *O. labeo* showed significant differences only in OW/OL% (P = 0.014). Finally, *C. labrosus* and *O.*

labeo showed differences in OS/[OLXOW] (P = 0.012). As shown in the LDA plot (Fig. 29), the first two axes showed a slight separation in the *sulcus acusticus* parameters between the three fish species analyzed. The mean shape of otoliths differed significantly between the *C. auratus*, *C. labrosus*, and *O. labeo* specimens (P < 0.001). The otolith contours are shown in Fig. 30a. Marked differences in the otoliths shape have also been confirmed by LDA indeed from the LDA plot of the first two discriminant functions, we can see that the three species were quite well separated (Fig. 30b) (Table 8-9).

Fish species	**Morphometric parameters**	**Weight**		**Total length**	
		ρ	p value	ρ	p value
C. auratus	OP^2/OS	ns	ns	ns	ns
	OS/(OLxOW)	ns	ns	ns	ns
	OW/OL %	ns	ns	ns	ns
	OL/TL	ns	ns	ns	ns
	SS/OS %	ns	ns	0.416	0.001
	CL/SL %	ns	ns	ns	ns
	OSL/SL %	ns	ns	ns	ns
C. labrosus	OP^2/OS	ns	ns	ns	ns
	OS/(OLxOW)	ns	ns	ns	ns
	OW/OL %	ns	ns	0.411	0.001
	OL/TL	-0.392	0.001	-0.366	0.0029
	SS/OS %	ns	ns	ns	ns
	CL/SL %	ns	ns	ns	ns
	OSL/SL %	ns	ns	ns	ns
O. labeo	OP^2/OS	ns	ns	ns	ns
	OS/(OLxOW)	ns	ns	ns	ns
	OW/OL %	ns	ns	ns	ns
	OL/TL	-0.658	0.001	-0.729	0.001
	SS/OS %	0.499	0.02	0.561	0.008
	CL/SL %	ns	ns	ns	ns
	OSL/SL %	ns	ns	ns	ns

Table 8. Pearson Correlation results between total length, weight and selected morphometric parameters of *C. auratus*, *C. labrosus* and *O. labeo*. P= 0.05 value was used to set the significant result., OP^2/OS (circularity), OS/(OLxOW) (rectangularity), aspect ratio (OW/OL; %), the ratio of the otolith length to the total fish length (OL/TL), percentage of the otolith surface occupied by the sulcus (SS/OS, %), percentage of the sulcus length occupied by the cauda length (CL/SL, %), percentage of the sulcus length occupied by the ostium length (OSL/SL, %). ns= not significant.

	OP^2/OS	OS/(OLxOW)	OW/OL %	OL/TL	SS/OS %	CL/SL %	OSL/SL %
Comparison between L and R otoliths:							
C. auratus	ns	ns	ns	ns	ns	ns	ns
C. labrosus	ns	ns	ns	ns	ns	p <0.001	p<0.001
O. labeo	ns	ns	ns	ns	ns	ns	ns
Comparison between species:							
C. auratus* vs *C. labrosus	P <0.001	P = 0.001	P <0.002	P = 0.002	ns	ns	ns
C. auratus* vs *O. labeo	ns	ns	P = 0.014	ns	ns	ns	ns
C. labrosus* vs *O. labeo	ns	P = 0.012	ns	ns	ns	ns	ns

Table 9. Results of t-test and ANOVA carried out on selected morphometric parameters between left and wright *sagitta* and among left *sagittae* of *C. auratus*, *C. labrosus* and *O. labeo*. Significant result was set at P= 0.05. OP^2/OS (circularity), OS/(OLxOW) (rectangularity), aspect ratio (OW/OL; %), the ratio of the otolith length to the total fish length (OL/TL), percentage of the otolith surface occupied by the sulcus (SS/OS, %), percentage of the sulcus length occupied by the cauda length (CL/SL, %), percentage of the sulcus length occupied by the ostium length (OSL/SL, %). ns= not significant.

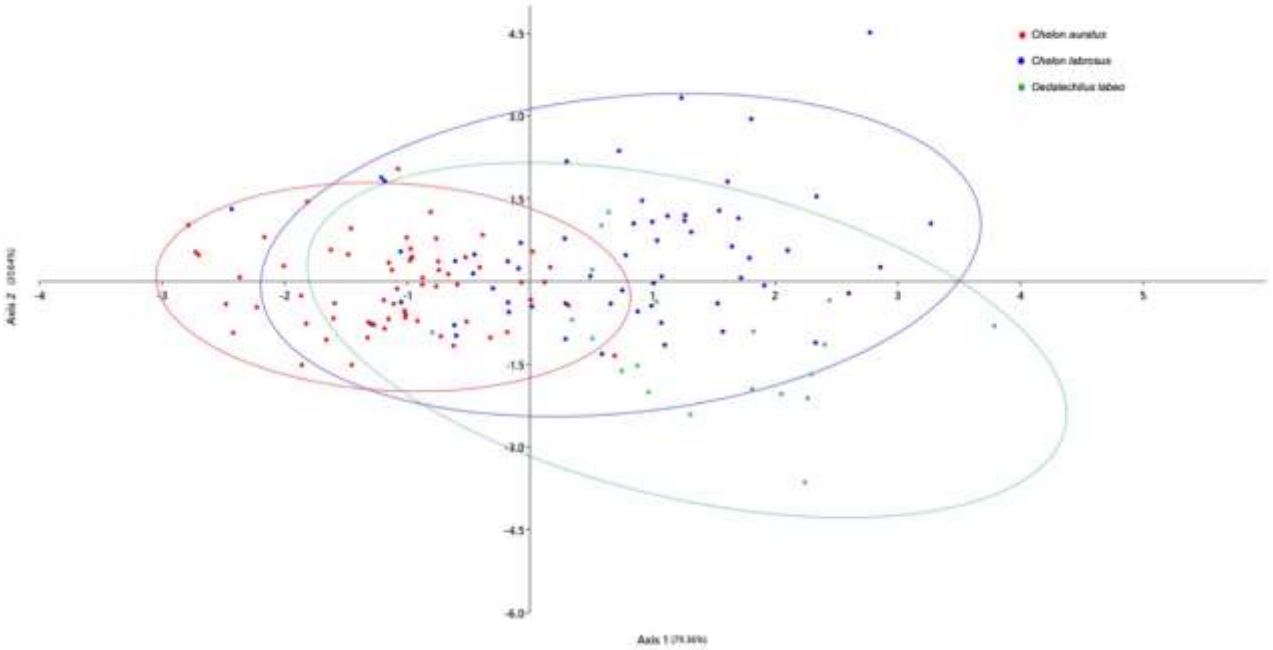

Figure 29. Linear Discriminant Analysis (LDA) of the sulcus acusticus computed between the species *C. auratus*, *C. labrosus* and *O. labeo*. The LDA was based on selected *sulcus acusticus* parameters: Sulcus acusticus area, sulcus aucusticus perimeter, sulcus acusticus length, ostium area, ostium perimeter, ostium length, ostium width, cauda area, cauda perimiter, cauda length, cauda width, percentage of the otolith surface occupied by the sulcus (SS/OS, %), percentage of the sulcus length occupied by the cauda length (CL/SL, %), percentage of the sulcus length occupied by the ostium length (OSL/SL, %). 95% probability ellipses are shown.

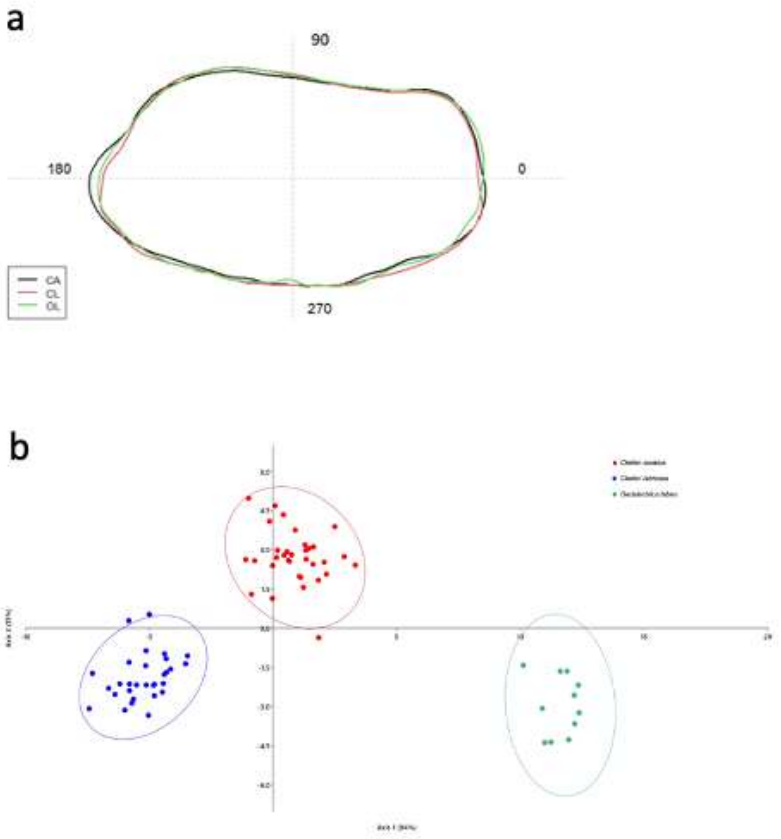

Figure 30: (a) Mean shapes of left otolith contours. CA is *Chelon auratus*, CL is *Chelon labrosus*, and OE is *Oedalechilus labeo.* (b) Linear Discriminant Analysis plot between the species *Chelon auratus*, *Chelon labrosus* and *Oedalechilus labeo*, calculated on elliptic Fourier descriptors. Ellipses include 95% confidence interval.

4.6 Scanning Electron Microscopy (SEM) Analysis.

SEM images of the three species of mugilidae studied give us an accurate view of the sagittas. In all the three species the *acuticus sulcus* was heterosulcoid with a supramedian position and flat *cullicles* (Homomorph). The *ostium* was widely opening in anterior margin and *cauda* was distinctly closed away from the posterior margin (ostial mode opening). In all the three species it was tubular with a more markedly curved shape in *C. labrosus* and *O. labeo* than *C. auratus* (Figure 31 d,b,c). In *C. auratus* the *ostium* was funnel-like (Figure 31a), while in the *C. labrosus* and *O. labeo* it resulted to be mostly rectangular (31 e,f). The anterior regions of *sagittae* were peaked in all the studied species, with an anti-rostrum absent or poorly developed and short and poorly pronounced *rostrum*, while posterior regions were flattened and slightly oblique in some *C. auratus* specimens.

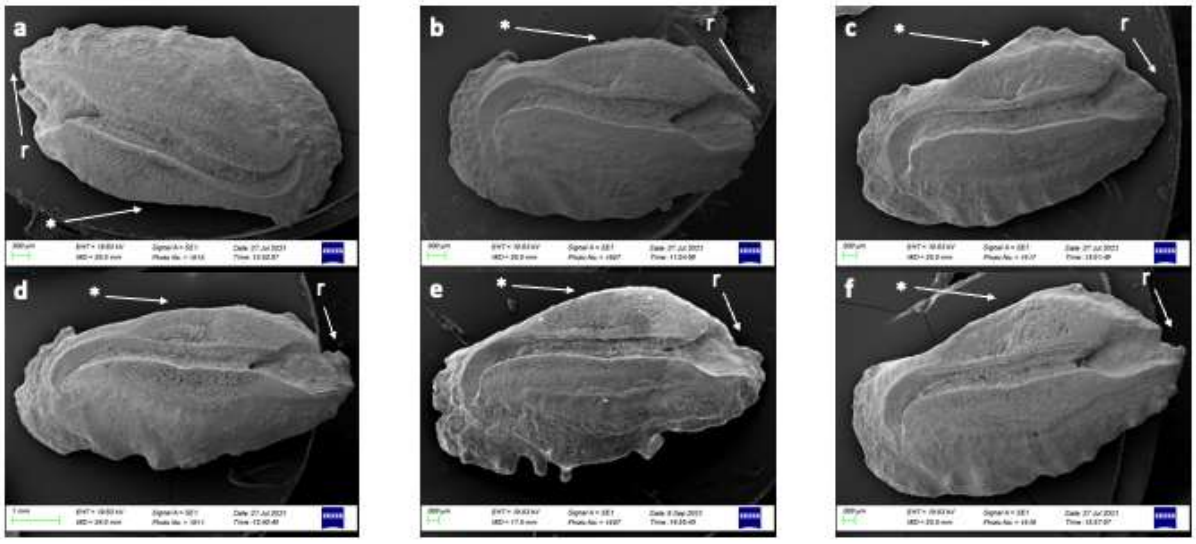

Figure 31. SEM imaging of left *sagittae* proximal surface; (a-d) C. auratus; (b-e) C. labrosus; (c-f) O. labeo. (r) Indicates the rostrum and (*) indicates the dorsal rim.

The external textural organization, SEM analysis revealed a polymorph transformation, closely related to otoliths mineralization process. All the analysed *sagittae* showed radial oriented crystalline units, with a chaotic orientation and not equally sized (Figure 32 c,b,e; 33 b,c; 34 b,c), probably due to polymorph composition of crystals. In all the three species studied, the aragonite was found in two crystal habits (Columnar habits and Distinct plates habits) on *cauda* surface with bigger, longer and narrower crystals (Figure 32 d,e; 31 b; 33 c,d,e), while in *ostium* they were smaller and shorter than in *cauda*, with a smooth surface (Figure 32 b; 33 d; 34 b).

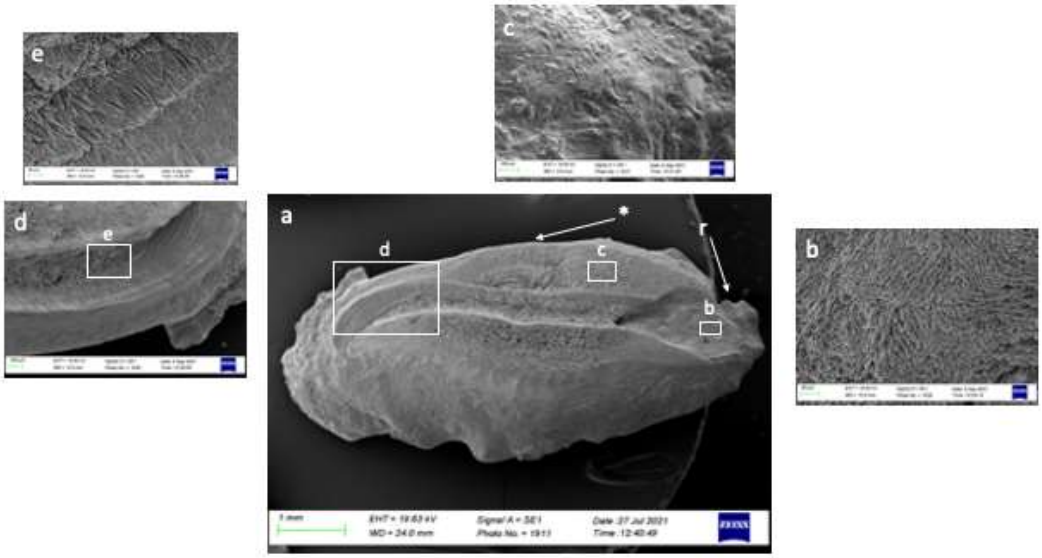

Figure 32. SEM imaging of left *sagitta* proximal surface in *C. auratus* (a), with details of external textural organization of *ostium* (b), area between *cauda* and dorsal rim (c) and *cauda* (d-e)*;* (r) Indicates the rostrum and (*) indicates the dorsal rim.

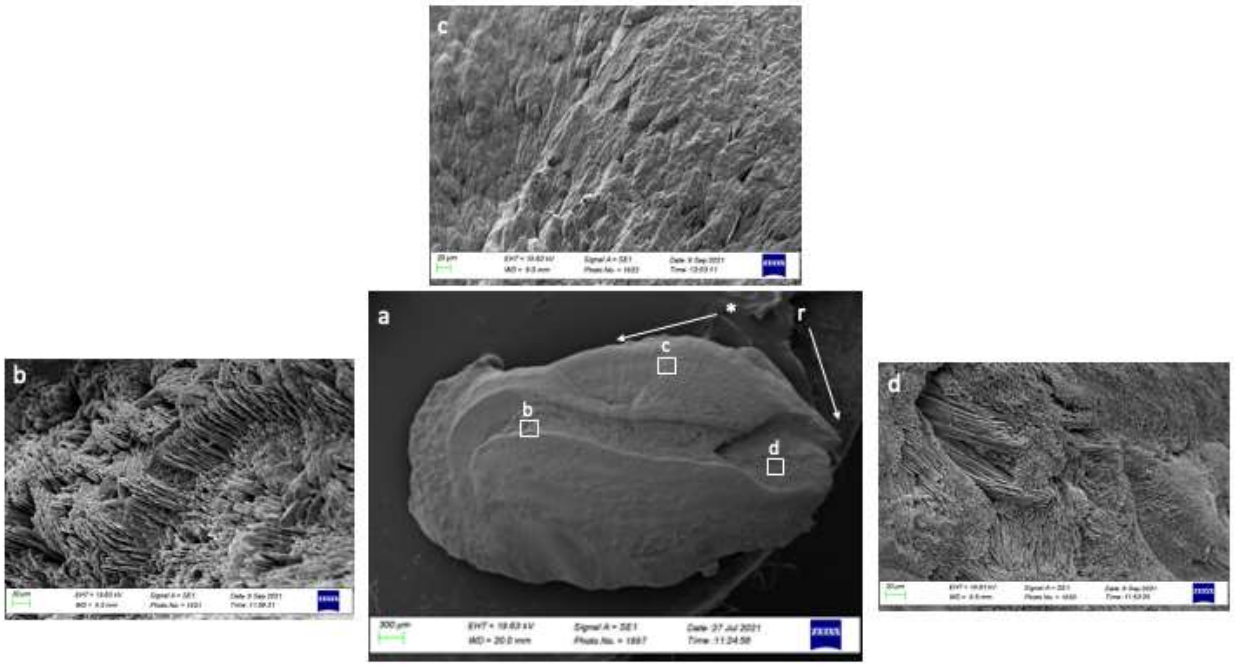

Figure 33. SEM imaging of left sagitta proximal surface in C. labrosus (a) with details of external textural organization of cauda (b), dorsal area (c) and ostium (d); (r) Indicates the rostrum and (*) indicates the dorsal rim.

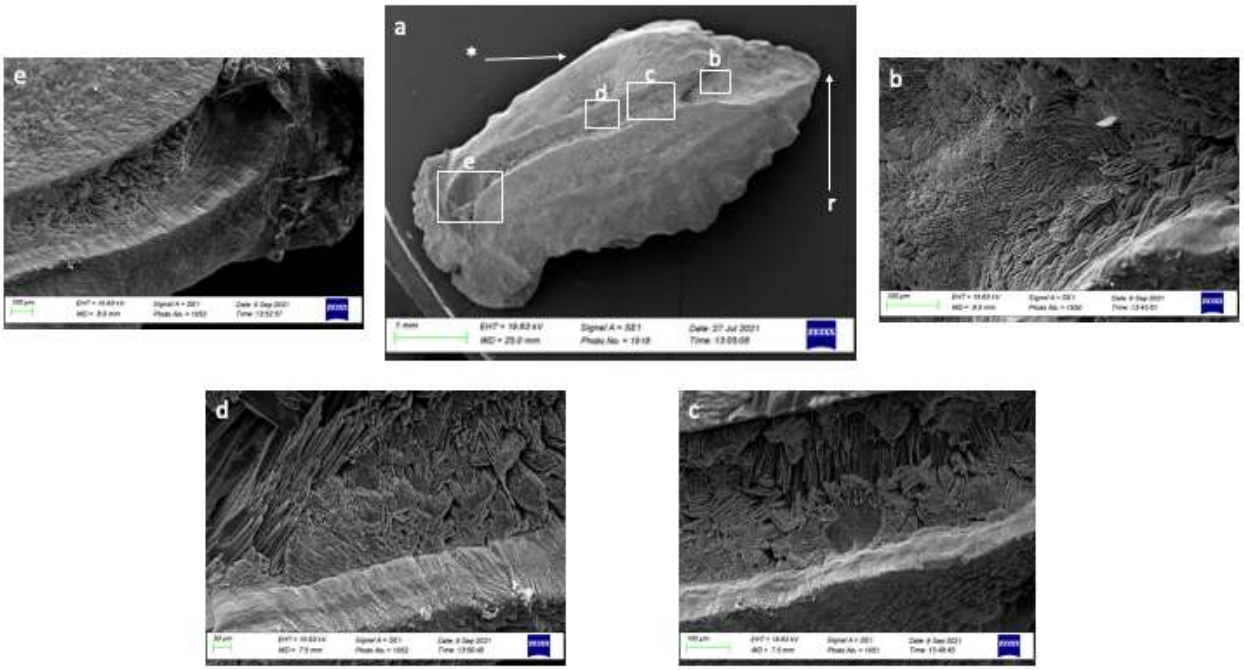

Figure 34. SEM imaging of left *sagitta* proximal surface in *O. labeo* (a) with details of external textural organization of *ostium* (b) and *cauda* (c-d-e)*;* (r) Indicates the rostrum and (*) indicates the dorsal rim.

Several polymorphs and habits of calcium carbonates were detected in many otoliths, particulary of *C. labrosus.* These crystalline habits showed different shapes and organizations: small needles locally oriented, long prisms shaped and large rhombohedral crystals. This last kind was detected on *C. labrosus sagitta* surface (Figure 35 b,c,d,e,f,g,h); the long prism shaped crystals (Figure 36 c,e) and small needles locally oriented (Figure 36 b,d)were detected on *cauda* surface of *O. labeo* and in *C. auratus.* SEM imaging showed also carbonate formations like "globular secretion" on *sagittae* surface of *C. labrosus* (Figure 37 b,c), with the evidence of large prismatic crystals (Figure 38 a,b,c).

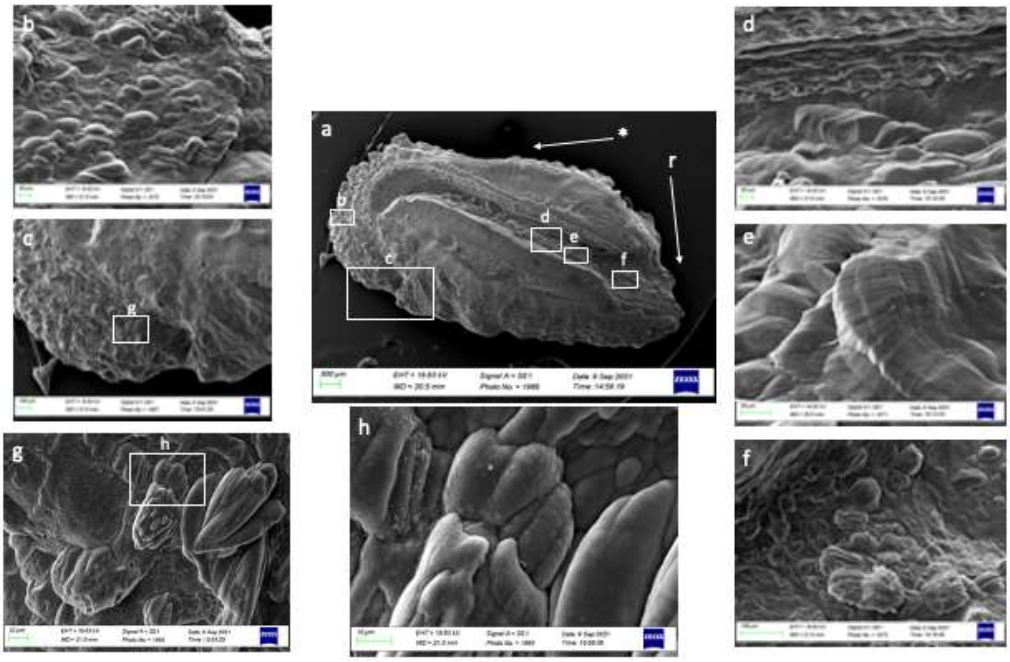

Figure 35. SEM imaging of left *sagitta* proximal surface in *C. labrosus* (a) with details of several calcium carbonates habits in posterior area (b), ventral area (c-g-h), *cauda* (d-e) and *ostium* (f); (r) Indicates the rostrum and (*) indicates the dorsal rim.

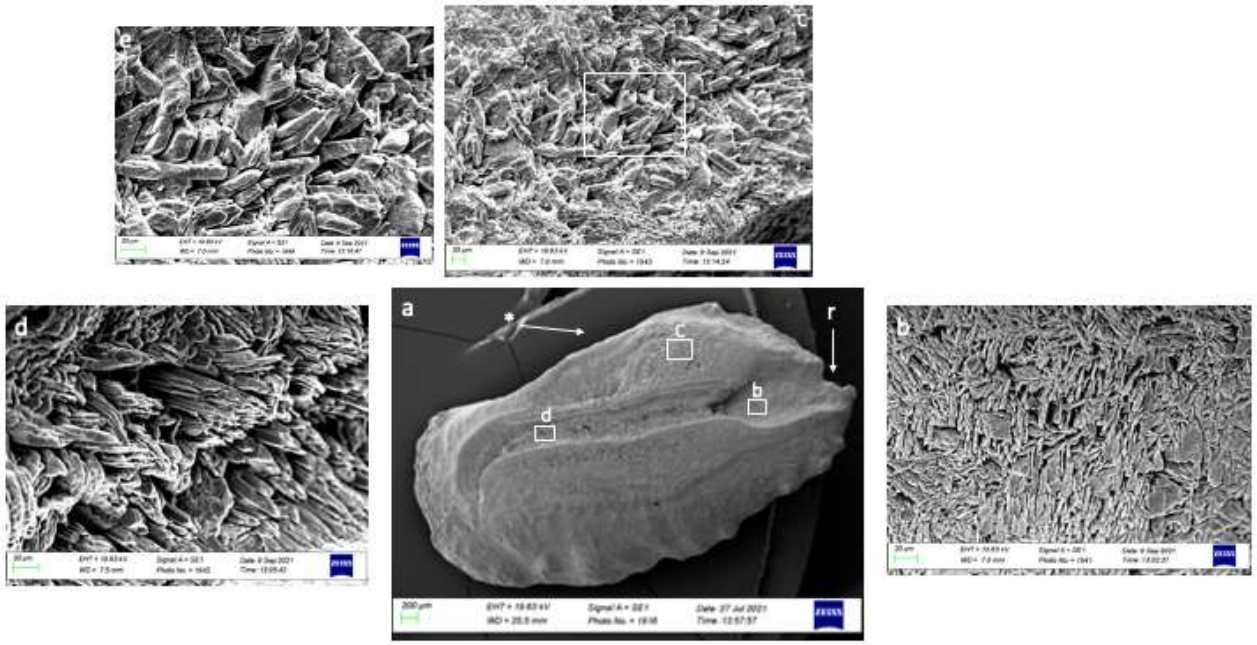

Figure 36: SEM imaging of left sagitta proximal surface in *O. labeo* (a) with details of several calcium carbonates habits in ostium (b), dorsal area (c-e) and cauda (d); (r) Indicates the rostrum and (*) indicates the dorsal rim.

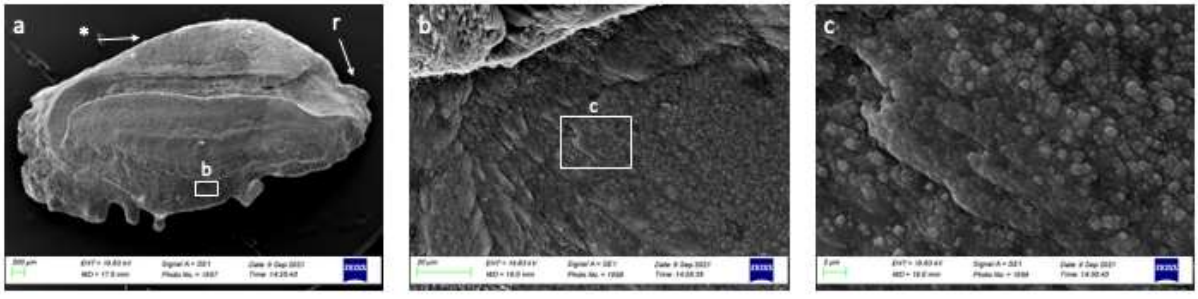

Figure 37: SEM imaging of left *sagitta* proximal surface in *C. labrosus* (a) with details of granular crystalline habit in ventral area (b-c); (r) Indicates the rostrum and (*) indicates the dorsal rim.

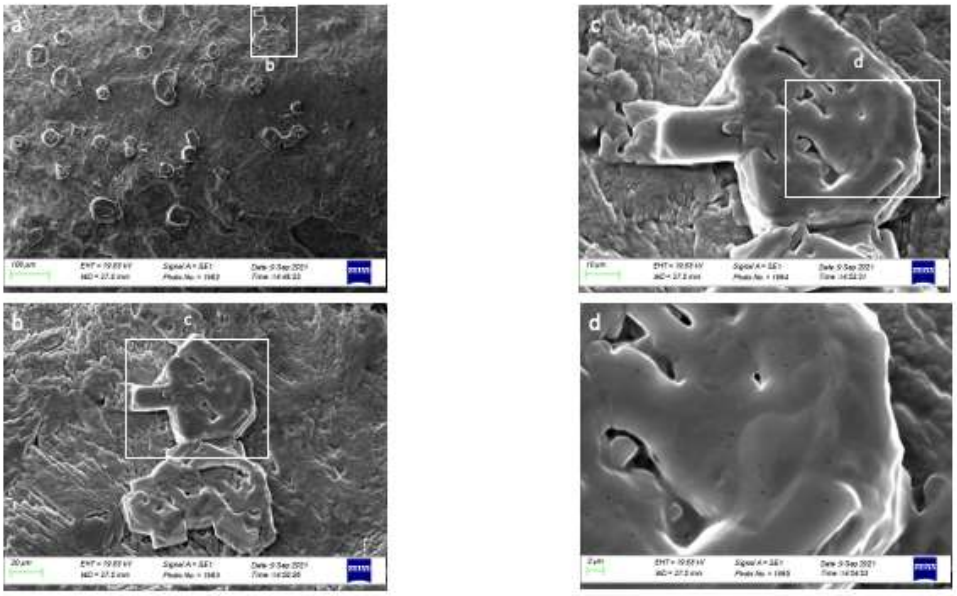

Figure 38: SEM imaging of large prismatic crystals in *C. labrosus* (a-b-c-d).

4.7 Microbiological Analysis

The microbiological analysis of the water samples carried out from June 2020 to June 2021 showed that the pH remained constant around 7 throughout the year, with a small increase to 8.14 in June 2021. The air temperature was higher in the summer and decreased in the winter, reaching the minimum temperature in February 2021. The water temperature reached a peak of 31 degrees in August and the lowest temperature in February was around 12, 13 degrees. Salinity was always between 27 and 31psu, with an increase from 31 to 37 in the period ranging from September 2020 to January 2021. The O_2 (mg/l) showed fluctuating values, in June 2020 it was around 9, in July it dropped to 5, and then in August it rose exponentially up to 11. Finally, in May 2021 it dropped to 6.5. The O_2 (%sat) showed constant values like O_2 all year round but low in July 2020 and May 2021(Table 10, App VI, 11, App VII).

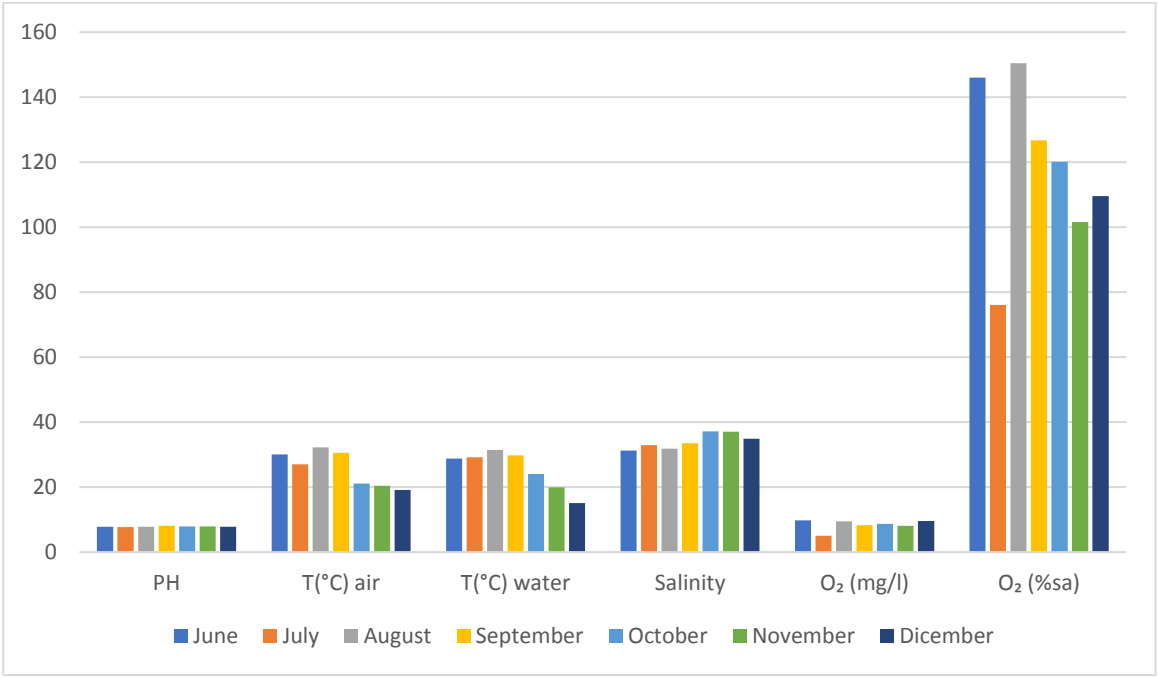

Figure 39. Parameters of pH, air temperature (°C), water temperature (°C), salinity (psu), oxygen (mg/l), and oxygen O_2 (%sat) from June 2020 to December 2020.

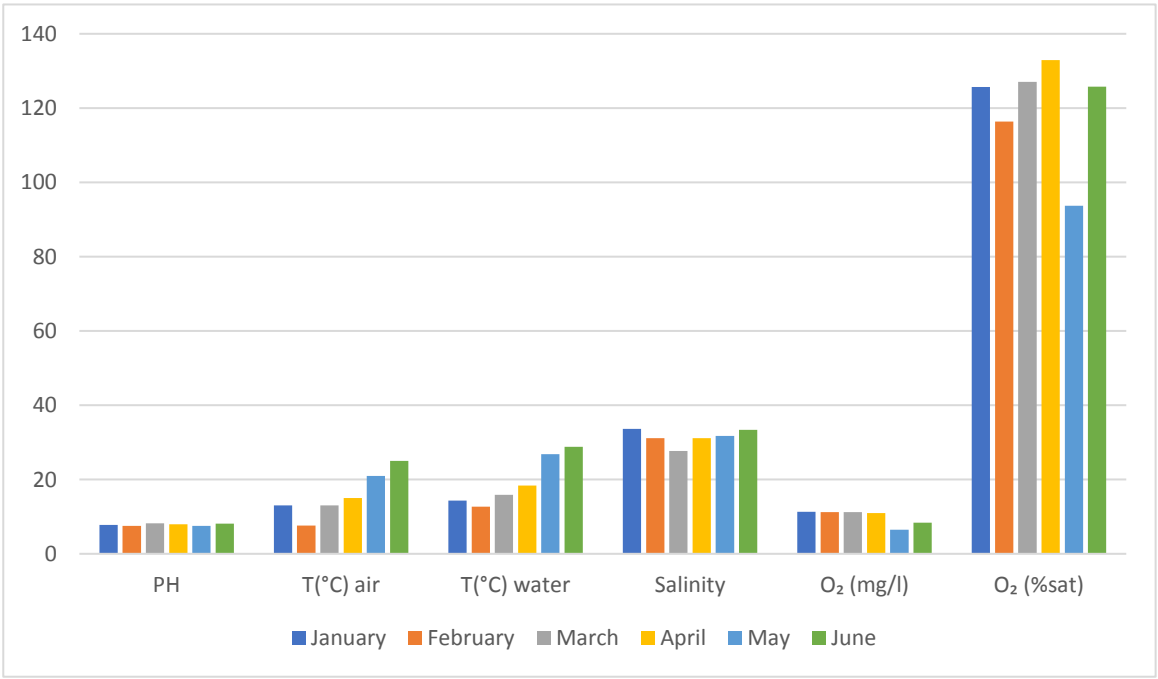

Fig. 40: Parameters of pH, air temperature(°C), water temperature(°C), salinity (psu), oxygen (mg/l), and oxygen O_2 (%sat) from January 2021 to June 2021.

5 DISCUSSION

5.1 Parasitological evaluation of gastro intestinal tract, Identification of Acanthocephala and Trematodes.

Parasitic diseases are a major problem in the culture and captive maintenance of brackish water fish. This study focused on three different species of Mugilidae. As we have seen, the most abundant species is *C. labrosus*, but the most parasitized species with a 50% positivity to trematodes is *O. labeo* even if the least represented among the fish that have been collected, because probably it enters this lake during the annual opening of the channels with the sea. The high prevalence of might suggest that this species might be highly the most predisposed to harbouring parasites. Furthermore, in all *O. labeo* specimens we observed an abundance of parasites at the intestinal level and a low number of the stomachal level. These data suggest to us that the intestine is the most affected organ. Parasite infection in fish may be the result of a single contact with intermediate hosts or it could be the result of multiple exposure to parasites, leading to the formation of parasite cysts near older infections or recovering infections (Faliex 1991). In this study along with fresh parasitological examination and subsequent molecular confirmation we identified the trematode *Haploporus benedeni* (Haploporidae Stossich,1887). The *Haploporus benedeni* life cycle is characterized by the free-swimming miracidium enters a gasteropod mollusk, in most cases Hydrobiidae: *Hydrobia acuta* or *Hydrobia ventosa*. The cercariae originate in the chairs and subsequently become encyst in the outdoor environment, finally Mugilidae infest themselves by ingesting cysts (Saad-Fares & Maillard 1985). Adult trematodes probably harm mullet minimally in natural habitats. In cases where mullets are trapped with little water and high snail densities, the danger increases. *C. labrosus* is the most abundant species found in Ganzirri Lagoon. Most of the specimens sampled had more or less the same body weight (BW) and total length (TL), with the exception of one specimen that had a BW of 1.453 g and a TL of 53 cm. This specimen showed an high trematodes abundance. The location of collecting could be distant many kilometres from where an infection originated and under different or opposite ecological conditions. For those parasites characterized by a complex life cycle, the salinity optima and tolerances evolved for molluscan and other intermediate hosts in the case of most trematodes,

and for crustacean intermediate hosts in the case of most cestodes, acanthocephalans and nematodes, bear more significance than the tolerance established for the parasite. Salinity can also regulate growth of the intermediate host and the host vulnerability to predators (Paperna 1975). An analysis carried out under the stereomicroscope showed 7,8 trematodes in the intestine and 55 trematodes in the stomach, *C. labrosus* presented the greatest variety of parasites. In two specimens, cysts were found, and their presence presumably is attributable to digenea trematodes metacercariae. Acanthocephala were found in two other specimens of *C. labrosus*. On microscopic examination the metasoma of the parasite was cylindrical, short, nearly cylindrical proboscis, slightly wider than longer, armed with a series of hooks arranged in three circles of six hooks, the first rows of hooks was larger. The neck was not clearly demarcated, about one-third the length of the proboscis. Trunk long, gently curved, robust. Elongated oval testes are located one behind the other in the middle third of the body. Female worms revealed a large number of ovarian spheres within the sac of ligaments. The spindle-shaped eggs measure up to 42 × 12 μm and contain the embryo. The morphological characteristics of the specimens, the shape and size of the proboscis, and the low number and position of spines on the proboscis clearly place this species within the genus *Neoechinorhynchus agilis* and are consistent with descriptions for *Neoechinorhynchus agilis Rudolphi*, 1819 belonging to *Acanthocephala: Neoechinorhynchus (Neoechinorhynchus) agilis (Rudolphi, 1819)* Van Cleave, 1916. The life cycle of the Acanthocephala involves the egg containing the larva which is passed into the water where it is ingested by an intermediate host (usually an amphipod or other crustacean). The larva enters the intermediate host and it develops into a cyst. When the intermediate host is ingested by a fish, the cyst matures into an adult worm or becomes embedded in the fish's tissues. The fish can then act as the final host, harboring the sexual reproductive phase of the parasite. Intermediate host, harboring the asexual reproductive phase of the parasite; depending on priority they are classified into first, second, and third intermediate hosts, or paratenic host through which the agent is mechanically transferred and in which it does not develop at all. The infected fish probably is ingested by the final host such as another fish, bird, or mammal (T. Mhaisen et al. 2014). *C. labrosus* is found in the eastern Atlantic Ocean and the Mediterranean Sea and it is the only recorded host of *N. agilis* according to this study. This *Acanthocephala* has traditionally been considered to be a parasite of *M. cephalus*. However, this is thought to be due to a lack of understanding of Mugilidae taxonomy when the original description of *N. agilis* was

published. Thus, it is impossible to define the type host for this worm. *C. labrosus* is probably a single typical host of *N. agilis*. The host specificity of the parasite may vary even though the species are close in ecology and genetics. Parasites are usually considered good biological markers of their host evolution and diversity (Mehmet Erturk 2005, Sarabeev et al. 2014). This hypothesis is supported by current knowledge about the diversity and distribution of *Neoechinorhynchus spp.* in mullet. We can infer that the species diversity of this genus may be the result of allopatric or allogenic speciation.

5.2 Identification of Five Stages of Granuloma Development from Early to Late Stage

The area investigated in the present study is the Ganzirri Lagoon (Northern Sicily), which is a transition area that compared to the waters of the Strait of Messina shows low hydro dynamism and high trophism. Because of its peculiarities, the Ganzirri Lagoon therefore represents a nursery area for many marine species because of its peculiarities. The ichthyic population studied involved three species of mugilidae: *C. labrosus, C. aurata* and *O. labeo;* the latter is typical of lagoon but it is in an evident minority compared to the other two. The family of Mugilidae includes coastal and brackish water marine species distributed throughout the temperate and tropical seas (Katselis George; Minos, George and Vidalis, Kosmas 2006). These fishes are of economic importance to fisheries and aquaculture as they are a major food source in several regions in the world. In the present study, we investigated and consequently identified five stages of granuloma development, from early to late stages. Granulomas were found in 51/150 studied specimens and some of them had multiple organs affected. A granuloma is a mass of tissue that regularly forms in response to any inflammation reaction, due to infection of microbial nature or presence of foreign material. Granulomatous reactions are found in several diseases and are characterized by a deficit in phagocytosis of the etiologic agent (Dubielzig et al. 2010, Arellano & del Pozo 2013). Granulomas can be necrotic and non-necrotic. Usually, a non-necrotic granuloma first appears and later progresses to a necrotic phase. In fish, necrotic granulomas are not easy to detect because their formation occurs internally (Reite & Evensen 2006). A granuloma consists of clusters of well-organized,

heterogeneous, dynamic and compact immune cells including macrophages, epithelial cells and fibroblasts (Sheffield 1990). When cells of the immune system encounter a pathogen a cascade of anti and pro-inflammatory signalling is initiated. This occurrence elicits the recruitment and accumulation of macrophages and other leukocytes in tissues, thus leading to the formation of granulomas. The chronic inflammatory response is a non-specific reaction to numerous factors such as bacteria, fungi, mycobacteria, noxious substances and parasites (Timur 1976, Noga et al. 1989). The first stage is phagocytosis exerted by macrophages. When the damage exceeds the phagocytic capacity of the host, the organism activates more complex mechanisms to confine the intruder in the host tissues, thus leading to the formation of granuloma (Kumar et al. 2015). The size, composition, and organization of this immune response vary according to the causative agent. In fish, the routes of infection can be numerous and transmission can occur orally, through feces or even through infected fish carcasses (Banks et al. 2014). Diseases caused by bacteria in fish can be classified into two types, non-granulomatous and granulomatous (Arellano & del Pozo 2013). The latter are a great threat to the aquaculture industry because chronic and necrotizing granulomas can lead to extensive chronic multifocal granulomatous response including multiple lesions throughout the affected organs which severely compromise the immune response of fish and ultimately its survival (Birkbeck et al. 2011). Granuloma formation is a dynamic process and many times the structure of these specific chronic inflammatory responses very often gives useful information about the timing, as well as even the evolution and prognosis of the disease. However, as observed experimentally by (Colorni et al. 1998) and recently also by (Ortega et al. 2014), granulomas can also be classified histologically into distinct developmental stages. We precisely identified 5 stages of granuloma formation: Stage I free larvae where the parasite is intact without any tissue reaction or cyst. Only 4 specimens out of 51 positive samples presented tissue changes as the free larvae stage. The second stage Encysted parasite, where the parasites resulted encysted in the parenchyma of various organs, in fact 25 samples out of 51 presented this stage of lesion involving more organs, among them the liver was the most involved organ. The parasite presented surrounded by a compact eosinophilic layer and because of the compression of the cysts the parenchyma cells were compressed. As reported by (Goubran et al. 2014, Félix et al. 2019) in this phase the inflammatory response is absent or poorly present, but if present it is characterized by a limited number of mast cells placed near the wall of the parasite or scattered in the surrounding parenchyma, and sporadically

macrophages. Studies reported by (Benedito-Palos et al. 2008) hypothesize that the lack of or poor immune response could be due to the ability of the parasite to escape the host immune system or regulate the mounting inflammatory process. In phase III (Early Stage) an inflammatory response begins to be observed being characterized by few sheets of macrophages surrounding larva. 20 samples out of 51 presented this stage of granuloma. In the stage IV (Intermediate stage granuloma), in this phase there is a clear response of the immune system to the host with several cell (macrophages, epithelioid cells, rare fibroblast at the periphery) layers around the parasite. Obviously, the immune response to the host differs depending on where the infection occurs. Four out of 51 specimens presented this stage of granuloma. Finally in stage V (Late-Stage Granuloma), represents the final and late stage of chronic inflammation, with a high number of immune cells, which led to the resolution of the infection of the parasite; the latter cannot be detected inside the lesion. Only three samples out of 51 were positive for this stage of granuloma. In this stage there is an excessive increase in collagen production, and a moderate increase in fibroblasts. This is because fibroblasts begin to degenerate after fulfilling their role, while collagen, which represents the final product of fibroblasts reaches maximum levels. Moreover, within the same tissue, mainly in the liver and once in the intestine, we found more granulomas belonging either to the same stage or to different stages. A feature that we noticed observing the samples under the microscope especially in the encysted, was that in the samples at the same magnification the granuloma had a completely different size, this makes us hypothesize the presence of different parasites within the same specimen. In addition, the existence of aggregates of macrophages associated with granuloma showed a very different presence not related to the stages of development of the granuloma, this makes us hypothesize that their presence could be explained by other factors such as age, stress, exposure to pollutants, but it could also be related to the species of fish.

5.3 Analysis of Intra-specific Morphological and Morphometric Differences in Otoliths

In order to have a clearer idea about the variability of otoliths and their relation with different habitats and environmental factors, it is fundamental to study the intra-specific morphological differences among sagittas. Many authors have carried out numerous studies just to evaluate how the morphology and the shape of the sagittas change in populations of the same species. In this way it is only possible to evaluate the stocks, and their correlation with environmental, biological and habitat variations. Very often the study of shape and morphology of different wild populations, to make comparative studies between the different areas analysed cannot fully explain the adaptive response of the sagittas to different environmental conditions or habitat, leading to morpho-functional differences between specific between different populations. To collect this date, it would be necessary to breed, under controlled environmental conditions, specimens belonging to different populations. In this way it would be possible to detect whether and which differences in the assays are due to the genetics of the animal or if they are the result of an adaptation of the animal to environmental variations and conditions (for example, phenotypic plasticity). This study highlights how the morphometric results of the sagittas of the Mugilidae in the Ganzirri area slightly differ from those ones described in the literature about the populations of the western Mediterranean Sea of the north-eastern Mediterranean, and the Atlantic Ocean. Samples of C. auratus from the area we studied showed a more rectangular sagitta, with a higher *sagitta* length to total fish length ratio and Rectangularity values, and a lower circularity and *sagitta* aspect ratio. The margins of anterior region were most regular in studied specimens than those from the Northeastern Mediterranean Sea (Çiçek et al. 2020), while the rostrum was more pointed than those from the Western Mediterranean Sea (Bauzà Rullan 1960, Tuset et al. 2008). Statistical analysis confirmed the positive correlation of the most pronounced sagitta size in the studied specimens. The positive correlation between ratio of *sulcus acusticus* surface to the entire *sagitta* and the increase in specimens' size was related to an accentuated sulcal growth, which could depend to species ecology and its adaptation to studied area. Moreover, in the case of *C. labrosus,* a different morphology was shown respect to those reported in the literature of the western Mediterranean and Atlantic Ocean organisms. It presented a much higher

rectangularity, while circularity was much lower; *sagitta* aspect ratio was the same and *sagitta* length to total fish length ratio was slightly higher. The irregular margins of anterior region were very similar to those seen in specimens from the North-eastern Mediterranean Sea, Western Mediterranean Sea and northern Atlantic Ocean (Bauzà Rullan 1960, Tuset et al. 2008, Çiçek et al. 2020), while the posterior region was very flattened. Statistical analysis proved a more accentuated increase in *sagitta* width than length related to fish length increase. A requirement which has been confirmed by the negative correlation between total fish length and *sagitta* length to total fish length ratio. Moreover, this species is the only one to show a slight difference between the left and the right *sagittas*, in particular regarding to the part of the acoustic groove, i.e the *cauda* length to *sulcus acusticus* length ratio and *ostium* length to *sulcus acusticus* length ratio. These small changes between left and right wagons are mostly likely due to ecology and food strategies. This was the first time in which these differences were detected in this species, confirming the peculiarity of specimens inhabiting Ganzirri Lagoon. Further analysis on specimens from Ganzirri Lagoon are required to confirm this hypothesis. Regarding to *O. labeo*, in the bibliography there are no studies related to morphometric calculations. It has a more rectangular *sagitta* with very regular rims in dorsal and ventral margins and very irregular anterior region than those showed by bibliography from the Northeastern Atlantic and Mediterranean Sea (Callicó Fortunato et al. 2014). The statistical analysis showed an increase in *sagitta* length negatively related to total fish length and weight. The positive correlation between *sulcus acusticus* surface to *sagitta* surface ratio and total fish length and weight has confirmed the most accentuated increasing in sulcus area of the entire *sagitta*. Moreover, we also observed a calcium carbonate overgrowth. It is not easy to find a direct correlation between environmental factors and variations in morphology and morphometric parameters of sagittas. Morphological differences between specimens from different geographic areas could lead to changes in sagitta among stocks and could depend on environmental characteristics of the Ganzirri Lagoon. This study may expand the knowledge about the morphological functionality of *sagitta* and adaptation of Mugilidae to different environmental factors of *Mugilidae*. Inter specific differences shown by results among the studied species primarily concerned circularity, rectangularity, *sagitta* aspect ratio and ratio of the *sagitta* length to the total fish length. All these differences were confirmed by the shape analysis. Indeed, contours have clearly showed a stronger circularity in *sagittae* of *O. labeo*, while a very marked rectangular shape in *C. auratus*, which also showed a longer *sagitta* with

the highest otolith width confirmed by highest values of *sagitta* aspect ratio and otolith length to total fish length ratio. The three species of mugilids revealed different characteristics. On considering life cycles *O. labeo* in particular compared to the other two It is mainly a marine species; but it is common to find it in Ganzirri Lagoon. It probably enters in this brackish coastal lake during the annual opening of canals linking to the sea. The lagoon is a transition area with a high water trophism and a low hydro dynamism, especially compared with the Strait of Messina waters. As confirmed by LDA analysis of the *sulcus acusticus,* the three Mugillidae species showed a few differences, they share the same habitats and ecological niches, they have dietary differences, *C. auratus* has habits of a pelagic predator, *O. labrosus* and *C. labrosus* have habits as both herbivores and benthic predators. Moreover *C. labrosus* showed a morphological difference of the intermediate *sagitta* between that of *C. aurata* and *O. labeo,* with a very marked rectangularity than *O. labeo* and a most marked circularity than *C. auratus*. All these peculiarities indicate that the area we studied represents a nursery area for many marine species, and an optimal environment to feed and protect against predators and strong currents of the area. Intraspecific morphological and morphometric differences in shape among sagittas represents a useful tool for species identification among the mugilidae because identification of species in this family is very difficult due to their high similarity (Whitfield et al. 2012). The SEM imaging, performed for the first time to investigate the *sagittae* external textural organization of *C. auratus, C. labrosus* and *O. labeo,* showed a very peculiar crystals organization. SEM imaging analysis proved the presence of aragonitic crystal with a various shape (circular, hexagonal and lamellar form) as described by previous research (Gauldie 1993). As showed by previous studies on *Poecilia mexicana,* Steindachner, 1863 (Schulz-Mirbach et al. 2011), also in the *sulcus acusticus* of some *O. labeo* specimens were detected large hexagonal crystal were detected. In previously mentioned paper, this peculiar crystalline habit was related to population living in well-lit surface environments. In *Acipenser brevirostrum,* Lesueur, 1818, specimens these hexagonal crystals were described as calcite-like crystals (Gauldie 1993)**.** Comparing our SEM images with those from this last study, the large rhombohedral crystals found in some *C. labrosus* specimens, they seemed like those described in *Macruronus novaezelandiae,* Hector, 1871, as static calcitic crystals. Similar prismatic calcite crystals were also found in *Cilus gilberti,* Abbott, 1899, and *Sciaena deliciosa*, Tschudi, 1846, specimens, as reported from other studies (Béarez et al. 2005). This carbonate habit was found in *sulcus acusticus* and near the posterior margin of a *C. labrosus*

specimen. Moreover, near the ventral margin of the same otolith was detected another peculiar crystal habit was detected, like the ones described in *Hoplostethus atlanticus* Collett, 1889, as small granular vateritic crystals (Gauldie 1993). Large crystals were detected in another specimen of *C. labrosus* and were like the overgrowth of calcium carbonate shown by a previous study on the otolith surface and an in vitro crystallization experiment (Bose et al. 2017). In addition, the presence of spherules on the surface of the sagitta in some specimens was also detected. The spherules could be the carbonate deposition layer, which give the otolith its globular surface. These, seemingly formed by several subunits, appeared to be similar to those described in the *Encheliophis boraborensis*, Kaup, 1856, (Çiçek et al. 2020). Such a globular carbonate deposit resulted to be similar to the calcium carbonate precipitate found on extracellular globules secreted by *Desulfonatronum lacustre* (Bauzà Rullan 1960, Mahé et al. 2021). Endolymph proteins in the inner ears of teleosts could induce carbonate precipitation as seen in this bacterium (Mahé et al. 2019), triggering the globular surface of otoliths with the presence of spherules, as shown in the SEM images of the species studied. The characteristics of Ganzirri Lagoon could be influential as it is a highly unstable environment, with fluctuations in salinity and eutrophication phenomena, which could influence carbonate precipitation triggered by endolymph proteins and consequently the crystal orientation and composition of otoliths. Further analyses of the microchemical composition of the sagittas are needed to confirm the presence and percentage of the different carbonate polymorphs. Continuous monitoring of the environmental parameters in this brackish lake may be a unique opportunity to find a correlation between crystalline variations in *sagittae* and physicochemical parameters in a natural environment.

6 CONCLUDING REMARKS AND FUTURE PERSPECTIVES

In conclusion, parasitic diseases represent a major problem for the fish's health and in some cases also for human health. Mugilids are very adaptable specimens, which is why they can be found in clear, pristine reef waters as well as in highly turbid estuaries, and can even survive in some of the most polluted waters in the world. As euralin specimens they are easily adapting to different habitats, for this reason they are very exposed to different pathogens. Parasites are organisms that live on the surface or inside the body of a host and benefit at the expense of the host, so the challenge remains between the parasite and the host. The former tries to survive inside the host and the host in turn tries to prevent the spread of infection. Parasites usually enter the host's body through the mouth or skin. Parasites that enter through the mouth are ingested and may remain in the intestines or cross the intestinal wall and invade other organs. Parasites usually enter the mouth through oro-faecal transmission. Some parasites can penetrate directly through the skin. Others are transmitted through insect bites. Rarely, transmission of parasites occurs by injections made with needles previously used by infected individuals. Mugilids undergo a significant ontogenetic change in diet, moving from feeding primarily on zooplankton in their larval stages to sediment in their later stages of development, algae (predominantly diatoms), planktonic organisms, and detritus (Cardona, 2015). Specimens that feed in fresh or brackish waters grow faster than others. This study represents a deepening knowledge of a wide range of morphometric and morphological characteristics in the otoliths of the three species of Mugilidae. In addiction this study focused on the identification of parasites taken fresh, from stomach and intestine, and an in-depth analysis of the different stages of granuloma formation. Thanks to SEM imaging, we obtained, a more accurate image of the otoliths in these three species and in addition, we studied their external textural organization in greater depth. This study provides the basis for a better understanding of the structure and eco-morphological role of the sagitta in the life cycle of *O. labeo C. labrosus and C. aurata*. Future studies using other methodologies such as, X-ray diffraction, auditory sensitive measurement, and CT scans may be useful to investigate the physiology of sagitta more thoroughly and its ecological adaptation to the environment. Such studies could be useful to help the identification of stocks and to improve the understanding of the distribution of the different Mediterranean populations and their differences, especially of *O. labeo*, although a typical species of this area, which is the least present in the Ganzirri Lagoon.

Moreover, studying the phenotypic plasticity of otoliths and the ecomorphological role of otoliths could be a valuable tool to compare the morphometry, structure, and crystalline composition of otoliths in different species of Mugilidae from different catchment areas, to evaluate how structures and sagittal features change according to different environments and habitats. This approach is essential to assess how the morphometry and shape of different sagittal areas, such as the sulcus acousticus, change under different environmental pressures. It is essential to learn more about the subsequent asymmetry between sagitta pairs in *O. labeo, C. labrosus and C. aurata*, as this may influence stock differentiation based on shape analysis between populations in different sub-areas. This characteristic of otolith morphometry and shape could be another response to environmental pressure, which could elucidate the role of phenotypic plasticity in sagitta development. Thus, this study represents a deepening of our knowledge of the inflammatory reaction associated with parasites in fish organs and the development and course of disease, as seen (Polinas et al. 2021), who studied 3 stages of granuloma development, while in this study instead we identified 5 states of granulomas (free parasite, encysted parasite, early-stage granuloma, intermediate stage, and late-stage granuloma). Moreover, histologic patterns of granulomatous response may be a reliable tool to estimate granulomas associated with parasitic infection, and to differentiate granulomas of different origins. Further studies should be performed to understand the mechanisms of granuloma formation by different parasite species in various experimental models, and at the same time to understand how they develop, and elaborate strategies capable of very early detection especially in species of high commercial interest for human consumption. This data is very important because it suggests the need for monthly monitoring in the studied area for a prolonged temporary period to determine the welfare status of fish but, above all, for the potential zoonotic implications that this disease may have for fishery and aquaculture operators.

The results of otolith analyses were used to draw up a manuscript, submitted to the journal Sustainability in the section Sustainability, Biodiversity and Conservation, Title: “Otoliths analyses highlight morpho-functional differences of three species of mullet (Mugilidae) from transitional water”

7 REFERENCES

Almeida LJ, Silva EJ Da, Freitas YM (1968) Microorganisms From Some Tropical Fish Diseases. J Fish Res Board Canada 25:197–201.

Antuofermo E, Pais A, Polinas M, Cubeddu T, Righetti M, Sanna MA, Prearo M (2017) Mycobacteriosis caused by *Mycobacterium marinum* in reared mullets: first evidence from Sardinia (Italy). J Fish Dis 40:327–337.

Arechavala-Lopez P, Uglem I, Sanchez-Jerez P, Fernandez-Jover D, Bayle-Sempere JT, Nilsen R (2012) Movements of grey mullet *liza aurata* and *chelon labrosus* associated with coastal fish farms in the western mediterranean sea. Aquac Environ Interact 1:127–136.

Arellano JLP, del Pozo S de C (2013) Manual de patología general. Elsevier.

Arundel JH (1967) Field procedure for counting gastro-intestinal worms in sheep and cattle. Aust Vet J 43:592–593.

Assis J, Gonçalves JMS, Veiga P, Pita C (2018) Spearfishing in Portugal: A baseline study on spearfishers' profiles, habits and perceptions towards management measures. Fish Manag Ecol 25:417–428.

Bacheler NM, Wong RA, Buckel JA (2005) Movements and Mortality Rates of Striped Mullet in North Carolina. North Am J Fish Manag 25:361–373.

Baldwin CC (2003) FAO species identification guide for fishery purposes. The living marine resources of the Western Central Pacific.

Banks JE, Stark JD, Vargas RI, Ackleh AS (2014) Deconstructing the surrogate species concept: A life history approach to the protection of ecosystem services. Ecol Appl 24:770–778.

Bauzà Rullan J (1960) Nueva contribución al conocimiento de los otolitos de peces actuales. Bolletí

la Soc d'Història Nat les Balear 6:49–69.

Béarez P, Carlier G, Lorand JP, Parodi GC (2005) Destructive and non-destructive microanalysis of biocarbonates applied to anomalous otoliths of archaeological and modern sciaenids (Teleostei) from Peru and Chile. Comptes Rendus - Biol 328:243–252.

Bellwood DR, Wainwright PC (2002) The History and Biogeography of Fishes on Coral Reefs. Coral Reef Fishes 5:5–32.

Belousova Y V (2019) First record of the trematoda larvae *Haplosplanchnus sp.* in gastropod *Hydrobia acuta* in the Black Sea. Parazitologiya 53:82–85.

Benedito-Palos L, Navarro JC, Sitjà-Bobadilla A, Gordon Bell J, Kaushik S, Pérez-Sánchez J (2008) High levels of vegetable oils in plant protein-rich diets fed to gilthead sea bream *(Sparus aurata L.)* : Growth performance, muscle fatty acid profiles and histological alterations of target tissues. Br J Nutr 100:992–1003.

Bianchi CN, Morri C (2000) Marine biodiversity of the Mediterranean Sea: Situation, problems and prospects for future research. Mar Pollut Bull 40:367–376.

Bignal EM, McCracken DI (2000) The nature conservation value of European traditional farming systems. Environ Rev 8:149–171.

Birkbeck TH, Feist SW, Verner-Jeffreys DW (2011) Francisella infections in fish and shellfish. J Fish Dis 34:173–187.

Boglione C, Bertolini B, Russiello M, Cataudella S (1992) Embryonic and larval development of the thicklipped mullet *(Chelon labrosus)* under controlled reproduction conditions. Aquaculture 101:349–359.

Bose APH, Adragna JB, Balshine S (2017) Otolith morphology varies between populations, sexes and male alternative reproductive tactics in a vocal toadfish Porichthys notatus. J Fish Biol 90:311–325.

2117 Bottari A, Bottari C, Carveni P (2005) Tectonic genesis of the salt marshes on the Sicilian coast of
2118 the Straits of Messina (Sicily). Alp Mediterr Quat 18:113–122.

2119 Bozzetta E, Prearo M, Penati V, Pungkachonboon T, Ghittino C (1995) Isolation and typing of
2120 mycobacteria in cultured tropical fish. Boll Soc Ital di Patol Ittica 7:13–21.

2121 Briggs JC (1995) Global biogeography. Elsevier.

2122 Brooks S, Harman C, Zaldibar B, Izagirre U, Glette T, Marigómez I (2011) Integrated biomarker
2123 assessment of the effects exerted by treated produced water from an onshore natural gas
2124 processing plant in the North Sea on the mussel *Mytilus edulis*. Mar Pollut Bull 62:327–339.

2125 Bullock GL, Stuckey HM, Chen PK (1974) Corynebacterial Kidney Disease of Salmonids: Growth
2126 and Serological Studies on the Causative Bacterium. Appl Microbiol 28:811–814.

2127 Cable RM, Hopp WB (1954) Acanthocephalan parasites of the genus *Neoechinorhynchus* in North
2128 American turtles with the descriptions of two new species. J Parasitol 40:674–680.

2129 Callicó Fortunato R, Benedito Durà V, Volpedo A (2014) The morphology of saccular otoliths as a
2130 tool to identify different mugilid species from the Northeastern Atlantic and Mediterranean Sea.
2131 Estuar Coast Shelf Sci 146:95–101.

2132 Cambrony M (1980) Identification et périodicité du recrutement des juvéniles de Mugilidae dans les
2133 étangs littoraux du Languedoc-Roussillon. Vie milieu 34:221–227.

2134 Carballo R, Campo Dall'Orto V, Lo Balbo A, Rezzano I (2003) Determination of sulfite by flow
2135 injection analysis using a poly[Ni-(protoporphyrin IX)] chemically modified electrode. Sensors
2136 Actuators, B Chem 88:155–161.

2137 Carpenter KE, Springer VG (2005) The center of the center of marine shore fish biodiversity: The
2138 Philippine Islands. Environ Biol Fishes 72:467–480.

2139 Chai J-Y, Murrell KD, Lymbery AJ (2005) Fish-borne parasitic zoonoses: status and issues. Int J

2140 Parasitol 35:1233–1254.

2141 Chai JY, Jung BK (2017) Fishborne zoonotic heterophyid infections: An update. Food Waterborne
2142 Parasitol 8–9:33–63.

2143 Chai T, Draxler RR (2014) Root mean square error (RMSE) or mean absolute error (MAE)? -
2144 Arguments against avoiding RMSE in the literature. Geosci Model Dev 7:1247–1250.

2145 Chaoui L, Kara MH, Faure É, Quignard JP (2006) L'ichtyofaune de la lagune du Mellah (Algérie
2146 Nord-Est): Diversité, production et analyse des captures commerciales. Cybium 30:123–132.

2147 Çiçek E, Avşar D, Yeldan H, Manaşirli M (2020) Comparative morphology of the sagittal otolith of
2148 mullet species (Mugilidae) from the Iskenderun Bay , north-eastern Mediterranean. Acta Biol
2149 Turc 33:219–226.

2150 Colorni A, Avtalion R, Knibb W, Berger E, Colorni B, Timan B (1998) Histopathology of sea bass
2151 *(Dicentrarchus labrax)* experimentally infected with *mycobacterium marinum* and treated with
2152 *streptomycin and garlic* (Allium sativum) extract. Aquaculture 160:1–17.

2153 D'Iglio C, Albano M, Famulari S, Savoca S, Panarello G, Di Paola D, Perdichizzi A, Rinelli P, Lanteri
2154 G, Spanò N, Capillo G (2021) Intra- and interspecific variability among congeneric *Pagellus*
2155 otoliths. Sci Rep 11:1–15.

2156 Daan N (1987) Fishes of the North-eastern Atlantic and the Mediterranean.

2157 Dall WH, Dorville E, Montagu G (2011) Testacea Britannica, or, Natural history of British shells,
2158 marine, land, and fresh-water, including the most minute : systematically arranged and
2159 embellished with figures / by George Montagu. White.

2160 Decostere A, Hermans K, Haesebrouck F (2004) Piscine mycobacteriosis: A literature review
2161 covering the agent and the disease it causes in fish and humans. Vet Microbiol 99:159–166.

2162 Dmitrieva L, Kondakov AA, Oleynikov E, Kydyrmanov A, Karamendin K, Kasimbekov Y,

2163 Baimukanov M, Wilson S, Goodman SJ (2013) Assessment of Caspian Seal By-Catch in an
2164 Illegal Fishery Using an Interview-Based Approach. PLoS One 8:e67074.

2165 De Domenico E (1987) Caratteristiche fisiche e chimiche delle acque nello Stretto di Messina. Doc
2166 Trav l'Institut géologique Albert Lapparent:225–235.

2167 Dubielzig R, Ketring K, McLellan G, Albert D, Davis FA (2010) Veterinary Ocular Pathology. Vet
2168 Ocul Pathol.

2169 Durand JD, Chen WJ, Shen KN, Fu C, Borsa P (2012) Genus-level taxonomic changes implied by
2170 the mitochondrial phylogeny of grey mullets (Teleostei: Mugilidae). Comptes Rendus - Biol
2171 335:687–697.

2172 Ebeling AW (1957) The Dentition of Eastern Pacific Mullets, with Special Reference to Adaptation
2173 and Taxonomy. Copeia 1957:173.

2174 el-Ganayni GA, Youssef ME, Handousa AE, Bou-Zakham AA, Hegazi MM (1989) Serum and
2175 intestinal immunoglobulins in heterophyiasis. J Egypt Soc Parasitol 19:219–223.

2176 van der Elst RP, Wallace JH (1976) Identification of the juvenile mullet of the east coast of South
2177 Africa. J Fish Biol 9:371–374.

2178 Eschmeyer WN, Fricke R, Van der Laan R (2015) Catalog of fishes: Genera. Species, Ref.

2179 Faliex E (1991) Ultrastructural study of the host-parasite interface after infection of two species of
2180 teleosts by *Labratrema minimus* metacercariae (Trematoda, Bucephalidae). Dis Aquat Organ
2181 10:93–101.

2182 Félix F, Van Bressem MF, Van Waerebeek K (2019) Role of social behaviour in the epidemiology
2183 of lobomycosis-like disease (LLD) in estuarine common bottlenose dolphins from Ecuador. Dis
2184 Aquat Organ 134:75–87.

2185 Ferguson JS, Martin JL, Azad AK, McCarthy TR, Kang PB, Voelker DR, Crouch EC, Schlesinger

2186 LS (2006) Surfactant protein D increases fusion of *Mycobacterium tuberculosis* - containing
2187 phagosomes with lysosomes in human macrophages. Infect Immun 74:7005–7009.

2188 Fernandez WS, Dias JF (2013) Aspects of the reproduction of *Mugil curema* Valenciennes, 1836 in
2189 two coastal systems in southeastern Brazil. Trop Zool 26:15–32.

2190 Fredj G, Giaccone G (1995) Particulariés des peuplements benthiques du détroit de Messine. Striati
2191 Messin Ecosyst Proc Symp held Messin 4-6 April 1991:119–128.

2192 Freeburg EDW (2014) Exploring the link between otolith growth and function along the biological
2193 continuum in the context of ocean acidification. University of Massachusetts Boston.

2194 Fullwood P, Marchini S, Rader JS, Martinez A, Macartney D, Broggini M, Morelli C, Barbanti-
2195 Brodano G, Maher ER, Latif F (1999) Detailed genetic and physical mapping of tumor
2196 suppressor loci on chromosome 3p in ovarian cancer. Cancer Res 59:4662–4667.

2197 Galaktionov K V., Skirnisson K (2007) New data on Microphallus breviatus Deblock & Maillard,
2198 1975 (Microphallidae: Digenea) with emphasis on the evolution of dixenous life cycles of
2199 microphallids. Parasitol Res 100:963–971.

2200 Gallardo-Cabello M, Espino-Barr E, Cabral-Solís EG, Puente-Gómez M, García-Boa A (2012) Study
2201 of the otoliths of stripped mullet *Mugil cephalus* Linnaeus, 1758 in Mexican Central Pacific. J
2202 Fish Aquat Sci 7:346–363.

2203 Gauldie RW (1993) Polymorphic crystalline structure of fish otoliths. J Morphol 218:1–28.

2204 Gauthier DT, Rhodes MW (2009) Mycobacteriosis in fishes: A review. Vet J 180:33–47.

2205 Gauthier M, Bidault F, Mosnier A, Bablishvili N, Tukvadze N, Somphavong S, Paboriboune P,
2206 Ocheretina O, Pape JW, Paranhos-Baccala G, Berland JL (2015) High-throughput mycobacterial
2207 interspersed repetitive-unit-variable-number tandem-repeat genotyping for *mycobacterium*
2208 *tuberculosis* epidemiological studies. J Clin Microbiol 53:498–503.

2209 Gautier D, Hussenot J (2005) Les mulets des mers d'Europe ; synthèse des connaissances sur les
2210 bases biologiques et les techniques d'aquaculture. L'Houmeau, Fr Ifremer:119.

2211 Genovese S (1961) Sul fenomeno dell'«acqua rossa» riscontrato nello stagno salmastro di Faro
2212 (Messina). Atti Soc pelor Sci fis mat nat 7:269–271.

2213 Ghadirnejad H, Ryland JS (1996) A study of food and feeding of grey mullets in the southern of teh
2214 Caspian Sea. GUTSHOP 96:137–144.

2215 Ghasemzadeh J (1998) Phylogeny and Systematics of Indo-Pacific mullets (Teleostei: Mugilidae)
2216 with special reference to mullets of Australia.

2217 Ghittino C, Bozzetta E (1994) Profilassi delle zoonosi di origine ittica. Med Vet Prev 7:5–6.

2218 Giaccone G, Scammacca B, Cinelli F, Sartoni G, Furnari G (1972) Studio preliminare sulla tipologia
2219 della vegetazione sommersa del canale di sicilia e isole vicine. G Bot Ital 106:211–229.

2220 González-Castro M, Ghasemzadeh J (2016) Morphology and Morphometry Based Taxonomy of
2221 Mugilidae. Biol Ecol Cult Grey Mullets:1–21.

2222 González-Castro M, Macchi GJ, Cousseau MB (2011) Studies on reproduction of the mullet *Mugil*
2223 *platanus Günther*, 1880(Actinopterygii, Mugilidae) from the Mar Chiquita coastal lagoon,
2224 Argentina: Similarities and differences with related species. Ital J Zool 78:343–353.

2225 González Castro M, Abachian V, Perrotta RG (2009) Age and growth of the striped mullet, *Mugil*
2226 *platanus* (Actinopterygii, Mugilidae), in a southwestern Atlantic coastal lagoon (37°32'S-
2227 57°19'W): A proposal for a life-history model. J Appl Ichthyol 25:61–66.

2228 Goubran HA, Kotb RR, Stakiw J, Emara ME, Burnouf T (2014) Regulation of Tumor Growth and
2229 Metastasis: The Role of Tumor Microenvironment. Cancer Growth Metastasis 7:CGM.S11285.

2230 Griffith DE, Brown-Elliott BA, Langsjoen B, Zhang Y, Pan X, Girard W, Nelson K, Caccitolo J,
2231 Alvarez J, Shepherd S, Wilson R, Graviss EA, Wallace RJ (2006) Clinical and molecular

2232 analysis of macrolide resistance in *Mycobacterium avium complex* lung disease. Am J Respir
2233 Crit Care Med 174:928–934.

2234 Grodzinski P, Liu RH, Chen B, Blackwell J, Liu Y, Rhine D, Smekal T, Ganser D, Romero C, Yu H,
2235 Chan T, Kroutchinina N (2001) Development of plastic microfluidic devices for sample
2236 preparation. Biomed Microdevices 3:275–283.

2237 Hamdy EI, Nicola E (1980) On the histopathology of the small intestine in animals experimentally
2238 infected with *H. heterophyes* . J Egypt Med Assoc 63:179–184.

2239 Harrison, I. J., Howes GJ (1991) The pharyngobranchial organ of mugilid fishes; its
2240 structure,variability, ontogeny, possible function and taxonomic utility. Bull Br Mus nat Hist
2241 57:111–132.

2242 Harrison TD (2002) Preliminary assessment of the biogeography of fishes in South African estuaries.
2243 Mar Freshw Res 53:479–490.

2244 Hassantabar F, Zorriehzahra MJ, Firouzbakhsh F, Thompson KD (2021) Detection of betanodavirus
2245 in wild golden grey mullet *(Chelon aurata)* in southern parts of the Caspian Sea using Real-
2246 time RT-PCR and immunohistochemistry. Iran J Fish Sci 20:1317–1335.

2247 Hastings PA (2011) Complementary approaches to systematic ichthyology. Zootaxa 2946:57–59.

2248 Hoeksema DF (1998) Note on the occurrence of *Hydrobia acuta* (Draparnaud, 1805) (Gastropoda,
2249 Prosobranchia: Hydrobiidae) in western Europe, with special reference to a record from S.
2250 Brittany, France : Hoeksema, D F : Free Download, Borrow, and Streaming : Internet A. Basteria
2251 61:101–113.

2252 Hotta H, Tung I-S (1966) Identification of fishes of the family Mugildae based on the pyloric caeca
2253 and, the position on inserted first interneural spine. Japanese J Ichthyol 14:62–66.

2254 Hubbs C (1976) The Diel Reproductive Pattern and Fecundity of Menidia audens. Copeia 1976:386.

2255 Hubert N, Meyer CP, Bruggemann HJ, Guérin F, Komeno RJL, Espiau B, Causse R, Williams JT,
2256 Planes S (2012) Cryptic diversity in indo-pacific coral-reef fishes revealed by DNA-barcoding
2257 provides new support to the centre-of-overlap hypothesis. PLoS One 7:e28987.

2258 Huval B, Wang T, Tandon S, Kiske J, Song W, Pazhayampallil J, Andriluka M, Rajpurkar P,
2259 Migimatsu T, Cheng-Yue R, Mujica F, Coates A, Ng AY (2015) An Empirical Evaluation of
2260 Deep Learning on Highway Driving. arXiv Prepr arXiv150401716.

2261 Jawad LA, Sabatino G, Ibáñez AL, Andaloro F, Battaglia P (2018) Morphology and ontogenetic
2262 changes in otoliths of the mesopelagic fishes *Ceratoscopelus maderensis* (Myctophidae),
2263 Vinciguerria attenuata and *V. poweriae (Phosichthyidae)* from the Strait of Messina
2264 (Mediterranean Sea). Acta Zool 99:126–142.

2265 Katselis George; Minos, George and Vidalis, Kosmas GH (2006) Phenotypic affinities on fry of four
2266 mediterranean grey mullet species. Turkish J Fish Aquat Sci 6:49–55.

2267 Katselis G, Hotos G, Minos G, Vidalis K (2006) Phenotypic affinities on fry of four Mediterranean
2268 grey mullet species. Turkish J Fish Aquat Sci 6:49–55.

2269 Khemis I Ben, Gisbert E, Alcaraz C, Zouiten D, Besbes R, Zouiten A, Masmoudi AS, Cahu C (2013)
2270 Allometric growth patterns and development in larvae and juveniles of thick-lipped grey mullet
2271 *Chelon labrosus* reared in mesocosm conditions. Aquac Res 44:1872–1888.

2272 Kobelkowsky AD, Reséndez AM (1972) Estudio comparativo del endoesqueleto de *Mugil cephalus*
2273 *y Mugil curema* (Pisces: Perciformes). An del Inst Biol Univ Nac Autónoma México Serie
2274 Cien:33–81.

2275 Kottelat M, Freyhof J (2007) Handbook of European freshwater fishes. Publications Kottelat.

2276 Kulbicki M, Parravicini V, Mouillot D (2015) Patterns and processes in reef fish body size. Ecol
2277 Fishes Coral Reefs 421:104–115.

2278 Kumar A, Sherlin HJ, Ramani P, Natesan A, Premkumar P (2015) Expression of CD 68, CD 45 and

2279 human leukocyte antigen-DR in central and peripheral giant cell granuloma, giant cell tumor of
2280 long bones, and tuberculous granuloma: An immunohistochemical study. Indian J Dent Res
2281 26:295–303.

2282 Lahav M, Sarig S (1967) Ergasilus sieboldi, Nordman infestation of grey mullet in Israel fish ponds.
2283 Bamidgeh, Bull Fish Cult Isr 19:69–80.

2284 Lewis JF, Johnson P, Miller P (1976) Evaluation of amniotic fluid for aerobic and anaerobic bacteria.
2285 Am J Clin Pathol 65:58–63.

2286 Lewis S, Chinabut S (2011) Mycobacteriosis and nocardiosis. Fish Dis Disord 3:397–423.

2287 Lombarte A, Tuset VM (2015) Morfometría de otolitos. Método Estud con otolitos principios y
2288 Apl:60–91.

2289 Luther G (1975) New characters for consideration in the taxonomic appraisal of grey mullets.
2290 Aquaculture 5:107.

2291 Mahé K, Ider D, Massaro A, Hamed O, Jurado-Ruzafa A, Gonçalves P, Anastasopoulou A, Jadaud
2292 A, Mytilineou C, Elleboode R, Ramdane Z, Bacha M, Amara R, De Pontual H, Ernande B (2019)
2293 Directional bilateral asymmetry in otolith morphology may affect fish stock discrimination
2294 based on otolith shape analysis. ICES J Mar Sci 76:232–243.

2295 Mahé K, Mackenzie K, Ider D, Massaro A, Hamed O, Jurado-ruzafa A, Gonçalves P, Anastasopoulou
2296 A, Jadaud A, Mytilineou C, Randon M, Elleboode R, Morell A, Ramdane Z, Smith J, Bekaert
2297 K, Amara R, de Pontual H, Ernande B (2021) Directional bilateral asymmetry in fish otolith: A
2298 potential tool to evaluate stock boundaries? Symmetry (Basel) 13:987.

2299 Marin E. BJ, Quintero A, Bussière D, Dodson JJ (2003) Reproduction and recruitment of white mullet
2300 (Mugil curema) to a tropical lagoon (Margarita Island, Venezuela) as revealed by otolith
2301 microstructure. Fish Bull 101:809–821.

2302 Matić-Skoko S, Ferri J, Kraljević M, Pallaoro A (2012) Age estimation and specific growth pattern

of boxlip mullet, *Oedalechilus labeo* (Cuvier, 1829) (Osteichthyes, Mugilidae), in the eastern Adriatic Sea. J Appl Ichthyol 28:182–188.

Mehlhorn K, Newell BR, Todd PM, Lee MD, Morgan K, Braithwaite VA, Hausmann D, Fiedler K, Gonzalez C (2015) Unpacking the exploration-exploitation tradeoff: A synthesis of human and animal literatures. Decision 2:191–215.

Mehmet Erturk S (2005) Retrospective Power Analysis: When? Radiology 237:743–744.

Minos G, Katselis G, Ondrias I, Harrison IJ (2002) Use of melanophore patterns on the ventral side of the head to identify fry of grey mullets (teleostei: Mugilidae). Isr J Aquac - Bamidgeh 54:12–26.

Mladineo I, Bott NJ, Nowak BF, Block BA (2010) Multilocus phylogenetic analyses reveal that habitat selection drives the speciation of Didymozoidae (Digenea) parasitizing Pacific and Atlantic bluefin tunas. Parasitology 137:1013–1025.

Montanini S, Stagioni M, Valdrè G, Tommasini S, Vallisneri M (2015) Intra-specific and inter-specific variability of the sulcus acusticus of sagittal otoliths in two gurnard species (Scorpaeniformes, Triglidae). Fish Res 161:93–101.

Montenat C, Barrier P, Di Geronimo I (1987) The Strait of Messina, past and present: a review. Doc Trav l'Institut géologique Albert Lapparent:7–13.

Noga EJ, Dykstra MJ, Wright JF (1989) Chronic inflammatory cells with epithelial cell characteristics in teleost fishes. Vet Pathol 26:429–437.

Oda M, Satta Y, Takenaka O, Takahata N (2002) Loss of urate oxidase activity in hominoids and its evolutionary implications. Mol Biol Evol 19:640–653.

Oğuz T, Öztürk B (2015) Mechanisms impeding natural Mediterranization process of Black Sea fauna. J Black Sea / Mediterr Environ 17:234–253.

2326 Ohji M, Arai T, Miyazaki N (2007) Comparison of organotin accumulation in the masu salmon
2327 *Oncorhynchus masou* accompanying migratory histories. Estuar Coast Shelf Sci 72:721–731.

2328 Ortega C, Liao R, Anderson LN, Rustad T, Ollodart AR, Wright AT, Sherman DR, Grundner C
2329 (2014) *Mycobacterium tuberculosis* Ser/Thr Protein Kinase B Mediates an Oxygen-Dependent
2330 Replication Switch. PLoS Biol 12:e1001746.

2331 Panfili J, Aliaume C, Anastasopoulou A, Berrebi P, Casellas C, Chang C-W, Diouf PS, Durand J-D,
2332 Hernandez DF, de León FJG (2016) *Grey Mullet* as Possible Indicator of Coastal
2333 Environmental Changes: the MUGIL Project. In: *Biology, Ecology and Culture of Grey Mullets*
2334 *(Mugilidae)*. Taylor and Francis London, p 514–521

2335 Paperna I (1975) Parasites and diseases of the grey mullet (Mugilidae) with special reference to the
2336 seas of the Near East. Aquaculture 5:65–80.

2337 Paperna I, Lahav M (1971) New records and further data on fish parasites in Israel. Bamidgeh.vol23
2338 233:43–52.

2339 Perlmutter A, Bograd L, Pruginin J (1957) Use of the estuarine and sea fish of the family Mugilidae
2340 (grey mullets) for pond culture in Israel. FAO.

2341 Pica T (2005) Second language acquisition research and applied linguistics. Handb Res Second Lang
2342 Teach Learn 18:263–280.

2343 Piersimoni C, Scarparo C (2009) Extrapulmonary infections associated with *nontuberculous*
2344 *mycobacteria* in immunocompetent persons. Emerg Infect Dis 15:1351–1358.

2345 Polinas M, Padrós F, Merella P, Prearo M, Sanna MA, Marino F, Burrai G Pietro, Antuofermo E
2346 (2021) Stages of Granulomatous Response Against Histozoic Metazoan Parasites in Mullets
2347 (Osteichthyes: Mugilidae). Animals 11:1501.

2348 Poluzzi A, Ligi M, Badalini M (1997) Bryozoan transport in high-energy environments (Strait of
2349 Messina, Sicily). G Geol 59:55–79.

2350 Pourahmad F, Nemati M, Richards RH (2014) Comparison of three methods for detection of
2351 *Mycobacterium marinum* in goldfish (Carassius auratus). Aquaculture 422–423:42–46.

2352 Prearo M, Zanoni RG, Campo Dall'Orto B, Pavoletti E, Florio D, Penati V, Ghittino C (2004)
2353 Mycobacterioses: Emerging pathologies in aquarium fish. Vet Res Commun 28:315–317.

2354 Prisic S, Dankwa S, Schwartz D, Chou MF, Locasale JW, Kang CM, Bemis G, Church GM, Steene
2355 H, Husson RN (2010) Extensive phosphorylation with overlapping specificity by
2356 *Mycobacterium tuberculosis* serine/threonine protein kinases. Proc Natl Acad Sci U S A
2357 107:7521–7526.

2358 Rangin C, Jolivet L, Pubellier M (1990) A simple model for the tectonic evolution of Southeast Asia
2359 and Indonesia region for the past 43 m.y. Bull la Société Géologique Fr VI:889–905.

2360 Rawson E (1973) Scipio, Laelius, Furius and the Ancestral Religion. J Rom Stud 63:161–174.

2361 Reay PJ, Cornell V (1988) Identification of grey mullet (Teleostei: Mugilidae) juveniles from British
2362 waters. J Fish Biol 32:95–99.

2363 Reite OB, Evensen Ø (2006) Inflammatory cells of teleostean fish: A review focusing on mast
2364 cells/eosinophilic granule cells and rodlet cells. Fish Shellfish Immunol 20:192–208.

2365 Requena L, Kutzner H, Escalonilla P, Ortiz S, Schaller J, Rohwedder A (1998) Cutaneous reactions
2366 at sites of herpes zoster scars: An expanded spectrum. Br J Dermatol 138:161–168.

2367 Routtu J, Grunberg D, Izhar R, Dagan Y, Guttel Y, Ucko M, Ben-Ami F (2014) Selective and
2368 universal primers for trematode barcoding in freshwater snails. Parasitol Res 113:2535–2540.

2369 Saad-Fares A, Maillard C (1985) Étude en microscopie électronique à balayage du kyste
2370 métacercarien de Saccocoelium tensum Looss, 1902 (Trematoda-Haploporidae). Ann Parasitol
2371 Hum Comparée 60:119–122.

2372 Sala C, Forti F, Di Florio E, Canneva F, Milano A, Riccardi G, Ghisotti D (2003) *Mycobacterium*

tuberculosis fura autoregulates its own expression. J Bacteriol 185:5357–5362.

Salati S, Moore F (2010) Assessment of heavy metal concentration in the Khoshk River water and sediment, Shiraz, Southwest Iran. Environ Monit Assess 164:677–689.

Sarabeev VL, Tkach I V., Shvetsova LS (2014) Taxonomic status of *neoechinorhynchus agilis* (Acanthocephala, neoechinorhynchidae), with a description of two new species of the genus from the Atlantic and Pacific Mullets (Teleostei, mugilidae). Vestn Zool 48:291–306.

Schultz LP (1946) A revision of the genera of mullets, fishes of the family Mugilidae, with descriptions of three new genera. Proc United States Natl Museum 96:377–395, 5 figs.

Schulz-Mirbach T, Riesch R, García de León FJ, Plath M (2011) Effects of extreme habitat conditions on otolith morphology - a case study on extremophile livebearing fishes (Poecilia mexicana, P. sulphuraria). Zoology 114:321–334.

Şeleci DA, Gümüş ZP, Yavuz M, Şeleci M, Bongartz R, Stahl F, Coşkunol H, Timur S, Scheper T (2015) A case study on in vitro investigations of the potent biological activities of wheat germ and black cumin seed oil. Turkish J Chem 39:801–812.

Senou H (1988) Phylogenetic interrelationships of the Mullets (Pisces: Mugilidae) . Unpubl PhD Thesis, Univ Tokyo, Japan (in Japanese):172.

Serventi M, Harrison IJ, Torricelli P, Gandolfi G (1996) The use of pigmentation and morphological characters to identify Italian mullet fry. J Fish Biol 49:1163–1173.

Sheffield EA (1990) The granulomatous inflammatory response. J Pathol 160:1–2.

Song J (1981) Chinese mugilid fishes and morphology of their cephalic lateral-line canals. Sinozoologia 1:9–22.

Spalding NJ, Phillips T (2007) Exploring the use of vignettes: From validity to trustworthiness. Qual Health Res 17:954–962.

2396 Spencer Cobbold T (1866) On the Discovery of Trichina. Lancet 87:224–225.

2397 Sunny KG (1971) Morphology of the vertebral column of Mugil macrolepis (Smith). Bull Dep Mar
2398 Ocean Univ Cochin 5:101–108.

2399 T. Mhaisen F, R. Khamees najim, H. Ali A (2014) Checklists of Acanthocephalans of Freshwater
2400 and Marine Fishes of Basrah Province, Iraq. Basrah J Agric Sci 27:21–34.

2401 Teichert-Coddington DR, Popma TJ, Lovshin LL (2017) Attributes of tropical pond-cultured fish. In:
2402 *Dynamics of pond aquaculture*. CRC press, p 183–198

2403 Thomson JM (1963) Synopsis of biological data on the grey mullet *Mugil cephalus* Linnaeus 1758.
2404 CSIRO Fish Oceanogr Fish Synopsis 1:1–77.

2405 Thomson JM (1997) The Mugilidae of the world. Mem Queensl Museum 41:547–562.

2406 Timur A (1976) Temperature dependence of compressional and shear wave velocities in rocks.
2407 SPWLA 17th Annu Logging Symp 1976 42:950–956.

2408 Tomás-Zapico C, Coto-Montes A (2005) A proposed mechanism to explain the stimulatory effect of
2409 melatonin on antioxidative enzymes. J Pineal Res 39:99–104.

2410 Tramontana M, Morelli D, Colantoni P (1995) Tettonica Plio-Quaternaria del sistema sud-garganico
2411 (settore orientale) nel quadro evolutivo dell'Adriatico centro-meridionale. Stud Geol Camerti,
2412 Vol Spec:467–473.

2413 Turan C (2014) Genetic studies on the Black Sea marine biota. Turkish Fish Black Sea Turkish Mar
2414 Res Found Publ Istanbul, Turkey.

2415 Turan C, Caliskan M, Kucuktas H (2005) Phylogenetic relationships of nine mullet species
2416 (Mugilidae) in the Mediterranean Sea. Hydrobiologia 532:45–51.

2417 Turan C, Gürlek M, Ergüden D, Yağlioğlu D, Öztürk B (2011) Systematic status of nine mullet

2418 species (mugilidae) in the Mediterranean sea. Turkish J Fish Aquat Sci 11:315–321.

2419 Tuset VM, Lombarte A, Assis CA (2008) Otolith atlas for the western Mediterranean, north and
2420 central eastern Atlantic. Sci Mar 72:7–198.

2421 Varello A, Carrera E (2014) Free vibration response of thin and thick nonhomogeneous shells by
2422 refined one-dimensional analysis. J Vib Acoust Trans ASME 136.

2423 Whitfield AK, Panfili J, Durand JD (2012) A global review of the cosmopolitan flathead mullet *Mugil*
2424 *cephalus Linnaeus 1758* (Teleostei: Mugilidae), with emphasis on the biology, genetics,
2425 ecology and fisheries aspects of this apparent species complex. Rev Fish Biol Fish 22:641–681.

2426 Witenberg G (1929) Studies on the trematode—family Heterophyidae. Ann Trop Med Parasitol
2427 23:131–239.

2428 Yam KC, D'Angelo I, Kalscheuer R, Zhu H, Wang JX, Snieckus V, Ly LH, Converse PJ, Jacobs
2429 WR, Strynadka N, Eltis LD (2009) Studies of a ring-cleaving dioxygenase illuminate the role of
2430 cholesterol metabolism in the pathogenesis of Mycobacterium tuberculosis. PLoS Pathog
2431 5:e1000344.

2432 Yamaguti S (1970) Digenetic trematodes of Hawaiian fishes. Digenetic trematodes of Hawaiian
2433 fishes.

2434 Youssef AI, Uga S (2014) Review of parasitic zoonoses in Egypt. Trop Med Health 42:3–14.

2435 Yu S-H, Mott K (1994) Epidemiology and morbidity of food-borne intestinal trematode infections.
2436 World Health Organization.

2437 Zampino D, Di Martino V (2000) Presentazione cartografica dei popolamenti a Laminariales dello
2438 Stretto di Messina. Biol Mar Medit 7:599–602.

2439 Zanoni RG, Florio D, Fioravanti ML, Rossi M, Prearo M (2008) Occurrence of *Mycobacterium spp.*
2440 in ornamental fish in Italy. J Fish Dis 31:433–441.

2441

8 APPENDIX

Appendix I

Total number of Granulomas in C. aurata, C. labrosus and O. labeo.

	N granuloma CA	N granuloma CL	N granuloma OL
Number of values	37	99	14
Minimum	0	0	0
25% Percentile	0	0	0
Median	0	0	0
75% Percentile	1	1	0
Maximum	5	4	1
Mean	0,6216	0,4747	0,07143
Std. Deviation	0,9818	0,8124	0,2673
Std. Error of Mean	0,1614	0,08165	0,07143

Appendix II

Stage of Granuloma in *C. aurata C. labrosus and O. labeo*

C. aurata

	Free	Encysted	Early stage	Intermediate stage	Late stage
Number of values	37	37	37	37	37
Minimum	0	0	0	0	0
25% Percentile	0	0	0	0	0
Median	0	0	0	0	0
75% Percentile	0	0	0	0	0
Maximum	0	2	3	1	1
Mean	0	0,2162	0,2432	0,05405	0,02703
Std. Deviation	0	0,4793	0,5965	0,2292	0,1644
Std. Error of Mean	0	0,0788	0,09807	0,03769	0,02703

2452 *C. labrosus*

2453

	Free	Encysted	Early stage	Intermediate stage	Late stage
Number of values	99	99	99	99	99
Minimum	0	0	0	0	0
25% Percentile	0	0	0	0	0
Median	0	0	0	0	0
75% Percentile	0	0	0	0	0
Maximum	1	2	2	1	1
Mean	0,0404	0,1818	0,1414	0,0202	0,0202
Std. Deviation	0,1979	0,4131	0,4043	0,1414	0,1414
Std. Error of Mean	0,01989	0,04152	0,04064	0,01421	0,01421

2454

2455

2456

2457 *O. labeo*

2458

	Free	Encysted	Early stage	Intermediate stage	Late stage
Number of values	14	14	14	14	14
Minimum	0	0	0	0	0
25% Percentile	0	0	0	0	0
Median	0	0	0	0	0
75% Percentile	0	0	0	0	0
Maximum	0	1	0	0	0
Mean	0	0,07143	0	0	0
Std. Deviation	0	0,2673	0	0	0
Std. Error of Mean	0	0,07143	0	0	0

2459

2460

2461

Appendix III

Distribiction of Granuloma in different organs in *C. aurata, C. labrosus and O. labeo*

C. aurata:

	Liver	Muscle	Spleen	Pancreas	Heart	Gill	Intestine	Stomach
Number of values	37	37	37	37	37	37	37	37
Minimum	0	0	0	0	0	0	0	0
25% Percentile	0	0	0	0	0	0	0	0
Median	0	0	0	0	0	0	0	0
75% Percentile	1	0	0	0	0	0	0	0
Maximum	5	1	0	0	0	0	1	0
Mean	0,5676	0,02703	0	0	0	0	0,02703	0
Std. Deviation	0,9586	0,1644	0	0	0	0	0,1644	0
Std. Error of Mean	0,1576	0,02703	0	0	0	0	0,02703	0

2466 ***C. labrosus***

2467

	Liver	Muscle	Spleen	Pancreas	Heart	Gill	Intestine	Stomach
Number of values	99	99	99	99	99	99	99	99
Minimum	0	0	0	0	0	0	0	0
25% Percentile	0	0	0	0	0	0	0	0
Median	0	0	0	0	0	0	0	0
75% Percentile	0	0	0	0	0	0	0	0
Maximum	4	2	1	1	1	1	2	1
Mean	0,3131	0,06061	0,0202	0,0101	0,0404	0,0101	0,0202	0,0202
Std. Deviation	0,6647	0,3136	0,1414	0,1005	0,1979	0,1005	0,201	0,1414
Std. Error of Mean	0,0668	0,03152	0,01421	0,0101	0,01989	0,0101	0,0202	0,01421

2468

2469

O. labeo

	Liver	Muscle	Spleen	Pancreas	Heart	Gill	Intestine	Stomach
Number of values	14	14	14	14	14	14	14	14
Minimum	0	0	0	0	0	0	0	0
25% Percentile	0	0	0	0	0	0	0	0
Median	0	0	0	0	0	0	0	0
75% Percentile	0	0	0	0	0	0	0	0
Maximum	1	0	0	0	0	0	0	0
Mean	0,07143	0	0	0	0	0	0	0
Std. Deviation	0,2673	0	0	0	0	0	0	0
Std. Error of Mean	0,07143	0	0	0	0	0	0	0

Appendix IV

Origin of granuloma in *C. aurata, C. labrosus and O. labeo*

	Metacercaria-CA	Bacteria-CA	Mixosporidian-CA	Metacercaria-CL	Bacteria-CL	Mixosporidian-CL	Metacercaria-OL	Bacteria-OL	Mixosporidian-OL
Number of values	37	37	37	99	99	99	14	14	14
Minimum	0	0	0	0	0	0	0	0	0
25% Percentile	0	0	0	0	0	0	0	0	0
Median	0	0	0	0	0	0	0	0	0
75% Percentile	1	0	0	1	0	0	0	0	0
Maximum	5	1	1	4	1	0	1	0	0
Mean	0,5135	0,08108	0,02703	0,3737	0,101	0	0,07143	0	0
Std. Deviation	0,9609	0,2767	0,1644	0,7638	0,3029	0	0,2673	0	0
Std. Error of Mean	0,158	0,04549	0,02703	0,07676	0,03044	0	0,07143	0	0

Appendix V

Mean, Standard Deviation, Standard Error and C.I of Mean of Lenth and Weight

Size		Mean	Std Dev	Std. Error	C.I. of Mean
TL-CA	37	19,757	1,924	0,316	0,642
BW CA	37	72,081	22,193	3,648	7,399
TL - CL	99	20,18	3,992	0,399	0,792
BW- CL	99	91,66	139,679	13,968	27,715
TL-OL	14	18,75	2,744	0,733	1,584
BW- OL	14	65,286	23,973	6,407	13,841

Appendix VI

Parameters of pH, air temperature (°C), water temperature (°C), salinity (psu), oxygen (mg/l), and oxygen O_2 (%sat) from June 2020 to December 2020.

	June	July	August	September	October	November	Dicember
PH	7,8	7,69	7,79	8,04	7,86	7,93	7,79
T(°C) air	30,4	27	32,2	30,5	21,8	20,4	19,1
T(°C) water	28,8	29,2	31,4	29,8	24	19,9	15,1
Salinity	31,2	32,88	31,83	33,5	37,14	37,03	34,92
O_2 (mg/l)	9,76	5,06	9,43	8,32	8,7	8,05	9,56
O_2 (%sa)	146	76,1	150,4	126,7	120,1	101,6	109,5

Appendix VII

Parameters of pH, air temperature(°C), water temperature(°C), salinity (psu), oxygen (mg/l), and oxygen O_2 (%sat) from January 2021 to June 2021.

	January	February	March	April	May	June
PH	7,74	7,52	8,24	7,91	7,53	8,12
T(°C) air	13	7,6	13	15	21	25
T(°C) water	14,3	12,7	15,9	18,4	26,8	28,8
Salinity	33,62	31,11	27,72	31,16	31,74	33,36
O_2 (mg/l)	11,31	11,24	11,26	10,98	6,5	8,4
O_2 (%sat)	125,7	116,4	127,1	132,9	93,7	125,8